Is Anti-Müllerian hormone regulated by TGFbeta Superfamily Binding Proteins?

Yui Kawagishi

A thesis submitted for the degree of Doctor of Philosophy
at the University of Otago, Dunedin, New Zealand
November 2015

Abstract

Anti-Müllerian hormone (AMH) is a gonadal hormone that induces part of the male phenotype. However, it is also present in the blood of both sexes, and is a putative local regulator of adult gonadal function. This suggests that AMH, like other members of the TGFβ superfamily, is a pleiotropic regulator. The TGFβ superfamily ligands share receptors and binding proteins (BPs), leading to context-dependent signaling. AMH is the only ligand with a unique type-2 receptor (AMHR2), but it shares type-1 receptors with other TGFβs. Its ability to interact with other TGFβ superfamily members via common BPs is unknown. This thesis investigated whether TGFβ-superfamily BPs can regulate the activity of AMH.

A (BRE)2-Luc reporter gene assay was established to measure AMH signaling, at physiological levels of AMH. The assay was optimized by varying key parameters, such as the cell type and the type of serum, and by refining the critical technical steps. P19 cells were selected in preference to DU145 and LNCaP cells, as they had superior growth characteristics and as the AMH-reporter assay had a higher signal-to-background ratio. P19 cells express AMH type-1 receptors. However, the expression of endogenous AMHR2 by P19 cells was minimal. Transfection of AMHR2 was therefore essential to produce robust AMH signaling by P19 cells. The receptor-binding component of AMH (AMH_C) and the physiological form of AMH ($AMH_{N,C}$) both activated the reporter assay, with physiologically-relevant EC50s.

The influence of fifteen TGFβ-superfamily BPs on AMH signaling was examined, using multiple screens. The influence of each BP on the AMH dose-response curve was examined, along with their effect on an EC50-like concentration of AMH. AMH_C and $AMH_{N,C}$ were both examined, enabling the influence of interactions on both the N and C terminal domains of AMH to be examined. The follistatins (FSs) had the greatest effect on AMH signaling, with their influence being maximal when AMH levels were low (adult circulating-like levels). FS288 appeared to be more potent than FS315.

Brorin, decorin and FS-like 4 also caused a statistically significant change in the dose-response curve. The effect of these BPs were small and were only evident when the concentration of AMH_C was low. Little or no effect was observed when the concentration of AMH was close to or above the EC50. Endoglin and chordin-like 2 reduced the bottom (zero AMH) of the dose-response curve, but did not affect the reporter activity produced by AMH. This suggests that endoglin and chordin-like 2 influence the reporter assay through a mechanism that is unrelated to AMH.

The assay was designed to detect AMH BPs, and different types of studies will be needed to identify how FS288, FS315, brorin, decorin and/or FS-like 4 affects the functions of AMH *in vivo*. The other eight BPs tested appeared to have little or no effect on AMH signaling.

AMH is partially secreted as an inactive precursor (proAMH), and the bioactivity of AMH *in vivo* may be influenced by when and where proAMH is cleaved to $AMH_{N,C}$. BPs potentially influences this process, but none of the BPs examined in the Thesis affected the cleavage of proAMH by one of its putative cleavage enzymes, furin.

AMH shares type-1 receptors and the intracellular signaling cascade with bone morphogenetic proteins (BMPs). This raised the possibility that AMH does not always signal as an independent regulator. In some contexts, AMH and BMP may interact to regulate gene expression. Consistent with this, AMH and BMP exhibited redundant or co-operative activation of the reporter, depending on the concentrations of each ligand. This question was largely outside of the scope of this thesis, and further testing of this hypothesis was not undertaken. However, these preliminary observations lay a foundation for the future research directions outlined in Chapter 6.

In summary, this thesis presents the first evidence that certain TGFβ-superfamily BPs may influence AMH signaling. FS288 was the most significant of these, and may be most important when AMH levels are low, as in men and women. In vivo experiments are needed to prove this. BPs such as FS288 may integrate the biological actions of AMH with those of other TGFβ-superfamily ligands.

Acknowledgement

Thank you so much to my supervisor Prof Ian McLennan for taking me on as a PhD student and for your phenomenal support and guidance throughout my PhD journey.

Thank you so much to my co-supervisor Dr Michael Pankhurst for your support and assistance. Thank you to the late Dr Elspeth Gold for your critical and helpful advice. Thank you to Mrs Brandi-Lee Leathart and Mrs Nicola Batchelor for your help in the lab. Also, thank you to my PhD committee members: Dr Louise Parr-Brownlie and Dr Stephen Bunn, for helping with the milestones of this thesis.

Thank you to my family for your support: Eriko, Yume, Toseko, Tatsuo, and Tatsuro Kawagishi, Dr Taisei Kawagishi and Mr Motoki Seito. Thank you to my friends for making my life in Dunedin better.

Finally, thank you to my dearest partner (and fellow PhD student), Mr Simon Tom Kelly for the big support and cheering me up always.

Table of Contents

List of Tables

List of Figures

Abbreviations

ACVR	activin receptor
ACVR1	Activin A receptor type-1 (ALK2)
ACVR1B	Activin A receptor type-1B (ALK4)
ACVR1C	Activin A receptor type-1C (ALK7)
ACVR2A	Activin A receptor type-2A
ACVR2B	Activin A receptor type-2B
ACVRL1	Activin A receptor-like kinase 1 (ALK1)
ALK	Activin receptor-like kinase
AMH	Anti-Müllerian hormone
AMH_C	C-terminal peptide of anti-Müllerian hormone
AMH_N	N-terminal peptide of anti-Müllerian hormone
$AMH_{N,C}$	Non-covalent complex of AMH_C and AMH_N
AMHR2	Anti-Müllerian hormone type 2 receptor
BMP	Bone morphogenic protein
BMPR	Bone morphogenic protein receptor
BMPR1A	Bone morphogenic protein receptor type 1-A (ALK3)
BMPR1B	Bone morphogenic protein receptor type 1-B (ALK6)
BP	Binding protein
BRE	Bone morphogenic protein receptor responsive element
Co-SMAD	co-mediator SMAD
CRIM1	cysteine-rich transmembrane BMP regulator 1
Ctrl	Control
DNA	Deoxyribonucleic acid
DU145	human epithelial prostate cancer cell line
EC	Effective concentration (see Section 4.1.1)
ELISA	enzyme-linked immunosorbent assay
ERK	extracellular signal-regulated kinase
FCS	fetal calf serum
FS	Follistatin
FS288	Follistatin 288
FS315	Follistatin 315
FSH	Follicle stimulating hormone

FS-like 1	follistatin-like 1
FS-like 3	follistatin-like 3
FS-like 4	follistatin-like 4
GDF	growth and differentiation factor
hAMH	human anti-Müllerian hormone
HBSS	Hank's balanced salt solution
HEK	human embryonic kidney
InhB	Inhibin B
IVF	in vitro fertilization
LAP	latency-associate peptide
LH	Luteinizing hormone
LNCaP	human epithelial prostate cancer cell line
Luc	Luciferase
MA-10	mouse Leydig tumor cell line
MEM-α	Eagle's minimum essential medium-alpha
mRNA	Messenger ribonucleic acid
P19	murine embryonic carcinoma cell line
PCOS	Polycystic ovary syndrome
PCR	polymerase chain reaction
PCSK	proprotein convertases of the subtilisin/kexin-type
PMDS	Persistent Müllerian duct syndrome
proAMH	uncleaved precursor of $AMH_{N,C}$
qPCR	quantitative polymerase chain reaction
Ren	Renilla Luciferase
rhAMH	recombinant human anti-Müllerian hormone
RNA	ribonucleic acid
RPMI	Roswell Park Memorial Institute medium1640 with 2 mM L-glutamine
R-SMAD	receptor activated SMAD
Sog	short gastrulation
TGFβ	Transforming growth factor beta
TGFβR1	Transforming growth factor beta receptor (ALK5)
Transf	Tranfection
TβR	Transforming growth factor beta receptor

Chapter 1: General introduction

1.1 Overview

Anti-Müllerian hormone (AMH, also known as Müllerian inhibitory substance) is a gonadal hormone, which mediates part of the classical pathway for male sexual development. AMH has been viewed as a classical hormone that has very few actions. However, AMH is a member of a large superfamily of cytokines, the transforming growth factor βs (TGFβs), which are amongst the most pleiotropic regulators known to Science. AMH is present in the circulation of boys and adults of both sexes for reasons that are not explained by historical thinking. The concentration of AMH in the circulation and in the gonads differs by orders of magnitude, depending on sex, age and tissue. The TGFβ superfamily is able to signal at diverse concentrations, in a context dependent manner, as their signaling is modulated by binding proteins (BPs), and by other mechanisms. This raises the possibility that BPs modulate AMH signaling, leading to context dependent signaling. This thesis describes the first exploration of this issue, with its main objective being to test whether known TGFβ BPs can influence AMH signaling in an *in vitro* model.

The thesis begins with an over-view of the classical biology of AMH, after which a broad overview of the TGFβ superfamily is presented. This is followed by a discussion of why AMH signaling may be modulated by BPs.

1.2 Anti-Müllerian hormone

1.2.1 AMH and male sexual differentiation

In the early stages of fetal development, the gonads are bipotential. Both sexes contain Müllerian and Wolffian ducts. In female mammalian embryos, the Müllerian ducts differentiate into the oviducts, uterus, cervix, and the upper third of the vagina [1]. In human male embryos, the Müllerian duct regresses between the sixth and ninth week of gestation [2, 3], whereas the Wolffian ducts develop into the embryologic precursors of the vas deferens, epididymis and seminal vesicles [4].

The regression of the Müllerian ducts is triggered by AMH, which is secreted by Sertoli cells of the embryonic testes [5]. The AMH-induced regression of the Müllerian duct is the hallmark function of AMH. This phenomenon is particularly well known, as it was one of the first examples of physiological cell death [6]. The role of AMH was first examined by experimental manipulation of embryos [7]. However, the best evidence for its role today comes from rare males with null mutations in both alleles of either the AMH or the AMH type-2 receptor (AMHR2) genes. These individuals exhibit retention of the Müllerian duct and undescended testis, a condition known as persistent Müllerian duct syndrome (PMDS) [4, 8, 9].

The Sertoli cells continue to produce AMH after the regression of the Müllerian ducts, suggesting that AMH has biological functions beyond the regression of the Müllerian duct [10]. One of these functions is the regulation of testicular development and function. The receptors for AMH are expressed by Leydig cells [11] with AMH being a determinant of the number of Leydig cells and the capacity of each Leydig cell to produce testosterone. The multiple effects of AMH on Leydig cells tend to

cancel each other out, with the result that testosterone levels are largely independent of the level of AMH [12-14]. The biological purpose of this AMH regulation is currently unknown.

1.2.2 AMH may have hormonal and local functions

The existence of AMH was first deduced from the phenotype of Freemartin calves, which are female calves with a male twin [15]. Freemartin calves lack the internal female reproductive tract structures, and exhibit virilized ovaries [16]. This phenotype arises because blood-borne AMH from the male fetus has been transmitted to the female fetus, due to anastomosis of their placenta. Consequently, AMH was originally thought to be a classical hormone. However, AMH is not universally regarded as a hormone, as physiologically, the regression of the Müllerian duct appears to be due to diffusion of AMH from the adjacent testis. The clearest evidence for this comes from humans with ovitestis. These individuals often exhibit unilateral loss of the Müllerian duct adjacent to the testis-like gonad with development of the female reproductive tract occurring adjacent to their ovary-like gonad (reviewed in [10]). Similarly, the regulation of Leydig cells by AMH is likely to be due to the local diffusion of AMH between neighboring Sertoli and Leydig cells.

AMH expression has also been detected outside of the gonads, including the mature brain [17], the prostate [18] and the uterus [19]. These sources presumably mediate local phenomena, as AMH in the circulation is entirely of gonadal origin [20, 21]. The functions of non-gonadal sources of AMH are almost entirely unknown, with the putative function being autocrine or paracrine protection of neurons against excitoxicity [22].

1.2.3 Circulating levels of AMH in males

The secretion of AMH begins immediately after the testes become morphologically recognizable, which is around 40 days gestation in humans [23]. This is the first testicular secretion, which continues throughout the life cycle, but with age-specific variation. Circulating AMH levels are close to maximum in the second trimester of pregnancy [23, 24]. The levels tend to decline slightly after that and briefly fall during the perinatal period. Consequently, the median AMH level in cord blood of male babies is only 150 pM [21, 24]. Circulating levels of AMH increase rapidly after birth and by 3-months of age boys can have nM levels [21] (Figure1-1). The levels of AMH are highest during late infancy between 6 months and 12 months of age, after then they gradually decline until puberty [25]. Circulating levels of AMH fall markedly during the pubertal transaction by an order of magnitude, giving adult male levels that range from 20-50 pM [26]. This is 3-4% of infant male levels [21] and 5 % of the level in boys [21, 25, 27]. The circulating AMH levels in men are stable until around 50 years old, after which they appear to gradually decline, but with significant variation between men [21, 26]. Some elderly men lack detectable levels of AMH [26].

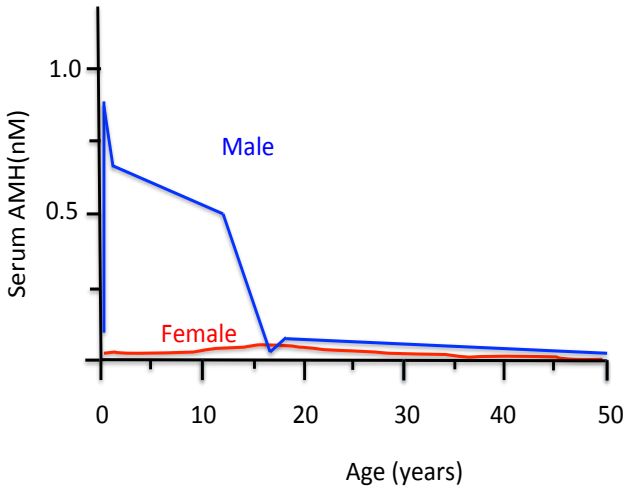

Figure 1-1. AMH levels in circulation

AMH shows sexually dimorphic pattern in circulation. Male (blue) AMH levels are very high during infancy and childhood, and decline at puberty. Female (red) AMH is undetectable during infancy and early childhood.

The levels of circulating AMH are highly variable in people of the same age and sex [21, 25]. For example, the range of circulating AMH levels in 5 to 6 year old boys is 0.5-2 nM [28] with these differences being stable throughout childhood [21, 28].

1.2.4 Hormonal functions of AMH

The reason why AMH levels are present throughout the life cycle of males is largely unknown. The receptors for AMH are broadly distributed in developing tissues (Sections 1.6.6, 1.6.7), and putatively contribute the generation of sex biases. To date, AMH has been implicated in the sexually dimorphic development of the lung [29] and the brain [17, 30]. The numbers of neurons in sexually dimorphic nuclei are regulated early in development and then undergo further changes at puberty. The initial sex

bias in the bed nucleus of the stria terminalis, for example, is absent in the AMH knockout mouse strain, $AMH^{-/-}$, mice, suggesting that AMH controls the developmental ("child") version of the nucleus. The subsequent pubertal changes are independent of AMH, and are presumably regulated by testosterone. Some non-reproductive behavior of mice, such as exploratory tendency, is dependent on AMH [30, 31]. In humans, the levels of AMH in 5 to 6 year old boys negatively associate with indexes of maturity, which is consistent with AMH having functions in humans [28].

The function of circulating AMH in adults is even less well studied, with no proven functions. One issue here is whether the levels of circulating AMH are sufficient to active AMH receptors (Section 1.7, Chapters 3 & 4). AMH levels in adult men correlate with the anatomical characteristics of their aorta, with AMH levels associating with various cardiovascular diseases [32]. This suggests that the cardiovascular system may be a target for adult AMH. AMH levels associate with atherosclerosis in female primates [33], suggesting that the adult functions of AMH may be non-dimorphic.

1.2.5 AMH and male germ cells

In adult men, a portion of the AMH produced by the Sertoli cells is secreted to the lumen of the seminiferous tubules. The concentration of AMH in these tubules and the epididymis appears to be very high, as the level of AMH in semen has been reported to vary between 3.5 pM - 0.5 nM. These values are extremely variable, spanning the lower range of serum levels of adult men to the upper range of the serum

levels observed in boys [34-37]. The function of this AMH has not been extensively studied but historic studies suggest that it may enhance the survival of sperm [38, 39].

1.3 Female actions of AMH

Historically, AMH appeared to be male-specific. However, the ovary also produces AMH, and the majority of current research into AMH relates to its ovarian function. Before discussing the role of AMH in the ovary, the formation of the ovary is briefly described.

1.3.1 Function of ovary

Granulosa cells surround each functional oocyte in an ovary: forming what is known as an ovarian follicle (Figure 1-2). At birth, a female baby has 1 million oocytes. The number of oocytes decreases during childhood and by menarche, young women have between 300,000 and 1,000,000 oocytes [40, 41]. During each ovarian cycle, multiple follicles begin to mature (see below) and then regress or progress to ovulation. Each of the steps in this process is actively regulated, with selection of the follicles to progress. In humans, only one follicle typically becomes dominant to ovulate. Consequently, the number of dormant follicles in ovaries (the ovarian reserve) progressively declines, leading to menopause.

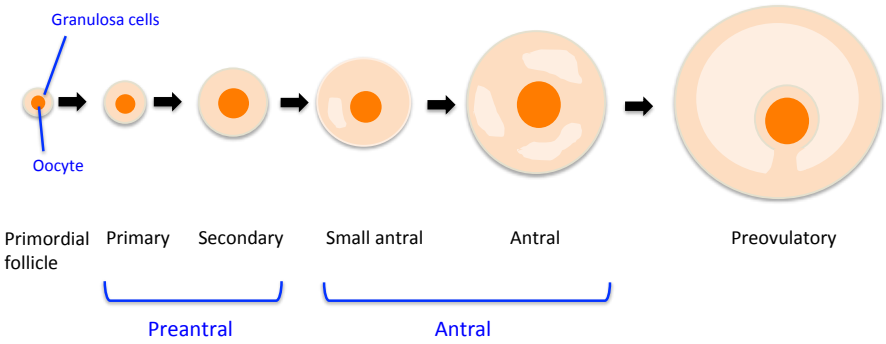

Figure 1-2. Folliculogenesis in ovary

Folliculogenesis have different developmental stages. There are three phases of follicles: primordial, preantral and antral. Preantral follicles includes primary and secondary follicles. Antral follicles have small antral follicles and large antral follicles.

Folliculogenesis occurs in the cortex of the ovary. Four major regulatory systems are involved: primordial follicle recruitment, preantral follicle development, selection, and atresia. There are three phases of follicles: primordial, preantral and antral. Primordial (or non-growing) follicles have flattened pre-granulosa cells associated with the oocyte. Preantral follicles are divided into two stages: primary and secondary follicles. Primary follicles have a single layer of cuboidal granulosa cells around the oocyte. Secondary follicles are preantral follicles with two or more granulosa cell layers surrounding the oocyte. Antral follicles are any follicles with a fully formed antrum. Antral follicles have two stages: small antral follicles and large

antral follicles. Large antral follicles are usually defined by the time when the follicle requires FSH to survive (Figure 1-2) [42].

The initial formation of primordial follicles occurs during fetal development. The primordial follicle consists of a small primary oocyte, a single layer of granulosa cells, and a basal lamina. The progression of immature follicles to subsequent stages is regulated by interactions between oocytes and their associated granulosa cells. These interactions are mediated by growth factors that act in an autocrine and paracrine fashion [43, 44]. Hormones have minimal importance at this stage. These regulatory processes lead to a continuous recruitment of primordial follicles to the preantral stage [43].

As follicles progress through the antral and pre-ovulatory phase, they become dependent on the cyclical secretion of the pituitary hormones: follicle-stimulating hormone (FSH) and luteinizing hormone (LH) [43]. As follicles grow, the number of granulosa cells increases and they begin to express AMH and inhibin B (InhB), leading to low levels of AMH in the blood of girls. Once puberty begins, FSH influences the selection of limited numbers of small, growing follicles during each ovarian cycle. From this smaller cohort of growing follicles, one follicle is typically selected as a dominant follicle (in humans). The dominant follicle(s) subsequently ovulates under the influence of LH [42]. The other follicles are removed by atresia. FSH needs to exceed a threshold concentration to enable FSH-dependent selection of follicles [45-47].

1.3.2 AMH regulation of the actions of FSH with folliculogenesis

The granulosa cells synthesize AMH, in a stage-specific manner. The primordial follicles lack AMH, with the onset of AMH production occurring in the early preantral follicles [48]. Antral follicles contain large numbers of granulosa cells, which are thought to be the primary source of circulating AMH [49]. However, the production of AMH is highest in the granulosa cells of preantral and small antral follicles, after which it ceases abruptly [48]. AMH is not produced by either atretic follicles or the corpus luteum [50]. The expression of AMH by growing follicles putatively modulates follicular growth. AMH also blocks the recruitment of non-dominant (preantral) follicles during the selection of a dominant follicle [13, 51] by decreasing the responsiveness of follicles to FSH [52]. Thus, AMH plays a role as a negative feedback signal of the number of growing follicles [53]. When this mechanism is absent, such as in $AMH^{-/-}$ mice, there is increased recruitment of small growing follicles. This does not lead to increased ovulation, as FSH affects multiple stages of follicular development. Consequently, AMH is controlling the rate at which the pool of follicles is depleted, without influencing litter size. Consistently, $AMH^{-/-}$ mice exhibit premature depletion of follicles [51] and polymorphic variants of AMH and its receptor are associated with the age of menopause in humans [54]. Given the above, there is the potential in the future for AMH to be used to delay the process of reproductive aging, and the onset of menopause.

1.3.3 Concentration of AMH in follicular fluid

In humans, the AMH concentration in follicular fluid relates to the size of small antral follicles. The median concentration of AMH is highest in small antral follicles with a

3 mm diameter (8 nM) and decreases thereafter, as follows: 2.8 nM in 9 mm, less than 0.7 nM in 12 mm, 18 pM in 16 mm [55]. The age of a woman does not affect the level of AMH in her follicles [56]. Consequently, AMH in pre-pubertal age girls are similar to older women. The concentration of AMH is not related to the concentrations of other hormones in follicular fluid, including androstenedione and testosterone [57]. The size of an ovulatory follicle is between 17-25 mm in diameter [58]

1.3.4 Circulating levels of AMH in females

During development, when AMH mediates aspects of male sexual differentiation, females have little or no AMH. The first expression of AMH in primary follicles occurs on the third postnatal day 3 in rats and mice [6, 59], and around 36 weeks of gestation in humans [60]. This initial production is very low, with AMH levels in the cord blood of female babies being less than 2.8 pM [61]. AMH levels rise rapidly during the "mini-puberty" that occurs after birth. Consequently, 3-month-old infant girls have significantly higher levels of circulating AMH (mean of 15 pM) with the levels decreasing by 12 months of age [62]. These levels of AMH overlap the adult male range [21, 25, 62] (Figure1-1), but are markedly below the lower limits for developing males (Section 1.1.3). Circulating AMH levels in girls only minimally increase throughout the pre-pubertal years [25]. From mid childhood to early adulthood (8-25 years old), AMH levels slightly increase as the profile of ovarian follicles matures [63].

The levels of circulating AMH in women peak around 25 years of age [63]. The

range of AMH values at this age show extreme variation between women [63, 64], with this range extensively overlapping with the range of AMH values in young men. The median AMH level progressively decreases after this age as the pool of ovarian follicles diminishes. AMH levels become undetectable at menopause [63], and elderly females lack AMH, unless they develop granulosa cell tumors [65]. The loss of circulating AMH is the first endocrine sign of menopause, and precedes the decline of estrogen and other ovarian hormones [46, 62, 66].

1.3.5 AMH as a biomarker of ovarian reserve

It is not currently possible to directly determine the number of primordial follicles in a living woman and her ovarian reserve can therefore also not be directly measured [46]. AMH levels fall in the circulation throughout reproductive life [67] and become undetectable at menopause [25]. Serum AMH levels correlate with the size of the primordial follicle pool and the measurement of serum AMH concentrations are commonly used to estimate the ovarian reserve of woman [68]. The levels of AMH do not vary during the menstrual cycle, in contrast to other ovarian hormones, such as estrogen. This increases the utility of AMH as a biomarker, as a woman's level of AMH can be examined at any stage of her menstrual cycle [69]. Estimation of ovarian reserve is particularly important at the beginning of *in vitro* fertilization (IVF) treatment, as it enables the attending clinicians to predict whether the woman will have a poor or over-response to the drugs used to induce super-ovulation [70].

1.3.6 Polycystic ovary syndrome

Polycystic ovary syndrome (PCOS) is the major cause of anovulatory infertility [71]. Up to 20% of females of reproductive age have PCOS [72, 73]. Anovulatory women with PCOS have abnormal granulosa cell function and this abnormality may influence the oocyte or embryo quality [74]. Their ovaries are also enlarged with increased numbers of follicles or cysts that have arrested developmental progression at the antral stage. Women with PCOS have significantly elevated levels of serum AMH level, suggesting that AMH may be involved in the generation of their follicular status [75]. This is due to increased numbers of preantral and antral follicles, and to increased production of AMH by cystic follicles [76]. Serum AMH levels appear to correlate to the level of severity of the PCOS, with AMH increasingly used in the clinical assessment of PCOS [77].

1.4 Summary of the biology of AMH

AMH appears to be a complex regulator that can act as a hormone or as a local regulator. It has different actions in males and females; it may additional have actions which are common to both sexes. The concentrations of AMH present in different biological fluids can be extremely different. Nanomolar concentrations of AMH are present in ovarian follicular fluid, the seminal fluids of adult men and the circulation of boys. In contrast, the level of AMH in the circulation of adult men and women rarely exceed a few tens of pM. How can one regulator signal at different concentrations and initiate disparate actions?

AMH is a member of the TGFβ superfamily, which has complex context dependent signaling. Before discussing the molecular biology of AMH, this thesis reviews the known characteristics of the TGFβ superfamily.

1.5 The TGFβ superfamily

1.5.1 Overview

The TGFβ superfamily is one of the main families of protein signaling molecules, which are variably described as cytokines or growth factors. The family has 35 mammalian members [78], which can be divided into two major TGFβ subfamilies, based on the similarity of their sequences. The two families are the TGFβ/activin/nodal subfamily and the bone morphogenetic protein (BMP)/growth and differentiation factors (GDFs) subfamily [79].

The TGFβ superfamily members typically show paracrine actions on cells near their site of synthesis [80], although the family also contains ligands that are best known as hormones. These include the activins and inhibins. The functions of TGFβ superfamily ligands are context dependent, cell type-specific and vary with the stage of development [81]. Consequently, a given TGFβ ligand can inhibit and stimulate the proliferation of a particular cell type [5]. The cellular functions regulated by this family include cell growth, adhesion, cell recognition, apoptosis, differentiation and migration [82, 83]. The TGFβ superfamily contributes to the development and function of most, if not all, tissues. The family has also been implicated in the pathogenesis of many human diseases, including cancer, neurological conditions, wound-healing disorders and fibrosis [80]. For this reason, the TGFβ superfamily has been extensively studied, with the lack of information relating to AMH being a notable exception to this generalization (Section 1.2).

The context dependent pleiotropic signaling of the TGFβ superfamily is generated from multiple layers of regulation, which include intra- and extra-cellular components.

These layers are briefly outlined below, with a particular emphasis on the multiple roles of BPs.

1.5.2 Ligands

1.5.2.1 Ligand expression and processing

Fundamentally, the actions of cytokines are defined by when and where they are expressed [84, 85]. With the TGFβs there is an added complexity as multiple ligands can activate the same receptor (Section 1.5.3.1). Consequently, the activation of a given receptor in a particular cell can be by a single ligand or by combination of ligands. For example, the TGFβ subfamily has three members, TGFβ1, TGFβ2, and TGFβ3, which can activate a common receptor. The expression of each isoform is different, but in some cellular environments more than one TGFβ isoform is present at the same site [86]. This results in null mutations of TGFβ ligands exhibiting a milder phenotype than the null mutations of TGFβ receptors [87, 88].

TGFβ superfamily ligands are synthesized as proprotein homodimers that share a conserved structure consisting of a signal sequence, a longer N-terminal domain and a shorter C-terminal receptor-binding domain. In most instances, the N- and C-terminal peptides dissociate after cleavage of the proTGFβ. However, some ligands form stable non-covalent complexes consisting of the N- and C-terminal peptide. In the case of the TGFβ subfamily, the N-terminal peptide is called the latency-associate peptide (LAP), although this terminology is not used for other TGFβ ligands [89].

The regulation of cleavage of the proTGFβs is one mechanism for controlling their bioactivity. This phenomenon may be particularly relevant to AMH, and is covered in Chapter 5.

1.5.2.2 Ligand availability

The activity of TGFβ ligands can be modified by BPs that either prevent or assist them reaching the sites where their cognitive receptors are. This can generate gradients of signaling, which are particularly important in morphogenesis. For example, short gastrulation (Sog) is a BMP BP, which is synthesized in the ventral-lateral region during the early patterning of an embryo, and diffuses from its site of synthesis. The BMPs in the early embryo are then transferred from regions of low Sog to regions of high Sog, creating a gradient of BMPs ligands, with the concentration of BMPs being highest in the ventral-lateral region (reviewed:[90]).

There are also BPs that can trap ligands, preventing their diffusion [79]. The combination of a sequestering BP and a ligand can create microscopic zones where signaling cannot occur immediately adjacent to zones where signaling is occurring. This type of mechanism is common in BMP signaling, and can be mediated by BPs such as noggin, and chordin [83, 91].

1.5.3 Receptors

All of the TGFβ superfamily signal through a receptor complex, which contains two type-1 receptors and two type-2 receptors. The type-1 and type-2 receptors are 50-60 kDa and 70-80 kDa, respectively [92]. Both types of receptors are serine-threonine kinases, with their kinase domain having approximately 40% homology [93]. This

contrasts with the other major cytokine families that predominantly signal through tyrosine kinases or g proteins.

1.5.3.1 Receptor specificity

Instead of each TGFβ ligand having different receptors, they share seven type-1 receptors and five type-2 receptors. For example, activin, nodal and BMPs share the same type-2 receptor: activin receptor type-2A (ACVR2A) (Figure 1-3). Activin and nodal share several type-1 receptors: ACVR1 (ALK2), ACVR1B (ALK4) and ACVR1C (ALK7). BMPR2 is another type-2 receptor for BMPs. Activin receptor-like 1 (ALK1) is a type-1 receptor for BMP9 and BMP10 [94].

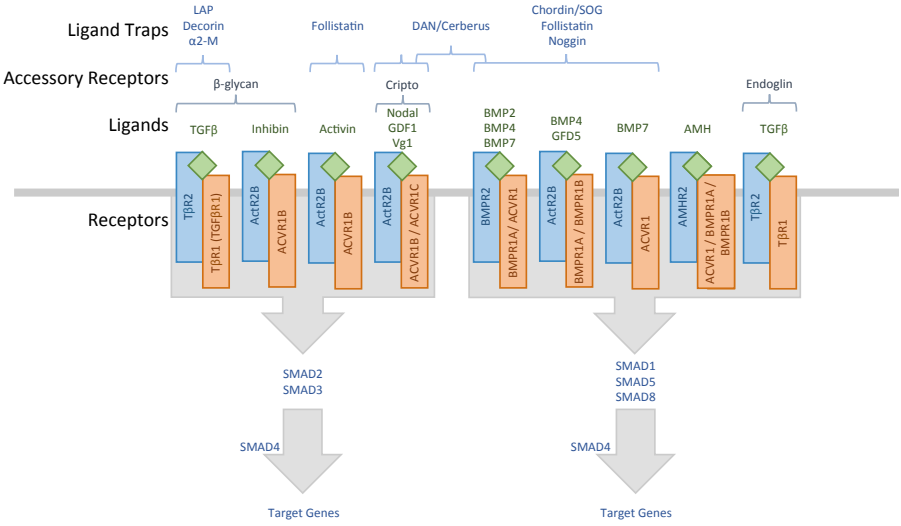

Figure 1-3. TGFβ superfamily ligands and receptors

TGFβ superfamily has a SMAD 2/3 pathway and a SMAD1/5/8 pathway. Ligand binding triggers the phosphorylation of one of the receptor, making phosphorylated R-SMAD. R-SMAD and SMAD 4 forms a complex, which enters the nucleus to induce transcription of target genes. AMH and BMP share type-1 receptors and SMAD 1/5/8 as a common downstream signaling pathway. Binding proteins of TFG-β superfamily are shared between ligands. AMH is the only ligand that it is not investigated for its binding proteins.

The specificity of receptors is context dependent, as various BPs can alter the ability of a ligand to bind to a receptor complex. These BPs can be membrane-embedded and were initially described as co-receptors or type-3 receptors. Co-receptors generally enhance the ability of ligands to bind to the receptors [83]. For example, betaglycan presents TGFβ to TGFβ receptors [95] and inhibin to activin receptors [96, 97]. The complex characteristics of betaglycan are discussed later (Section 1.5.4.1).

1.5.3.2 Receptor expression

The expression levels of the various type-1 and type-2 receptors are different, with respect to target cells and the stage of development [95, 96]. As noted above, many receptors can form multiple different complexes. Signaling within the TGFβ superfamily is therefore also dependent on which combinations of receptors are produced by specific cells, not exclusively by the pattern of expression of any one receptor.

1.5.3.3 Receptor inhibition

Some of the TGFβ superfamily ligands can bind to receptors, but are unable to activate an intracellular pathway [96, 98]. These ligands act as competitive inhibitors of other ligands that induce a downstream response. For example, Lefty (also known as left-right determination factor) can inhibit the binding of Nodal to its receptors [99, 100], whereas inhibin A and inhibin B compete with the activins [96, 97].

1.5.4 Binding proteins

The TGFβ-superfamily BPs contributes to multiple functions outlined in the Sections above. Each BP only binds to a subset of the TGFβ superfamily ligands (Table1-1). For example, follistatin (FS) binds to the activins with high affinity and to the BMPs with lower affinity [101, 102]. The binding specificities of the BPs are typically different to the receptors, and the combination of receptors and BP generate a large number of differing signaling contexts.

Some of the TGFβ superfamily BPs can be grouped into families: most notably the chordins, follistatins, noggins, and the cerberus/ DAN family [103]. Most BPs regulate one or more of the BMPs, but there is no consistent relationship between BP families and the ligand or receptor subfamilies (Figure 1-3, Section 4.3.2). The BPs have diverse functions ranging from accessory receptors to ligand traps, with some of the BPs being able to operate through different mechanisms at different sites [79, 80]. Examples of this are discussed in the following Section.

There is no consistent stoichiometry for the relationship between BPs and ligands: chordin and BMP bind on a one-to-one basis (chordin:BMP) [104]; chordin-like 2 – BMP, FS – Activin, FS-like 3 – Activin A all bind with a 2:1 ratio [104-106], whereas betaglycan has three binding sites, each of which has unique characteristics (Section 1.5.4.1). The stoichiometry of some of the ligand – BP interactions has yet to be defined.

Table 1-1. Binding proteins and ligands

Binding proteins	Binds to	Reference
Betaglycan	TGFβ, BMP with inhibin	[107]
Brorin	BMP	[108]
Chordin	BMP	[109, 110]
Chordin-like1	BMP	[109]
Chordin-like 2	BMP	[109]
DAN	BMP, chordin, FS, noggin	[111]
Decorin	TGFβ1/2	[112]
Endoglin	activin, BMP, TGFβ	[113]
FS	activin, BMP, TGFβ1	[114-116]
FS-like 1	activin, BMP	[117]
FS-like 3 (FLRG)	activin, BMP, TGFβ1	[118]
FS-like 4	BMP(?)	Note
Noggin	BMP	[119]
α2-macroglobulin	activin, betaglycan, BMP1, TGFβ as a carrier protein	[120, 121]

Note. FS-like 4 has been discovered recently and the binding characteristics are unknown. However, the data sheet of R&D systems reported that FS-like 4 inhibited the ability of BMP6.

As noted in the previous sections, the TGFβ-superfamily BPs can exert diverse influences. In some instances, a single BP can generate opposing actions, depending on the context of the cell. This mechanism is exemplified by betaglycan, as outlined in the next Section.

1.5.4.1 Betaglycan, an example of a complex binding protein

Betaglycan is an 853 amino acid proteoglycan, which was originally known as the type-3 TGFβ receptor [122]. Betaglycan regulates aspects of both the BMP and TGFβ subfamily ligands. When betaglycan is absent, TGFβ1 and TGFβ3 can activate TβR2, but TGFβ2 cannot. However, when betaglycan is present, it binds all three TGFβ isoforms, and then transfers them to TβR2. Under this circumstance, TGFβ2 is equally potent as TGFβ1 and TGFβ3 [88, 96, 123, 124]. Betaglycan enhances BMP signaling by increasing BMP ligand binding to BMPR1A and BMPR1B [125] and by regulating the trafficking and cell localization of BMP receptors [126].

Betaglycan has two different forms: a membrane-bound form and a soluble form, created by cleavage of the membrane-form adjacent to the extracellular portion of the trans-membrane domain. The soluble form is therefore not anchored to the membrane, and is unable to transfer TGFβs bound to it to the TGFβ receptors. Soluble betaglycan therefore, inhibits TGFβ signaling, by sequestering the TGFβs [95, 124, 127]. Consequently, betagylcan can be a BP that enhances TGFβ2 signaling, or a BP that inhibits all TGFβ signaling, depending if the target cell secretes the enzymes that cleaves it.

Inhibin cannot directly bind to activin receptors, unless assisted by betaglycan. Betaglycan binds inhibin with high affinity (Kd: 600pM). The resulting betaglycan-inhibin complex then transiently associates with ACVR2. This transient complex then naturally dissociates creating free betaglycan leaving inhibin bound to ACVR2 [96]. That is, betaglycan is acting like a chaperone to change the conformation of inhibin to one that has high affinity for ACVR2. The binding of inhibin to ACVR2 inhibits the binding of activin to this receptor, which in turn blocks the recruitment of the activin type-1 receptor [96, 128]. Betaglycan thus determines whether inhibin is able to antagonize activin signaling. As with the TGFβs, this situation can be reversed by the target cell, as the soluble form of betaglycan can bind inhibin, preventing it reaching ACVR2. Betaglycan also assists inhibins to antagonize BMP signaling, although this effect has been less studied, and is less well characterized [96, 107].

The inhibin and TGFβ binding sites on betaglycan are separate, but the two sites interact. If TGFβ binds to betaglycan then inhibin cannot bind. This leads to the situation where TGβs are able to block the inhibin-mediated inhibition of activin signaling, by preventing inhibins binding to betaglycan. The TGFβs can enhance activin signaling independent of the TGFβ receptors [79]. This example shows that TGFβ superfamily signaling is context dependent, as multiple layers of interactions regulate whether an intracellular cascade is triggered.

1.5.5 SMADs: Intracellular signaling

This thesis is focused on the extracellular regulation of AMH activity, and does not investigate the intracellular mediates of AMH action. The intracellular actions of the

TGFβs are therefore only briefly discussed. The SMADs are the main intracellular mediators of TGFβ signaling, although TGFβ can also activate other pathways. The SMAD pathway is sometimes referred to as the canonical signaling for TGFβ [80], with non-SMAD pathways being described as non-canonical signaling. Two main SMAD signaling pathways exist and act depending on which receptor-specific SMAD is activated (Figure 1-3). The TGFβ/activin-like pathway activates SMAD 2/3 whereas and the BMP-like pathway involves SMAD 1/5/8 [79]. Each type-1 receptor activates only certain SMADs. ACVR1B (ALK4), TGFBR1 (ALK5) and ACVR1C (ALK7) are specific for SMAD2/3, while ACVRL1 (ALK1), ACVR1 (ALK2), BMPR1A (ALK3) and BMPR1B (ALK6) are specific for SMAD 1/5/8. Non-canonical pathways for AMH have not been identified, which may reflect a lack of investigation of this possibility.

SMADs consist of three domains. The C-terminal domain binds to the type-1 receptor and also interacts with other proteins [129]. When receptor-activated SMADs (R-SMAD) are phosphorylated on the C-terminal, they can associate with the common-mediator SMAD (Co-SMAD), SMAD 4. Two R-SMADs and a single SMAD 4 makes a complex, which is shuttled into the nucleus. In the nucleus, this complex binds to chromatin and regulates the expression of the target gene with other transcription factors [130]. SMAD6 and SMAD7 are inhibitors that negatively regulate signaling strength and duration, creating negative feedback [131]. While receptors are active, both R-SMAD phosphorylation and SMAD nuclear accumulation are maintained but this ceases after receptor activity is lost [83]. The mechanism of SMAD phosphorylation and nuclear accumulation is straightforward compared with other signaling pathways like extracellular signal-regulated kinase

(ERK) activation by the Ras-Raf-MEK pathway downstream of EGF receptor signaling [83]. R-SMADs are dephosphorylated by a signal-independent and constitutively active phosphatase. This feeds nuclear R-SMADs back into the cytoplasm [83].

1.5.6 Summary

AMH is an atypical member in TGFβ superfamily and it has been thought to have a hormonal regulation without having BPs or sharing those with other members. To date, no BPs for AMH have been identified and it has been believed the regulation of AMH is less complicated than other members in the family are. The following sections discuss whether AMH is atypical, and if not, whether BPs for AMH participates in the regulation of AMH signaling.

1.6 The molecular biology of AMH

The following section discusses the molecular aspects of AMH, with particular reference to the TGFβ superfamily. AMH has a unique place in this family. It is the only ligand that has its own specialized type-2 receptor, placing it outside of the major TGFβ subfamilies. It is a subfamily in its own right. The evolutionary origin of AMH is unresolved, with recent phylogenetic trees of the TGFβ superfamily placing it on different branches. Some analyses suggest that AMH may be most closely related to the GDNF ligands, which are not consistently regarded as TGFβ superfamily members, as their receptors differ from other TGFβs and as their intracellular cascade is unrelated the SMAD pathway. Other analyses suggest that AMH's closest relation is the inhibin A subunit, whereas others consider AMH to be adjacent to GDF15 on the phylogenetic tree. All analyses agree that it is most distant from the BMPs, which is paradoxical as AMH shares type 1 receptors with the BMPs, and as AMHR2 and BMPR2 are closely related to each other [78, 132-134].

Until recently, AMH was thought to be like a classical hormone, with a few specialist functions. This contrasts with the pleiotropic nature of the superfamily as a whole. For these reasons, AMH is generally considered to be TGFβ-like, rather than a conventional member of the TGFβ superfamily. This conception has shaped research into AMH. The following section compares and contrasts the molecular biology of AMH with other members of the TGFβ superfamily, as a means of understanding its biology.

1.6.1 The AMH gene

The AMH gene is 2.75 kb long and contains five exons [135]. The fifth exon encodes part of the C-terminal peptide (AMHc), which binds to AMH receptors (Section 1.4.6). This is the only portion of the gene that has significant homology to the TGFβ superfamily [135, 136]. The other exons are, however, conserved between mammalian species, with the promoter and coding regions showing 65-80% and 70-75% homology between bovine, human, mouse and rat [6].

The coding region of AMH is most closely related to the inhibin, activins and TGFβs [83], which is somewhat paradoxical as AMH shares type-1 receptors with the BMPs (Figure1-3).

1.6.2. The AMH protein

The AMH protein is a 140-kDa glycoprotein, which consists of two identical monomers, each of which contains 555-560 amino acids, depending on the species [136-138]. AMH, like other members of the TGFβ superfamily, has three domains: the first is a signal sequence of 20 amino acids, which enables it to be secreted as a

535 amino acid proprotein (proAMH) [139]. ProAMH is subsequently cleaved at position 451/452 to form a 25 kDa C-terminal peptide (AMH_C) and a 110 kDa N-terminal peptide (AMH_N) [135, 139] (Figure1-4).

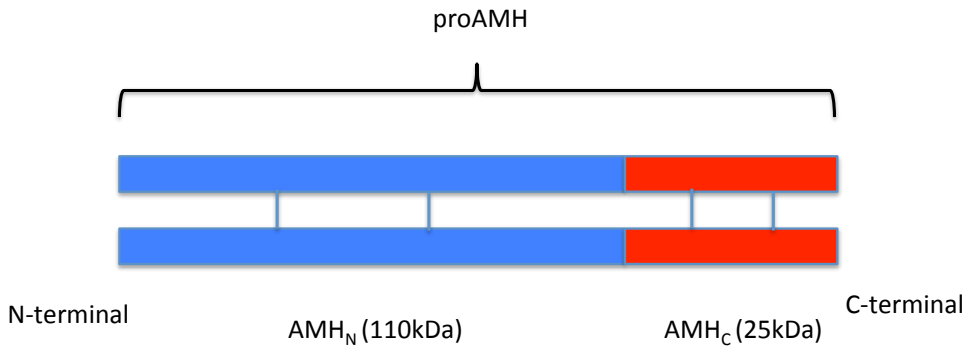

Figure 1-4. Structure of AMH protein

ProAMH has an N-terminal and C-terminal domain, which give rise to AMH_N and AMH_C after cleavage. The two AMH homodimers are linked by disulphide bonds (blue lines).

AMH_C and AMH_N remain as a non-covalent complex ($AMH_{N,C}$) after cleavage of proAMH, with AMH_C only separating from AMH_N as $AMH_{N,C}$ binds to the AMH receptor [140-142]. The formation of a stable complex ($AMH_{N,C}$) may facilitate the biological functions of AMH. Some of the functions of AMH are paracrine, and require AMH to diffuse through embryonic tissues (Section 1.1.2). The C-terminal fragments of TGFβ superfamily ligands tend to be insoluble in physiological conditions, which limits diffusion [98]. However, the formation of N- and C-terminal complexes increases the solubility of TGFβ superfamily ligands, facilitating their diffusion [98]. AMH fits this pattern, as AMH_N enhances and stabilizes the effect of AMH_C in an *in vitro* assay of the regression of the Müllerian duct [140]. Furthermore, mutations in AMH_N cause PMDS in humans, indicating that the N-terminal domain is required for normal AMH function, even though it does not bind to the AMH receptor [143].

Similarly, hormones must be soluble to remain in the circulation, and the N-terminal region may therefore be critical for AMH to remain in the circulation [144] (see Section 1.5.2).

In addition to regulating solubility, the N-terminal domains of the TGFβ superfamily have other functions, which includes regulating the intracellular trafficking of the ligand. The N-terminal domain of AMH may also serve this function, as mutant forms of human AMH (hAMH) that lack the C-domain are secreted more rapidly than wild-type hAMH, when transfected into CHO cells [145].

In summary, the functions of the N-terminal domain of AMH are incompletely understood, but appear to be conserved with a proportion of the other members of the

TGFβ superfamily. Most TGFβ ligands can only act over short distances, and the low homology of the N-terminal domain of AMH to other TGFβ superfamily ligands may simply reflect that it belongs to a small but significant portion of the family that mediates long-distance signaling, through hormonal and paracrine mechanisms.

1.6.3 Cleavage variants of AMH

Serine proteases such as plasmin creates AMH cleavage variants (AMH_{25-254} and $AMH_{255-560}$) [146]. These are not detected in the blood of healthy people but were observed in the blood of a patient with a sex cord tumor [147] and in equine granulosa cell tumors [148]. Naturally occuring mutations that alter amino acids 194 or 195 lead to PMDS [149, 150]. This raises the possibility that AMH may be cleaved at the 194/195 as part of normal physiology, but this has not been experimentally verified. In transfected cell lines, AMHΔ194 is not secreted, which is attributed to misfolding of the protein [145]. The properties of AMHΔ195 are unknown. There are no commercial or in-house suppliers of the cleavage variants of AMH, and the physiological significance of the variants is unknown. Consequently, these variants were not studied as part of this thesis.

1.6.4 Forms of AMH in the circulation

At the beginning of this thesis, the forms of AMH in the circulation had not been investigated, with the exception of a single study, which examined a single man with a sex chord tumor. This man's level of AMH was supraphysiological, enabling his AMH to be examined by western blots, without prior concentration by immunoprecipitation [147]. All of this man's AMH was cleaved, with a minority being the alternative cleavage form (Section 1.6.3). The forms of AMH in the circulation of healthy individuals were examined by the Otago AMH Neurobiology

Group at the University of Otago. The AMH in the circulation of boys, men and women was found to be a mixture of proAMH and $AMH_{N,C}$ [141]. Free AMH_C and the cleavage variants of AMH were not detected. The absence of AMH_C in the circulation is consistent with its physiochemical properties (Section 1.4.2). As a consequence of this discovery, the thesis has examined proAMH, as well as the AMH-receptor-binding forms of AMH.

ELISAs for AMH do not distinguish between proAMH and $AMH_{N,C}$ [10]. Therefore, the levels of AMH reported in Sections 1.1.3 and 1.2.4 represent an aggregate measure of proAMH and $AMH_{N,C}$, which the Otago Neurobiology Group refers to as total AMH. Different population groups have different ratios of proAMH and $AMH_{N,C}$. Boys and girls have a higher proportion of proAMH than men or women [151]. As well as differences between groups, there is also variation between individuals of the same sex and age.

1.6.5 Cleavage of proAMH

Multiple enzymes have been shown to cleave proAMH to $AMH_{N,C}$ *in vitro*, but there is currently no proof of which enzymes are physiological regulators of proAMH cleavage *in vivo*. Some of the proprotein convertases of the subtilisin/kexin-type (PCSK) cleave proAMH at 451/452, including PCSK3 (furin), PCSK5, and PCSK6 [152]. Plasmin also cleaves AMH into 57kDa N-terminal and 12.5 kDa C-terminal fragments. It can also cleave proAMH between Arg 427 and Ser 428, generating the alternatively cleaved form of AMH (Section 1.6.3) [6]. The PCSK enzymes and plasmin both cleave the pro-form of multiple cytokines. Consequently, the rate/extent

of the cleavage of proAMH may be linked to the rate/extent of other regulators, such as the proBMPs. The cleavage enzymes themselves are subject to complex regulation. Plasmin is formed by the cleavage of plasminogen, with this cleavage subject to complex interactions between activators and inhibitors [153].

Sertoli cells and granulosa cells express the enzymes that cleave proAMH *in vitro*. The level of these enzymes and their regulators vary during testicular development, the seminiferous cycle [154], ovarian development, the ovarian cycle, the stage of follicular development [155] and pregnancy [156]. The cleavage-enzymes have both intracellular and extracellular forms [157]. Consequently, proAMH is potentially cleaved by the cells that synthesize it and/or by other cell types.

When recombinant proAMH is added to organ cultures of the Müllerian duct, regression occurs [139, 142], even though proAMH is unable to activate AMHR2. This suggests that the Müllerian duct is able to activate proAMH, which creates a scenario where the bioactivity of AMH depends of the level of cleavage enzymes in the target tissues. When enzymes are present, the associated AMH receptors can be activated by both circulating proAMH and $AMH_{N,C}$. When enzymes are absent, only the $AMH_{N,C}$ will be able to activate the receptors, leading to a smaller AMH signal than in tissues that can cleave proAMH. ProAMH also appears to be cleaved within the gonads. The majority of AMH in ovarian follicular fluid is proAMH, indicating that the granulosa cells that synthesize AMH do not extensively cleave it intracellularly. However, the majority of AMH in the circulation of women is $AMH_{N,C}$. This indicates that proAMH may be cleaved as it passes from the ovarian follicles to the blood. Alternatively, proAMH may be cleaved outside of the ovary,

and then returned to the blood. The former appears to be the case for adult mice, as recombinant human $AMH_{N,C}$ ($rhAMH_{N,C}$) does not accumulate after intravenous injection of rh-proAMH (Pankhurst, personal communication).

In summary, the cleavage of proAMH appears to be part of the regulation of the bioactivity of AMH. However, there is insufficient evidence to explain in detail when and where this occurs. The potential regulation of proAMH cleavage by TGFβ BPs is discussed in Chapter 5.

1.6.6 AMH type-2 receptor

AMHR2 is thought to be specific to AMH, and conversely all AMH signaling is thought to be dependent on AMHR2 [158, 159]. This is in marked contrast to other TGFβ superfamily ligands, and lays the foundation for the presumption that AMH is unlike any other TGFβ superfamily ligand. The strongest evidence for the one-to-one relationship between AMH and AMHR2 is that $AMH^{-/-}$ and $AMHR2^{-/-}$ mice [160] and humans [158, 161] have the same overt clinical phenotype, PMDS. However, most of the actions of TGFβ superfamily ligands involve redundant signaling, with the result that the phenotype of null-mutations of ligands only reveals part of their signaling function. Other experiments are therefore needed to identify the full range of signaling of a ligand and a receptor. To date, the possibility that proAMH or $AMH_{N,C}$ can signal through other receptors outside of the Müllerian duct has not been extensively tested. Similarly, the ability of other TGFβ superfamily ligands to bind to AMHR2 has not been systematically examined.

The human AMHR2 gene is located in chromosome 12, contains 13 exons [162], and encodes a 63 kDa protein of 573 amino acids. The signal sequence, the extracellular, transmembrane and intracellular regions contain 17, 132, 21, and 403 of the 573 amino acids respectively [162]. The intracellular region contains a serine/threonine kinase domain. Rats and mice have two splicing variants of AMHR2, which partially lack either the binding site or the kinase domain [163]. The physiological function of these variants is unknown. There is a 30% overall homology between AMHR2 and the other TGFβ superfamily type-2 receptors [4, 158]. AMHR2 is phylogenetically near to BMPR2 [83], and interacts with the same type I receptors as BMPR2. This raises the possibility that AMH and BMP signaling may have some commonalities, even though the AMH and BMP ligands are only distantly related.

AMHR2 is present in the reproductive tissues of both sexes. It is expressed at very high levels in the developing testis and at lower levels in the mature testis [11]. The Leydig cells are primarily responsible for this expression [164-166]. AMHR2 is expressed in the mesenchymal cells surrounding the Müllerian ducts of both sexes [167], but AMHR2 is not expressed in the epithelium of the Müllerian duct. Consequently, the AMH-induced regression of the Müllerian duct is an indirect effect [168]. AMHR2 mRNA has also been detected in the rat prostate, human prostate cancer cells, and prostate cancer cell lines [169, 170]. In females, AMHR2 mRNA is present in the granulosa cells of the ovaries, the endometrium of the uterus, the uterine cervix and the mammary gland [11, 170-173].

AMHR2 is also expressed outside of the reproductive tracts, with levels that are high relative to other cytokine receptors [17]. This was initially overlooked, as the levels

of AMHR2 in the testis are two orders of magnitude higher than in other tissues [17]. The initial surveys of AMHR2 expression were set to detect high levels, creating the impression that all non-reproductive tissues had little or no expression of AMHR2. More recently, functional levels of AMHR2 expression has been detected in the lungs [174, 175], breast [176], endometrium [170], and in various neurons in the central nervous system [17, 22, 30]. A detailed study of AMHR2 expression has yet to be published, but preliminary data suggests that AMHR2 is expressed in many tissues [10] .

1.6.7 AMH type-1 receptors

AMH has two known type-1 receptors: ACVR1/ALK2 and BMPR1A/ALK3 [1]. ACVR1 and BMPR1A, like AMHR2, are both expressed in the mesenchyme surrounding the Müllerian duct [177]. ACVR1$^{-/-}$ [178] and BMPR1A$^{-/-}$ [179] mice exhibit embryonic lethality, and are unsuitable for analyzing AMH signaling *in vivo*. However, when either the ACVR1 or the BMPR1A gene is conditionally inactivated in cells that express AMHR2, then PMDS occurs with incomplete penetrance [1]. When both genes are inactivated in AMHR2-expressing cells, PMDS invariably occurs in male mouse embryos, indicating that ACVR1 and BMPR1A are functionally redundant in the mesenchymal cells surrounding the Müllerian duct [1]. PMDS also occurs when antisense probes are used to inactivate ACVR1, but not when BMPR1A is similarly inactivated [180].

BMPR1B/ALK6 is also a putative receptor [79]. However, BMPR1B$^{-/-}$ male mice exhibit normal regression of the Müllerian duct [181], indicating that BMPR1B is not

essential for the hallmark function of AMH. In an immature Sertoli cell line, BMPR1B inhibits AMH signaling [181]. This raises the possibility that BMPR1B is involved in negative feedback for AMH signaling. If so, then the absence of BMPR1B would not be expected to cause PMDS, as AMH signaling would be expected to be abnormally enhanced, rather than attenuated.

The human ACVR1, BMPR1A and BMPR1B proteins have a mass of 57, 60, 57 kDa, respectively [162, 182]. The genes for the human ACVR1, BMPR1A, and BMPR1B gene are, respectively, located in chromosome 2 and consists of 18 coding exons, chromosome 10 and consists of 15 coding exons, and chromosome 4 and consisting of 17 coding exons [183]. Each type-1 receptor has an extracellular domain, transmembrane domain, and serine/threonine kinase domain in the intracellular region [162]. The human ACVR1 protein consists of 509 amino acids, comprising a signal sequence (20 amino acids), extracellular (103 amino acids), transmembrane (23 amino acids) and intracellular domains (363 amino acids). The intracellular region contains a serine/threonine kinase domain. The human BMPR1A protein consists of 532 amino acids, comprising the signal sequence (23 amino acids), and extracellular (129 amino acids), transmembrane (24 amino acids) and intracellular regions (356 amino acids). Human BMPR1B protein consists of 502 amino acids, comprising a signal sequence (13 amino acids) and extracellular (113 amino acids), transmembrane (22 amino acids) and intracellular regions (354 amino acids) [162].

The AMH type-1 receptors are shared by different type-2 receptors [93] which are activated by the BMP subfamily [79, 184] (Figure1-3). For example, BMP7 binds to the complex of ACVR2B and ACVR1. BMP2, BMP4 and BMP7 bind to the

complex of BMPR2 and BMPR1A or BMPR1B. BMP4 and GFD5 bind to the complex of ACTR2B and BMPR1A or BMPR1B [79].

In males, ACVR1 is expressed in the urogenital ridges of fetal and adult murine testis, which is similar to the AMHR2 expression pattern [180, 181]. BMPR1A is expressed in mitotic spermatogonia during the first week postnatal, in the germ line compartment of the postnatal murine testis [185] and in the peri-Müllerian mesenchyme[1][177]. BMPR1B is expressed in the urogenital ridges at a very low level, and is not detectable in the fetal murine testis [180]. In adults, BMPR1B is expressed in the epithelial layer of the Müllerian duct but not in the mesenchymal layer of mice [181]. The complete removal of Müllerian duct is an essential aspect of male sexual differentiation, and it is therefore unsurprising that BMPR1B is absent in the Müllerian mesenchymal cells, as inhibition here would appear to be undesirable. Consequently, this does not exclude the possibility that BMPR1B is part of the AMH signaling pathway at other sites.

In females, ACVR1 is also expressed in the urogenital ridges of the fetal and adult murine ovary [180, 181]. BMPR1A is expressed in granulosa cells and conditional knockout of *BMPR1A* in murine granulosa cells is sub-fertile with reduced spontaneous ovulation [186]. BMPR1B is expressed in murine urogenital ridges at a very low level [180] and in the granulosa cells of the mature murine ovary [186]. However, BMPR1B is barely detectable in the fetal murine ovary [180]. In adult mice, BMPR1B is only expressed in the oocytes of small antral follicles and in the granulosa cells of large antral follicles [180, 187]. Disruption of BMPR1B in mice generates infertility [187]. This indicates that the expression pattern of BMPR1B and

AMHR2 are not identical in the ovary. In addition, AMH Type-1 receptors generally show a less follicle-stage-specific expression pattern than AMHR2. These observations are consistent with the type-1 receptors having roles in BMP signaling in rodents [188] as well as roles as receptors for AMH signaling.

1.7 Is AMH signaling regulated by binding proteins?

AMH, like other members of the TGFβ superfamily, is a pleiotropic regulator, but this only recently been recognized. The exploration of AMH signaling has been based almost solely on the presumption that AMH only signals through one simple mechanism, which is exemplified by the regression of the Müllerian duct. The TGFβ superfamily ligands share receptors and BPs, leading to context dependent signaling. AMH is the only ligand for AMHR2 but AMH shares type 1 receptors with other TGFβs. It is therefore conceivable that AMH may also share BPs with other TGFβ superfamily members. The concentration of AMH in the circulation of adults is low compared to that of boys, which in turn appears to be low relative to the concentrations within the gonads. Despite this, the AMH in the circulation appears to have function. This suggests that the regulation of AMH signaling may be more complex than has previously been thought. This complexity may be explained if BPs modulate and integrate the activities of AMH, either by regulating its ability to bind to the AMH receptors and/or by controlling the cleavage of proAMH into the AMH-receptor competent form, $AMH_{N,C}$. This aim of this thesis was therefore to undertake the first test of whether the bioactivity of AMH can be affected by any of the known TGFβ-superfamily BPs.

Chapter 2: Materials and Methods

2.1 Luciferase reporter assay

2.1.1 Maintenance of the cell lines

The human epithelial prostate cancer cell lines, DU145 and LNCaP (American Type Culture Collection), were incubated in T75 flasks filled with Roswell Park Memorial Institute (RPMI) medium 1640 (Gibco) supplemented with 2 mM L-glutamine, 10 mM HEPES, 1 mM sodium pyruvate (Sigma), 25 mM glucose (Sigma), 17.85 mM sodium bicarbonate (Sigma) and 10% fetal calf serum (FCS, Invitrogen) at 37 ºC in a 5% CO_2, water-jacketed incubator (Forma scientific, model 3111). The FCS was derived from females, unless otherwise stated.

When the cells reached 80 to 90% confluency, they were washed with Hank's Balanced Salt Solution (HBSS, Invitrogen) then incubated at 37 °C for 5 minutes in a solution containing 0.05% trypsin-EDTA (Life Sciences). The cells were spun at 2,000 *g* for 5 minutes and the pellet re-suspended in 1 ml of fresh media supplemented with 10% FCS. One third of the cell suspension was then plated in a new 75 ml flask containing 10 ml of RPMI supplemented as described in the paragraph above (unless otherwise stated). The remaining cells was mixed with 15% dimethyl sulfoxide to prevent the formation of ice crystals during the freezing process, and 0.5 ml aliquots were stored at -80 °C for subsequent culturing.

The P19 murine embryonic carcinoma cell line (American Type Culture Collection) was maintained in Eagle's Minimum Essential Medium-alpha (MEM-α, Sigma) instead of RPMI, but was otherwise maintained as described above.

2.1.2 Transfection of cells

2.1.2.1 Transfection vectors

The transfection vectors were prepared by Dr. Suneeth Mathew (Otago Neurobiology Group). In one of the transfection vectors ((BRE)2-Luc), a firefly luciferase gene is driven by a BMP responsive element (BRE), which enables the activation of the AMH signaling cascade to be measured (Chapter 3.1.1). This vector was kindly donated by Dr. Peter ten Dijke (The Netherlands Cancer Institute) [189] and amplified in ultra-competent *E-coli* DH5α cells by Dr. Suneeth Mathew. The CMV-Amhr2 plasmid contains *AMHR2* gene has been previously described [163]. The phRL-SV40 vector contains a *Renilla reniformis* luciferase under the control of the SV40 promoter, and was kindly donated by Prof. Warren Tate. pcDNA3.1(+) (Invitrogen) was used as a control vector [163] in experiments examining whether the presence or absence of CMV-Amhr2 influenced BMP signaling.

2.1.2.2 Transient transfection

This process began when the cells reached 80% confluency. The transfection medium was prepared before the cells were harvested. First, FuGENE6 (Roche) transfection reagent was diluted in serum-free MEM-α according to the manufacturer's instructions. Three µl of FuGENE6 was added for each µg of transfection vector DNA, with the volume of medium relating to the number of wells. The transfection vectors were diluted in milliQ-H_2O, and added to the mixture of FuGENE6 and medium. The final amount was 20 ng of AMHR2, 20 ng of (BRE)2-luc and 0.2 ng of phRL-SV40 per well, unless otherwise indicated. pcDNA was used as control vector, when needed. This mixture was then incubated for between 30 minutes and 1 hour at room temperature, whilst the cells were harvested.

The cells were trypsinized as previously described (Section 2.1.1). The concentration of cells was determined with a hemocytometer. The cells were then diluted with medium to obtain a final plating density of 10,000 cells per well on a 96-well plate, unless otherwise indicated. The medium contained 10% female FCS, unless otherwise stated. The diluted cells were then mixed with the vector, FuGENE6 and medium solution. One hundred µl to the final mixture of cells and reagents was then

added per well, using a 96-well plate. Un-transfected cells were used as controls in some experiments.

2.1.3 Incubation of the transfected cells with ligands and binding proteins

2.1.3.1 Forms of AMH

The early methods for purification of AMH used diethylaminoethyl ion exchange, dye-affinity or immunoaffinity chromatography from the testes [6]. More recently, studies have used recombinant AMH preparations from various sources, including bacteria, tobacco and Chinese hamster ovary cells [6]. One unresolved issue with these preparations is whether the post-translational modification of AMH is normal when a human gene is transferred to another species. For this reason, the recombinant AMH used in this project was predominantly from a human cell line (next paragraph). Whilst this is superior to other alternatives, it is not perfect because the cells used are not a physiological source of AMH, and may therefore process AMH differently to granulosa and Sertoli cells.

Recombinant hAMH was produced by PX' Therapeutics (Grenoble, France), under contract to the University of Otago. This rhAMH was produced from HEK293 cells, which is a cell-line derived from human embryonic kidney. These cells were transfected with an rh-proAMH vector. The HEK293 cells predominantly secreted uncleaved proAMH, but with low level of $AMH_{N,C}$ [141]. When $AMH_{N,C}$ was required, the rh-proAMH was cleaved by furin, as described in Section 2.4.1

In some experiments, AMH_C was used. The AMH_C used in these experiments was derived from transfected *E Coli*, and was purchased from R&D systems (Table 2-1).

Table 2-1. Binding proteins and ligands catalog numbers

Protein	Catalog number	Species
Betaglycan	242-R3	Human
Brorin	6147-FW	Human
Chordin	758-CN	Mouse
Chordin-like1	1808-NR	Human
Chordin-like 2	2520-CH	Human
DAN	755-DA	Mouse
Decorin	143-DE	Human
Endoglin	1097-EN	Human
FS288	5386-FS	Human
FS315	4889-FN	Human
FS-like1	1694-FN	Human
FS-like3 (FLRG)	1288-F3	Human
FS-like 4	4890-FN	Human
Noggin	6057-NG	Human
α2-macroglobulin	1938-PI	Human
AMH_C	1737-MS	Human
BMP2	355-BM	Human
BMP4	314-BP	Human
Activin A	338-AC	Human

2.1.3.2 TGFβs and binding proteins

The BPs and TGFβ-superfamily ligands were purchased from R&D systems. The catalogue numbers are listed in Table 2-1. These BPs and ligands were reconstitutes according to manufacturer's instructions and then stored at -80 °C. The aliquots were made to prevent repeated freeze thaws. These aliquots can be stored for 12 months at -80 °C.

2.1.3.3 Preparation of solutions containing ligands and binding proteins

The AMH, TGFβ-superfamily ligands and BPs to be added to cultured cells were diluted in medium, immediately prior to their addition to the cells. When combinations of ligands and/or BPs were added to the same well, they were mixed in medium and incubated together for 5 minutes at 37 °C in a storage plate, before addition to the culture medium.

2.1.3.4 Stimulation of P19 cells with ligands and BPs

One hundred µl of solution with the transfected cells were plated for 24 hours before the ligands and BPs were added, unless otherwise stated. When 96-well plates were used, 50 µl of the culture medium was removed from each well. Sixty µl of the solution containing the ligands and BPs was immediately added to each well. The plate was then gently swirled to mix the added and existing media, after which the plate was incubated for 24 hours incubation at 37 °C.

$AMH_{N,C}$ contains furin. The effect of furin on the reporter assay was tested by comparing the activity of four nM of AMH_C, in the presence and absence of 0.02 IU/µl of furin buffer (Chapter 3.2.1.5).

2.1.4 Luciferase enzyme assay

The medium was removed and rinsed with 200 µl per well of HBSS. The remaining medium and HBSS was removed, followed by adding 20 µl per well of passive lysis buffer (Promega). A tilter shaker shook the plate for 1 hour, with the wells being scratched with pipette tips to disrupt cells after 30 minutes of this incubation. The cell lysates were then assayed immediately, or frozen at -80 °C for subsequent assay, which was typically undertaken on the next day. Once the procedures were established (Chapter 4ff), the samples were routinely frozen before assay, to ensure consistency between experiments. After thawing, the lysates were triturated with a pipette to re-suspend them.

The luciferase activity was measured using the Dual-Luciferase® reporter assay system (Promega), according to the manufacturer's instructions. 10 µl aliquots of the samples were loaded on a 96-well plate and incubated for 2 seconds with 50 µl of the firefly luciferase buffer and the firefly luminescence measured for 10 seconds using a Victor X3 2030 (Perkin Elmer) plate reader. The reaction was then quenched by adding 50 µl of the *Renilla reniformis* luciferase buffer for 2 seconds followed by a 10 seconds *Renilla* luminescence measurement with shaking. This enzymatic activity is temperature-dependent. Thus, the measurement was undertaken at 23-24 °C to minimize the variability of the measurement.

Experiments included controls wells that had not been transfected with the (BRE)2-Luc vector, or any other vector. These were used to estimate the zero-value for the luciferase assays.

2.1.5 Calculations and statistics

2.1.5.1 Normalisation

The absolute intensity of the fluorescence in a well in a reporter assay is determined by the extent of the activation of the reporter (the desired variation) plus numerous unavoidable influences. The latter includes small well-to-well and day-to-day variation in the number of cells, small day-to-day variation in the transfection efficiency, variation in room temperature, and the concentrations (and age) of the chemicals used to generate the fluorescence. The procedures required to produce informative reporter assays are well understood, with broad agreement. Firefly luciferase assays were initially unreliable due to variation in cell number, with this being overcome by co-transfection with a vector that causes constitutive expression of a second luciferase (Renilla). The two forms of luciferase can be independently measured and the ratio of the firefly to renilla luciferase activities provides a measure of the activation of the target reporter that is insensitive of cell number, and most of the variables that lead to day-to-day variation in the absolute level of firefly luciferase activity in the assay. This technique is known as the dual-luciferase reporter assay [189].

The level of reporter activity in the AMH reporter assay varies with the concentration of AMH and with the level of AMHR2 expression ([163] and Chapter 3). These two variables are independent of each other. The abundance of AMHR2 molecules determines the maximum activation of the intracellular cascade, but theoretically (and by observation) the dose-response curve is determined by the binding constants between AMH and AMHR2. Ideally, the level of AMHR2 should not vary from day to day. However, for technical reasons it was necessary to transiently transfect the P19 cells with AMHR2 (Chapter 3), for each batch of each experiment. Each experiment included wells with a high concentration of AMH (BP experiments) or BMP (AMH-BMP interaction experiments), which had been experimentally shown to maximally activate the reporter system. This value was defined as 100% activation in each experiment, with the no AMH wells being defined as 0% activation. All other values were linearly scaled. The zero and 100% values were defined from the control wells that lacked BPs. Consequently, any BP that increased the top value will yield values greater than 100%, whereas BP that suppressed basal reporter activity would yield negative values. This normalization thus does not mathematically bound the assay to values between 0 and 1.

The zero-value for the firefly and *Renilla reniformis* luciferase assays were subtracted for the observed values, before the ratio of the firefly to *Renilla* activities calculated for each well.

2.1.5.2 Number of data points included in each dose-response curve

The sigmoidal shape of a dose-response curve requires more data points to definite than a straight line. The Departmental statistical adviser, Mr Andrew Gray, was asked to undertake a power calculation. He recommended 50 points per curve. In this thesis, most experiments used 60 points for each dose-response curve, for the reasons outlined below. This number is very large compared to the norms of biomedical experiments.

The design of a dose-response curve needs to balance opposing influences, with there being no consensus on how to do this. From a purely statistical standpoint, the ideal design is 60 different doses (concentrations) with no replicate. Here each point is

imprecise, but the estimation of the curve parameters has maximum precision. However, this is rarely done in biomedical science, as the generation of a large number of dose can introduce experimental error leading to a false positive that has high statistical certainty.

The data from the reporter assay was initially variable, and the first part of the thesis involved an investigation of the source of this variation (Chapter 3). The purpose of this was to increase the signal-to-noise ratio of the assay. Equally, the purpose was to develop an understanding of what the sources of variation in the assay were. This enabled the experiments to be designed in a manner that minimized the risk of false positive and false negatives.

The reporter assays is sensitive to the speed of processing various steps. Practice and the use of devices such as multi-pipettes increased signal-to-noise. However, in the absence of robotic processing of the experiment, there was a practical necessity to minimize the size of individual experiments. This involved collection of data in three batches. This is a common issue with experimental design: for example, with genetically-modified mice, it is often necessary to examine mice from different litters on different days, as there are insufficient mice with the appropriate genotype in a single litter.

The collection of data in three batches was also undertaken for a separate reason. False positives can arise through minor procedural issues: For example, the addition of a BP to a well will dilute the AMH in the well. An exactly equal volume of control must be added. If the setting on the multi-pipette moved (or was incorrectly set) when adding the BP or control solution, then a small systematic difference would be created. Similarly, if the concentration of the BP were in error, then this would not be detected if the experiment were completed as a single batch. Each BP was prepared three times, as the experiment was done in three batches – consequently, the experiment would detect if a significant error was made in preparing a BP (or other critical components).

It is common to make measurements in triplicates. When the values of the three data points that make up a triplicate are not in close agreement, then the measurement is

suspect and should be repeated. Similarly, when a dose-response curve is generated in three batches, then any significant differences between the batches would indicate a possible problem, requiring the experiment to be repeated.

2.1.5.3 Calculation of EC50, top and bottom values of dose-response curves

A dose-response curve was calculated using the "sigmoidal dose-response (variable slope)" function of Prism (6.0, GraphPad Software Inc), with the outputs including estimates of the EC50, top and bottom values for the curve, along with the standard errors for each of the estimated parameters. When two curves were being compared, for example AMH plus and minus a BP, the data was log transformed by Prism and the two curves compared using the "log (agonist) vs. response - variable slope (four parameters)", with statistical assessment of the HillSlope, logEC50, top and bottom values being obtained. All results with a p value of < 0.05 are recorded.

2.1.5.4 Statistical comparison of mean values

The mean values of groups were compared using one-way or two-way ANOVA, with the p-values being corrected for multiple tests using Bonferroni's method, when appropriate. The statistical calculations were undertaken using Prism and SPSS Statistics (IBM Corporation), here and elsewhere in the thesis. All results with a p-value of < 0.05 are recorded.

2.1.6 Method Development

The initial results contained high variation within and between experiments. This variation was reduced as outlined below.

2.1.6.1 Solution for technical variation

The assay was initially undertaken using 24-well plates, which involved inefficient use of cells and other reagents. The assay proved to be sufficiently sensitive for the procedure to be downscale to 96-well plates, with all experiments using P19 cells

involving 96-well plates. The addition of reagents to wells, one well at a time, introduced variation due to pipetting and degraded the assay by extending the time cells were outside of the incubator. The use of 96-well plates enabled multi-pipettes to be used, with the reagents being pipetted from storage plates (Section 2.1.3.3). This strategy greatly reduced experimental variation.

2.1.6.2 Efficiencies relating to the maintenance of cells

P19 cells are smaller than DU145 or LNCaP cells. At the beginning of the growth, they mainly grew as a monolayer. However, when the cells were close to confluency, they started to grow as aggregation clusters. This made it difficult to count the number of cells, as the clusters were not readily separated by trypsin. This also introduced the risk of generating cells with diverse characteristics, as there is variation in the environment within and outside of clusters. Therefore, the cell confluency was carefully checked to avoid the cell clusters. If clustering occurred, the clustered cells were discarded.

The entire medium was initially changed after 24 hours incubation, which stressed the cells. Only part of the medium was therefore changed, typically 50% (Section 2. 1.3.3).

The wells on the edge of the 96-well plates have a different environment to other wells, which can affect the rate of evaporation of the medium and the availability of CO_2. The outside wells were therefore not used, and were filled with HBSS or medium to produce a constant environment.

The characteristics of cell lines can change over time, with this being unavoidable. The use of trypsin to split cell cultures is necessary, but this also damages cells. When cells were needed for experiments, the flasks were seeded at a high density to provide cells for experiments. In between experiments, the flasks were seeded at a lower density to minimize the number of passages. Cells were also frozen, to enable cultures to be re-established from low passage cells. If the appearance or growth characteristics of cells changed, then cultures were terminated and the stocks re-established from frozen cells.

The dimethyl sulfoxide used during the cryopreservation is toxic to cells, and freeze-thaw procedures can introduce variation. Cells were grown from at least one passage after freezing before being used in experiments. Any flasks with atypical cells were not used.

Similar experiments were undertaken in batches in as tight a timeframe as possible, to ensure that each part of the thesis program was internally consistent.

2.1.6.3. Optimizing the lysis step

The incubation time for cell lysate was optimized, which involved increasing it from 15 minutes to 1 hour, and adding a mixing and scratching procedure 30 minutes after homogenization the cells (Section 2.1.4). A routine freeze-thaw step was introduced, with a re-suspension step (Section 2.1.4).

2.2 Detection of TGFβ-superfamily receptors

The expression of the TGFβ-superfamily receptors by DU145, LNCaP and P19 cells were examined by PCR. Quantitative analysis of the level of expression in P19 cells was also undertaken using real-time PCR.

2.2.1 RNA extraction

Medium in the T75 flask was removed and 1 ml of TRI reagent (Sigma-Aldrich) added to the cells and pipetted several times to form a homogenous lysate. After 5 minutes, 0.2 ml of chloroform was added to the lysates, which were shaken for 15 seconds and then stood for 2 minutes at room temperature. After centrifugation at 14,500 g for 15 minutes at 4 °C, the aqueous phase was transferred to a fresh tube and 0.5 ml of 2-propanol was added and mixed. The samples were stored at -20 °C overnight, and then centrifuged at 12,000 g for 10 minutes at 4 °C. The supernatants were removed and the RNA pellets washed by adding a minimum of 1 ml of 75% ethanol. Each sample was vortexed and then centrifuged at 7,500 g for 5 minutes at 4 °C. The samples were placed in a 65 °C heating block to dry. Fifty µl of

autoclaved Diethylpyrocarbonate-treated water was added to each sample, and the samples heated for 5 minutes at 65 °C, after which they were vortexed and stored at -20 °C.

2.2.2 DNase treatment of RNA

The RNA samples were incubated for 30 minutes with TURBO DNase in TURBO DNase buffer (TURBO DNA-free kit, Ambion) to remove genomic DNA contamination. The reaction was stopped by the addition of DNase inactivation reagent. After incubation for 2 minutes, the samples were centrifuged at 10,000 g for 1.5 minutes. The supernatant was collected, and the concentration of RNA in it measured.

2.2.3 Measurement of RNA concentration

Measurements of RNA concentration were undertaken using the NanoDrop spectrophotometer (Thermo Scientific). The spectrophotometer was initialized and blanked using 2 µl of distilled water, after which 2 µl of each sample was analyzed. The quality of the RNA samples was confirmed by loading them onto 1.5% agarose (Invitrogen) gels containing 0.5 µg/ml of ethidium bromide and run at 100 volts for 60 minutes for visualization with a UV transilluminator (Biometra, TI1).

2.2.4 cDNA synthesis

The DNase-treated RNA was converted to cDNA (complementary DNA) using the SuperScript VILO cDNA synthesis kit (Invitrogen). 1 µg of RNA was mixed with 4 µl of the VILO reaction mix and 2 µl of the Superscript enzyme mix. The synthesis was achieved using the protocol described in Table 2-2. The concentration of the resulting cDNA was estimating using a NanoDrop spectrophotometer. Samples with no reverse transcriptase control (RT^-) were made as controls.

Table 2-2. cDNA synthesis condition

Step	Temperature (°C)	Duration (min)
1	25	10
2	42	60
3	85	5

2.2.5 PCR reactions

PCR (polymerase chain reaction) was performed in a thermal cycler (MJ research) in a 20 µl reaction mixture containing cDNA, 5 µM of the primers (Table 2-3), 10 mM of dNTPs (Invitrogen), 0.05 U/µl of Taq DNA polymerase, 10X Taq reaction buffer containing 2 mM of $MgCl_2$ (New England Biolabs), 0.1 mM cresol red and 10% sucrose (Univar). Equal amounts of cDNA were loaded for each sample, with β-actin used as a loading control. The PCR was performed in a thermal cycler (MJ research) following the cycle conditions described in Table 2-4. The primers sequences are listed in Table 2-3. The samples, along with the controls, were then loaded onto 1.7% agarose (Invitrogen) gels containing 0.5 µg/ml of ethidium bromide and run at 100 volts for 30 minutes for visualization with a UV transilluminator (Biometra, TI1). No template controls (water) and RT^- controls were included in each experiment.

The gels were photographed with an RGB digital camera. The image was converted to grayscale in Photoshop CS6 (Adobe Systems Integrated), and then inverted to generate a black on white image. The images were not otherwise manipulated. Irrelevant bands have been cropped from some figures.

Table 2-3. Primers used for PCR

Gene Detected	Mouse Primer	Sequence	Product size(bp)
ACVR2A	ActR2A-F	5’-AGCAAGGGGAAGATTTGGTT-3’	178
	ActR2A-R	5’-GGTGCCTCTTTTCTCTGCAC-3’	
BMPR2	BMPR2-F	5’-AGGATCAGGTGAAAAGATCAAGAGA-3’	165
	BMPR2-R	5’-GCAAGGTACACAGCAGTGCTAGATT-3’	
AMHR2	AMHR2-F	5’-GCTCCAGAGCTCTTGGACAA-3’	89
	AMHR2-R	5’-AGTAGTAGCGCCAGAGAGTAAA-3’	
ACVR1	ALK2-F	5’-GATCAACAGAGGCCAAACATACCTA-3’	274
	ALK2-R	5’-AGATGGATTCTGTTCTGACAACCA-3’	
BMPR1A	ALK3-F	5’-GTCTATTCCAGGGCAGATTTCCTA-3’	160
	ALK3-R	5’-CCTGCTTAACATCTGACGCAAGT-3’	
BMPR1B	ALK6-F	5’-ATACCAGCTTCCCTATCACGACCT-3’	277
	ALK6-R	5’-TGAAATTCTTGCTCTGTCCACAAGTA-3’	
ACVR2B	ActR2B-F	5’-CAGGGACTTCAAAAGCAAGAATGT-3’	189
	ActR2B-R	5’-AGGAAGGCGTCTCTCTGGAAGTT-3’	
GAPDH	GAPDH-F	5’-CTTCATTGACCTCAACTA-3’	300
	GAPDH-R	5’-TTCACACCCATCACAAAC-3’	
β-actin	beta actin-F	5’-TCGTCGACAACGGCTCCGGCATGT-3’	520
	beta actin-R	5’-CCAGCCAGGTCCAGACGCAGGAT-3’	

Gene Detected	Human Primer	Sequence	Product size(bp)
ACVR2A	ActR2A-F	5’-CAGTGCAGAGTGGGCAAGTTAACA-3’	222
	ActR2A-R	5’-AAGCATTCCTTACGCGGAGATCTG-3’	
BMPR2	BMPR2-F	5’-GATGTTCTTGCACAGGGTGTTCCA-3’	239
	BMPR2-R	5’-TGACTTCACAGTCCAGAGATTCAG-3’	
AMHR2	AMHR2-F	5’-AGGCCTGACAGCAGTCCACCA-3’	255
	AMHR2-R	5’-TTGAGGATGGGCCAAGGCAGC-3’	
ACVR1	ALK2-F	5’-AAACCAGCCATTGCCCATCG-3’	283
	ALK2-R	5’-TACCATTGCTCACCATCCGC-3’	
BMPR1A	ALK3-F	5’-TGGGCAAATGGCGTGGCGA-3’	280
	ALK3-R	5’-TGTGCAGGTGGCACAGACCAC-3’	
BMPR1B	ALK6-F	5’-GCAGCACAGACGGATATTGT-3’	630
	ALK6-R	5’-TTTCATGCCTCATCAACACT-3’	
ACVR2B	ActR2B-F	5’-CTCCCTCAGGGATTACCTCA-3’	428
	ActR2B-R	5’-AGGGCAGCATGTACTCATCC-3’	
β-actin	beta actin-F	5’-TCACCCACACTGTGCCCATCT-3’	295
	beta actin-R	5’-CAGCGGAACCGCTCATTGCCA-3’	

Table 2-4. PCR cycle conditions

DU145, LNCap

β-actin

Step	Number of cycles	Temperature (°C)	Duration
Initial denaturation	1	95	2 mins
denaturation	35	95	15 secs
Annealing	35	70	15 secs
Extention	35	72	30 secs
Final extension	1	72	3 mins

AMHR2

Step	Number of cycles	Temperature (°C)	Duration
Initial denaturation	1	95	2 mins
denaturation	35	95	15 secs
Annealing	35	60	60 secs
Extention	1	72	3mins

ACVR1, BMPR1A

Step	Number of cycles	Temperature (°C)	Duration
Initial denaturation	1	95	2 mins
denaturation	35	95	15 secs
Annealing	35	65	15 secs
Extention	35	72	30 secs
Final extension	1	72	3 mins

ACVR2A, BMPR2

Step	Number of cycles	Temperature (°C)	Duration
Initial denaturation	1	95	2 mins
denaturation	35	95	15 secs
Annealing	35	62	15 secs
Extention	35	72	30 secs
Final extension	1	72	3 mins

BMPR1B

Step	Number of cycles	Temperature (°C)	Duration
Initial denaturation	1	95	2 mins
denaturation	35	95	15 secs
Annealing	35	60	15 secs
Extention	35	72	45 secs
Final extension	1	72	3 mins

ACVR2B

Step	Number of cycles	Temperature (°C)	Duration
Initial denaturation	1	95	2 mins
denaturation	35	94	20 secs
Annealing	35	60	30 secs
Extention	35	72	45 secs
Final extension	1	72	10 mins

P19 cells

all genes above

Step	Number of cycles	Temperature (°C)	Duration
Initial denaturation	1	95	2 mins
denaturation	35	95	20 secs
Annealing	35	60	20 secs
Extention	35	72	30 secs
Final extension	1	72	5 mins

2.2.6 Quantitative PCR reactions

The quantitative PCRs were performed using SYBER Green Master Mix (Applied Biosystems) and the gene-specific primers used for PCR (Table 2-3). A 3-step PCR procedure was carried out using the protocol described in Table 2-5. The efficiency of each primer set was known from previous in-house use of the primers, and varied between 1.8 and 1.9. The relative copy number of each gene was calculated by reference to a standard curve with known levels of cDNA for each gene.

Table 2-5. qPCR cycle condition

Number of cycles	Temperature (°C)	Duration
1	95	15 min
45	95	20 sec
45	60	20 sec
45	72	30 sec
1	95	5 sec
1	65	1 min

2.3 Do binding proteins interfere with an AMH ELISA?

2.3.1 Preparation of the samples

The binding of $AMH_{N,C}$ and each of 6 BPs (chordin, chordin-like1, endoglin, FS288, FS315, FLRG) were assayed using the AMH gen II enzyme-linked immunosorbent assay kit (ELISA (Beckman Coulter, A79765, analytical sensitivity 0.08 ng/ml)). Thirty five µl of 29 pM of $rhAMH_{N,C}$ (Section 2.1.3.1) and 35 µl 20 nM BPs were mixed and incubated for 30 minutes at 37 °C. The concentration of AMH selected is in the middle of the standard curve, and corresponds to the AMH value of a typical young adult. The BPs were added at large molar excess (greater than 500 times) to ensure that even a weak effect of the BP was detected. The BPs selected were those that affected the AMH dose-response curve in Chapter 4. Twenty µl of this premix were pipetted to the ELISA plate and incubated for 30 minutes on an orbital shaker.

2.3.2 ELISA protocol

The ELISA was undertaken according to the manufacturer's protocol, with the assistance of Ms. N. Batchelor for the detection steps. Standards were prepared in a pre-incubation plate (25 µl standard plus 125 µl assay buffer) and mixed and incubated on orbital shaker at room temperature for 1 hour. A hundred twenty µl standards were pipetted to the wells. A hundred µl of assay buffer were pipetted to the samples. The wells were incubated, shaking at 300 rpm on an orbital microplate shaker, for 1 hour at room temperature. Each well was aspirated and washed five times with washing solution, using an automatic microplate washer (ThermoScientific). The plate was then inverted onto absorbent material; to remove residual washing solution and 100 µl of the antibody-biotin conjugate solution added to each well. The plates were incubated for 1 hour at room temperature, on an orbital microplate shaker at 300 rpm. Each well was aspirated and washed five times with wash solution using an automatic microplate washer. Residual wash solution was removed by inversion, as described above, and 100 µl of the TMB chromogen solution added to each well. The wells were incubated, shaking at 300 rpm on an orbital microplate shaker for 10.5 minutes at room temperature. The plates were

covered with a black box to avoid exposure to sunlight. A hundred µl of the stopping solution was added to each well and the absorbance of the solution was read in the well within 30 minutes using a microplate reader set to 450 nm. The intra-assay CV for this ELISA in the Otago Neurobiology Laboratory has been previously described [190, 191]. [190, 191[Pankhurst, 2015 #2078].

Samples were measured in triplicate. Standard curves were generated using a quadratic curve, as recommended by Beckman Coulter.

2.4 Assessment of AMH cleavage with binding proteins

2.4.1 Furin treatment of AMH

Recombinant human AMH (PX'Therapeutics) at 10 mM was reacted with 8 units of furin (New England Biolabs) in 40 µl of reaction buffer consisting of 100 mM HEPES, pH 7.4, 2.4 mM Ca^{2+}, 140 mM Na^{+}, 4 mM K^{+} (Cl^{-}). The reaction was allowed to progress for 24 hours at 37 °C and was then stopped by freezing the sample at -20 °C.

2.4.2 Optimizing the incubation time and the concentration of proAMH

Two1.2 nM rhAMH and one 6 nM solutions were reacted with 8 units of furin (New England Biolabs) in 11.25 µl of reaction buffer consisting of 100 mM MES, pH 7.5, 0.3mM Ca^{2+}, 12 mM Na^{+}, and 107 mM K^{+} for 4 hours or 8 hours at 37 °C. In order to stop the reaction, Laemmli buffer was added and the samples were heated to 95 °C for 5 minutes.

2.4.3 Preparation of binding protein samples

BPs were diluted with 0.05% v/v Tween-20 to become either 133 nM (Brorin, chordin-like1, decorin, noggin, FS-like1, FLRG, FS288, DAN, chordin-like2) or 66 nM (chordin, betaglycan, endoglin, FS-like 4, α2-macroglobulin). The final concentration of these proteins in the following preparation was either 10 nM or 20 nM, respectively.

2.4.4 Furin cleavage with binding proteins

An aliquot of the rh-proAMH was used in the following experiments (2.1.3.1). Each of 14 BPs were added to the rhAMH (PX'Therapeutics) at 10 mM and each BP preparation was reacted with 8 units of furin (New England Biolabs) in 40 µl of reaction buffer consisting of 100 mM HEPES, pH 7.4, 2.4 mM Ca2+, 140 mM Na+, 4 mM K+. The reaction was allowed to progress for 4 hours at 37°C. In order to stop the reaction, Laemmli buffer was added and the samples were heated to 95 °C for 5 minutes. Two control aliquots of rhAMH were incubated in the same treatment with or without the addition of furin to the reaction buffer.

2.4.5 Electrophoresis and Western blotting

SDS-PAGE was run using 10% Tris-glycine bisacrylamide gels with a 4% stacking gel using the Xcell Surelock Mini-Cell system (Invitrogen) at 100 volts for 2 hours. Proteins were transferred to a 0.4-µm nitrocellulose membrane (Whatman) at 30 volts for 1 hour. Blotting membranes were blocked with Odyssey blocking reagent (Licor) for 30 minutes, probed with 0.1–0.2 mg/mL polyclonal goat anti-human MIS/AMH propeptide antibody (AF2748; R&D Systems), visualized with IRDye680 donkey anti-goat IgG antibody (Licor) applied at 0.66 mg/mL and scanned on an Odyssey infrared scanner (Licor).

2.4.6 Image quantification

The proportion of proAMH to $AMH_{N,C}$ was measured using densitometry. The density of the faint bands in the Western blots was quantified without image manipulation, using Image J software (NIH, http://rsbweb.nih.gov/ij/).

Chapter 3: Establishment of an AMH reporter assay

3.1 Introduction

One of the main objectives of this thesis was to examine if BPs can enhance or inhibit the ability of AMH to activate AMHR2. The focus is limited to interactions between BPs and either AMH or the extracellular portions of AMH receptors. Indirect interactions involving intracellular cascades were not examined. The first step in this investigation was to develop a reporter assay for the activation of AMH receptors. The assay development makes use of the commonality of TGFβ-superfamily signaling pathways. The relationship between AMH and BMP signaling is therefore outlined below, after which the assay is described.

3.1.1 AMH signaling cascade

AMH has a unique type-2 receptor, but it shares type-1 receptors with the BMPs (Chapter 1.6.1). Consequently, the SMAD intracellular signaling pathway for AMH is shared with the BMP ligands. The SMAD 1/5/8 pathway mediates the hallmark function of AMH. SMAD 1 and SMAD 8 are both expressed robustly in the mesenchymal cells of the Müllerian duct, while SMAD 5 is expressed at a lower level [181]. When Smad 1, 5 and/or 8 are conditionally knocked out in AMHR2-expressing cells, the male mice exhibit PMDS, with variable penetrance. When all three genes (Smad 1, 5, 8) are deleted, then all male mice exhibit PMDS. However, when only 1 or 2 of Smad 1, 5 or 8 are deleted, the male mice exhibit either partial or no regression of the Müllerian ducts. Therefore, there is functional redundancy between the three Smads for AMH signaling, with all three needed for full function [1]. Similarly, when AMH is added to Sertoli or Leydig cell derived cell lines, SMAD 1 is phosphorylated and accumulates in the nucleus, after binding to the co-SMAD 4 [192].

3.1.2 Luciferase reporter gene assay

3.1.2.1 Design of the assay

BMP signaling can be measured by a BMP reporter assay *in vitro*, without interference from other cytokines such as TGFβ1, bFGF and VEGF [189]. The assay uses a (BRE)2-Luc vector [163], which contains a firefly luciferase reporter gene under the control of a BMP responsive element BRE promoter (Figure 3-1). When BMP is added to the reporter cells, the SMAD 1/5/8 pathway is activated. After translocation to the nucleus, the activated SMAD 1/5/8 binds to the (BRE)2-Luc vector, leading to transcription and translation of the firefly luciferase gene. The cells can then be lysed and the luciferase activity assayed by detecting the intensity of the light emitted when luciferase substrates are added. This value correlates with the amount of reporter gene expression induced by BMP ligand binding. Any variation in the transfection efficiency with the (BRE)2-Luc vector can affect the sensitivity of the assay. This can be negated by co-transfecting the cells with a vector containing Renilla *reniformis* luciferase under the control of a constitutive SV40 promoter, and reporting the results as the ratio of the firefly and Renilla *reniformis* luciferase activities. This also controls for the number of cells in a well.

AMH shares the type-1 receptors and the intracellular signaling cascade with BMP (Chapter 3.1.1). Consequently, AMH signaling can be measured using the (BRE)2-Luc reporter assay, provided the cells express AMHR2 [163, 193] (Figure 3-1). At the start of the thesis, a basic AMH assay was available in the laboratory, but this assay was insufficiently sensitive to use as a screen for the influence of BPs on AMH signaling. The first step was therefore to optimize the assay, by varying the cell type, the amount of serum, and factors such as the length of incubation in AMH after transfection.

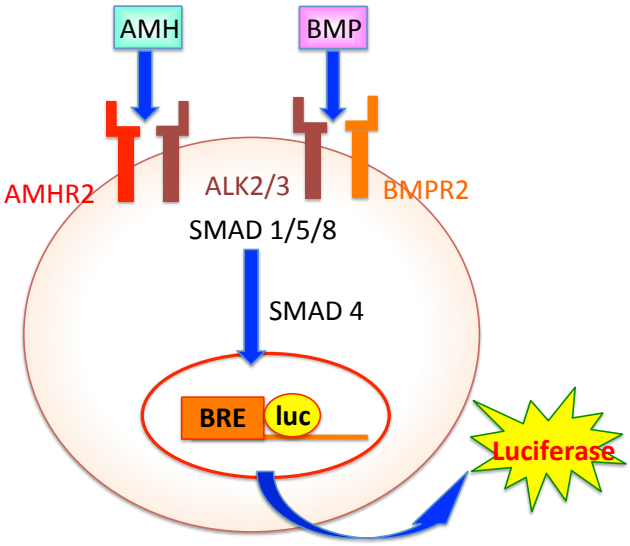

Figure 3-1. Luciferase reporter assay

AMH and BMP share the same type-1 receptors and the following intracellular signaling cascade by SMAD 1/5/8. The (BRE)2-Luc vector contains the firefly luciferase coding region under the control of the BRE promoter. The luciferase level from transfected cells with this vector can be majored as amount of gene expression by the AMH and BMP ligand binding.

3.1.2.2 Selection of cell line

Several cell lines were investigated as vehicles for the reporter assay. The ideal cell line should express the AMH receptors, have a robust intracellular response to AMH, be easy to maintain and proliferate rapidly. They should also preferably have limited expression of BMPR2, to minimize any interference from BMPs produced by the cell line. At the start of the thesis, the description of AMHR2 in cell types was very incomplete, and only a few cell lines were known to respond to AMH, most notably the prostate cancer cell lines DU145 [169] and LNCaP [169, 193]. These cell lines have previously been used for AMH assays [169, 193]. Both cell lines are old, and have been widely distributed. This can lead to the accumulation of mutations and divergence between cell lines located in different laboratories. Therefore, the assessment of these cell lines included measurement of the expression of TGFβ-superfamily receptors, as well as monitoring of their growth characteristics.

DU145 and LNCaP are both human cell lines, with the proliferation of DU145 cells being testosterone-independent and LNCaP cells being testosterone-dependent [169]. Neither DU145 nor LNCaP cells had the required characteristics, leading to the testing of P19 cells. P19 cells are a murine embryonic carcinoma, which are known to respond to BMP and activin [194]. The P19 cells have limited expression of AMHR2 and consequently their use in an AMH reporter assay required transfection with AMHR2 [195].

3.1.2.3 Selection of culture medium

Serum promotes the growth of most cell lines, and assists in their recovery after transfection. However, AMH is a hormone and the addition of serum may therefore interfere with an AMH reporter assay, due to the presence of either AMH or some other TGFβ-superfamily member, particularly BMPs. The alternative is to use a defined medium, but defined media have added growth factors, with the identity of the factors being a commercial secret. Consequently, the influence of serum on the growth of cells and the sensitivity of the reporter assay was closely monitored. Female fetuses lack significant levels of AMH, and female FCS hypothetically is superior to other serum for an AMH assay. However, at the start of the thesis, female FCS was not available in New Zealand. A source of female FCS was obtained towards the end of the first year, and was tested within the assay.

3.1.3 Aims of Chapter 3

In summary, the purpose of the work described in this Chapter was to produce an AMH reporter assay that (1) had a high signal to background ratio, (2) could be used to screen multiple BPs over an extended period, with (3) results that were reproducible from week-to-week. This work forms the basis for the majority of the subsequent experiments described in Chapter 4.

3.2 Results

3.2.1 Selecting a cell line

DU145 and LNCaP cell lines were established at the University of Otago, and the initial phase of development of the assay was restricted to these two cell lines.

3.2.1.1 Expression of TGFβ-superfamily receptors

Each of the type-1 AMH receptors, ACVR1 (Figure 3-2A), BMPR1A (Figure 3-2B), and BMPR1B (Figure 3-2C) were detected in the DU145 and LNCaP samples. The ACVR1 and BMPR1A bands were much stronger than the BMPR1B in both the DU145 and LNCaP samples. The LNCaP sample showed weaker bands than the DU145 sample for all the type-1 receptors. No bands were observed in the H_2O and RT^- negative controls and the β-actin band was of similar strength in the DU145 and LNCaP samples (Figure 3-2D).

A strong AMHR2 band was detected in both the DU145 and the LNCaP cells (Figure 3-3A). Likewise, a strong BMPR2 band and moderate ACVR2A and ACVR2B bands were detected in the DU145 sample (Figure 3-3B, C). These receptors were also present in the LNCaP sample, although the BMPR2 and ACVR2A bands were of lower intensity, with the ACVR2A band being close to the level of detection (Figure 3-3B, C). No bands were observed in the H_2O and RT^- negative controls.

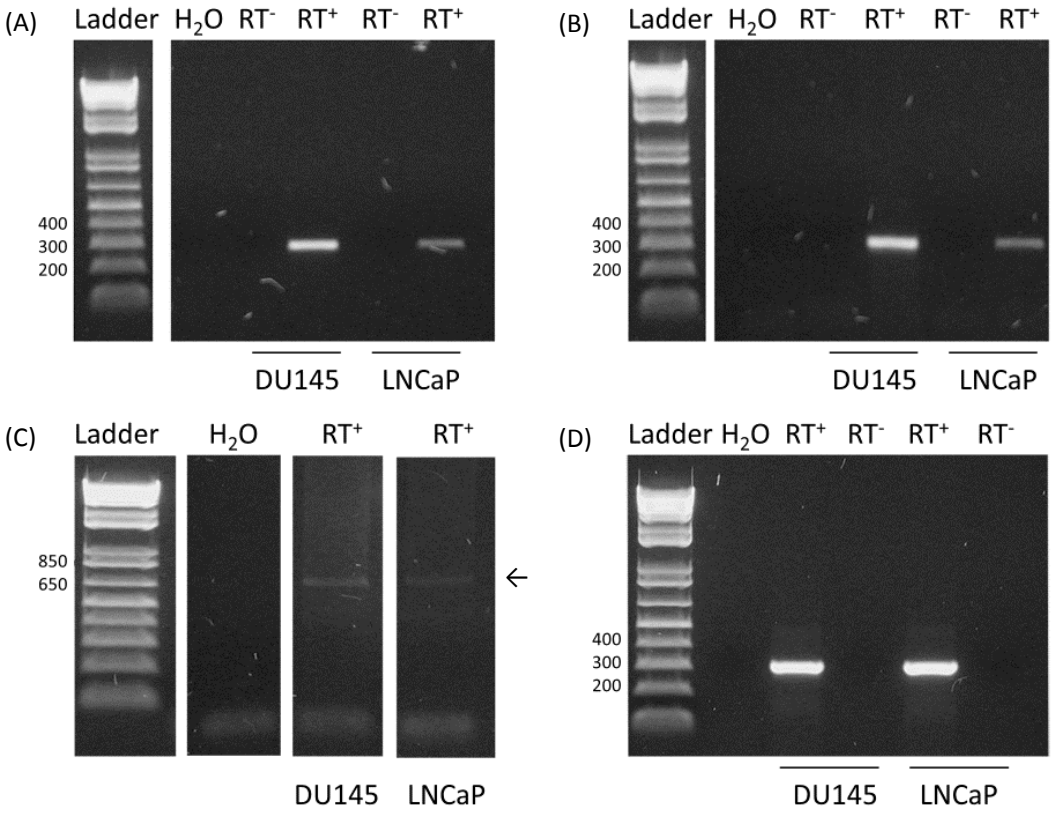

Figure 3-2. Expression of AMH type-1 receptors

cDNA was prepared from DU145 and LNCaP cells and gene specific primers were used for PCR as described in Chapter 2.2.5. (A) ACVR1, (B) BMPR1A, (C) BMPR1B, (D) β-actin. H_2O and RT^- were used as negative controls. (C) The lane orders were swapped to provide consistency.

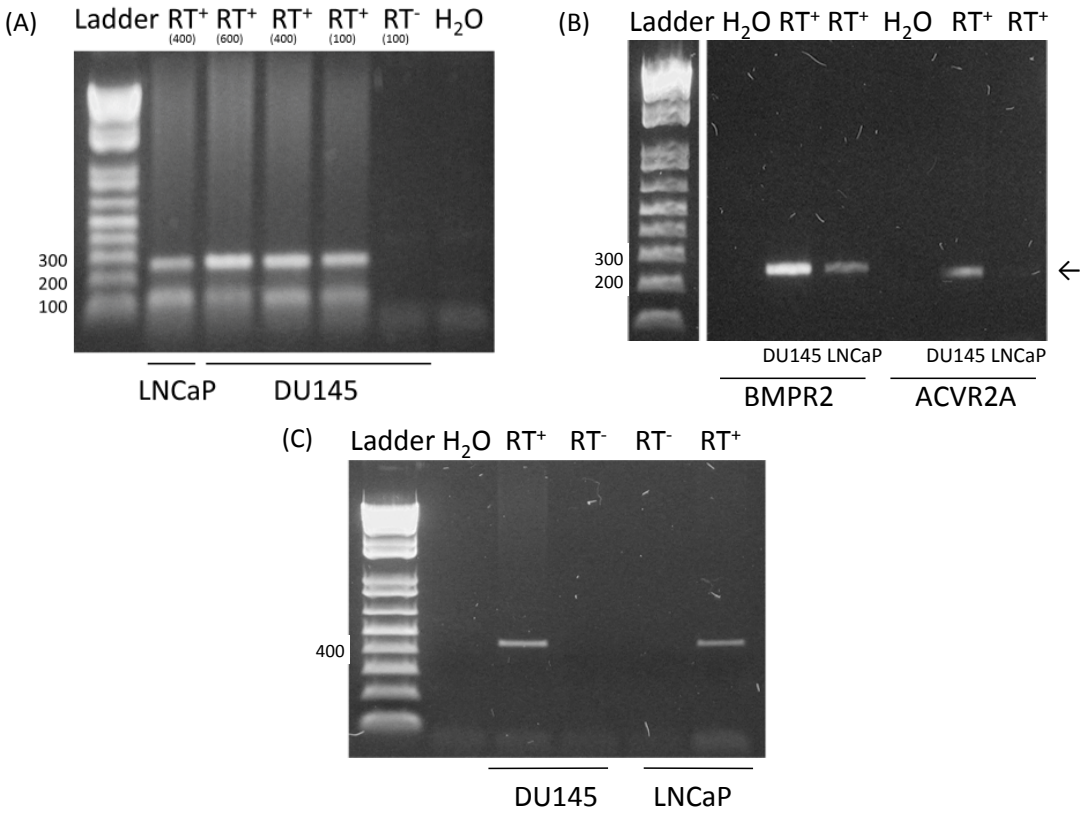

Figure 3-3. Expression of TGFβ type-2 receptors

cDNA was prepared from DU145 and LNCaP cells and gene specific primers were used for PCR as described in Chapter 2.2.5. (A) AMHR2 (cDNA amount used are shown (ng/µl)), (B) BMPR2 and ACVR2A, (C) ACVR2B. H_2O and RT^- were used as negative controls.

3.2.1.2 Growth of cell lines

The LNCaP cells grew more slowly than the DU145 cells, and typically took 1 to 2 days longer for 24-well-cultures to be ready to use. The growth of cells was even more prolonged in flasks. The LNCaP cells also tended to aggregate rather than grow as a monolayer. This made it difficult to accurately count the cells, separate the cells for re-plating and lyse the cells at the end of the experiment. Aggregation also creates a non-uniform environment, as the surface and middle of the cluster have different

cell-to-cell and cell-to-medium interactions. Lastly, the LNCaP cells died within 48 hours after transfection without dihydrotestosterone (data not shown).

3.2.1.3 Establishment of the assay

Transfection stresses cells. Therefore, the first experiments tested whether endogenous expression of AMHR2 in the DU145 cells was sufficient to produce a viable reporter assay. AMH_C was added to DU145 cells that had been transfected with the (BRE)2-Luc reporter. No dose-response curve was observed (Figure 3-4). Several possible explanations for this observation were tested.

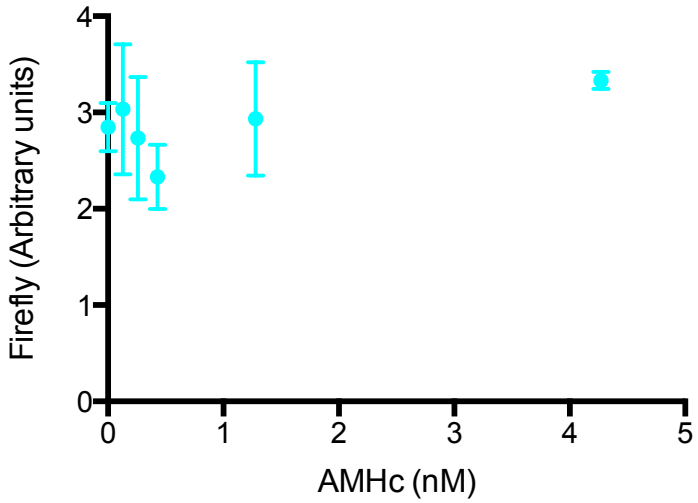

Figure 3-4. Dose response curve to AMH_C

DU145 cells were transfected with (BRE)2-Luc (0.2 µg/100,000 cells) and plated at a density of 50,000 cells per well. They were then incubated with culture media supplemented with female 10% FCS for 24 hours. They were then incubated with various concentration of AMH_C for 24 hours. Each dot represents the mean ± the standard error of the mean of 3 wells.

First, the culture contained 10% FCS, which may have sufficient AMH to saturate the reporter. However, the background response was similar when FCS and female FCS

were used. Furthermore, no significant response to AMH_C was observed when female FCS was used (Figure 3-5).

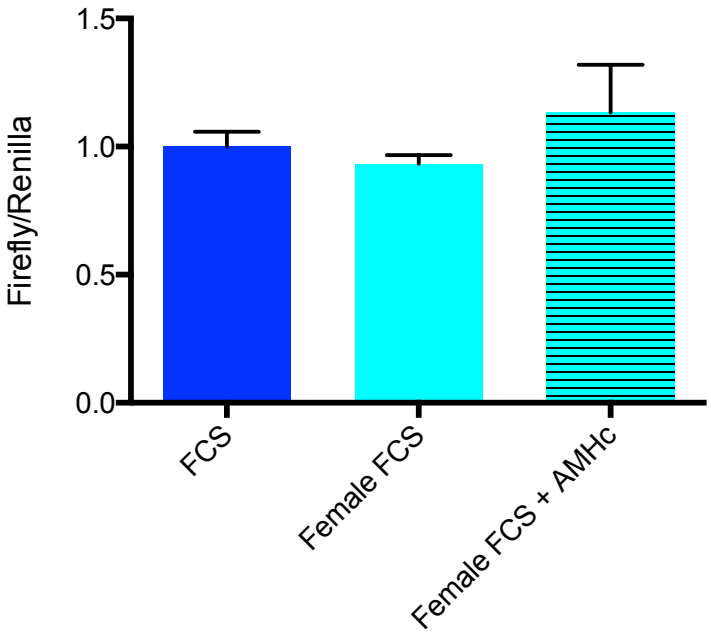

Figure 3-5. Female FCS did not affect the reporter assay

DU145 cells were transfected with (BRE)2-Luc (0.2 µg/100,000 cells) and phRL-SV40 (0.2 µg/100,000) and plated at a density of 50,000 cells per well. They were then incubated in culture media supplemented with 10% FCS, 10% Female FCS, or Female FCS containing 4.3 nM AMH_C for 48 hours. The ratio of the firefly luciferase to *Renilla reniformis* luciferase was calculated and normalized to the ratio obtained after transfection. The bars represent the mean plus the standard error of the mean of 3 wells. Neither female FCS nor AMH_C were significantly different to FCS, $p > 0.05$, one-way ANOVA.

Second, the (BRE)2-Luc reporter and luciferase assay were tested. The DU145 cells express BMPR2, enabling the reporter to be tested by the addition of BMP2. BMP2 significantly increased reporter activity (left panel Figure 3-6), indicating that the reporter construct and luciferase assay were working. AMH_C did not induce reporter activity in the same assay, suggesting either that the AMH was inactive or that the

level of AMHR2 may have been insufficient. When DU145 cells were transfected with AMHR2, AMH_C produced as much reporter activity as BMP2 (right panel, Figure 3-6). This verified that the AMH_C was active. However, the background level of reporter activity was increased in the transfected cells, with this observation being replicated by repeating the experiment. Hence, the signal-to-noise of the assay was low. The higher background in the AMHR2 transfected cells was observed with both FCS and female FCS (Figure 3-7). In Figure 3-7, the cells with female FCS had a higher reporter activity, but this was not significantly different and was not a replicable result (see Figure 3-5).

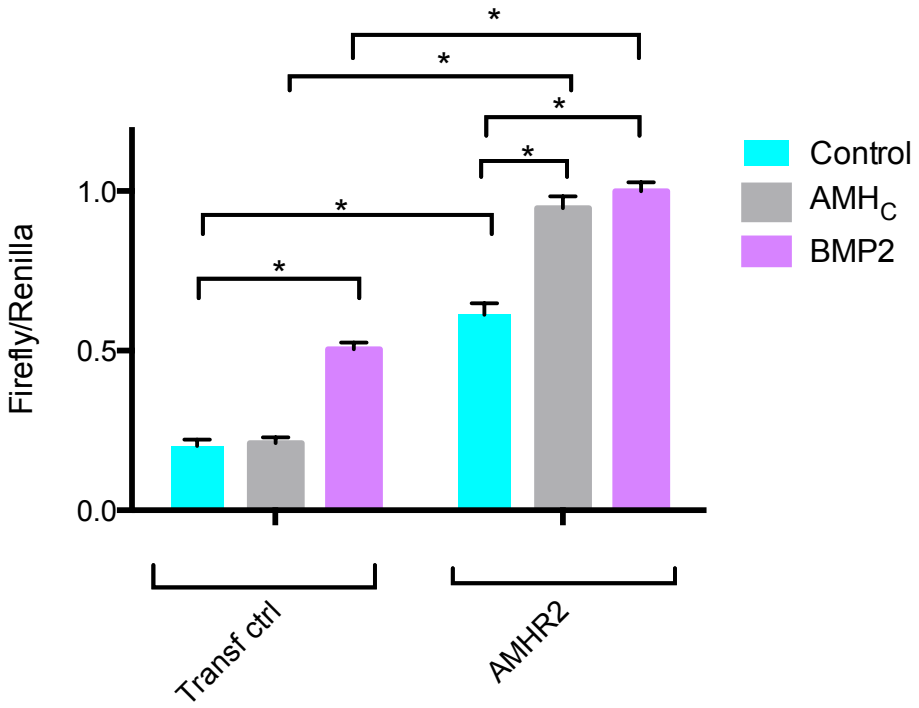

Figure 3-6. DU145 cells transfected with AMHR2 respond to AMH$_C$

DU145 cells were transfected with or without AMHR2 (0.2 ug/100,000 cells) along with (BRE)2-Luc (0.2 ug/100,000 cells) and phRL-SV40 (0.002 ug/100,000 cells), and plated at a density of 100,000 cells per well. The cells were then incubated in culture media supplemented with 10% female FCS for 24 hours. Half the culture medium was removed and mixed with AMH$_C$, BMP2 or no additional factor, and the returned to the cells for 24 hours. The final concentration of AMH and BMP2 was 4.3 nM and 7.7 nM, respectively. The ratio of the firefly luciferase to *Renilla reniformis* luciferase was calculated and normalized to the ratio obtained after transfection. The data is the combined results from 2 replicate experiments, with a total of 7 wells per group. The bars represent the mean + the standard error of the mean. The * indicate the groups were significantly different from each other, 2-way ANOVA with an adjusted p value of $p < 0.0001$.

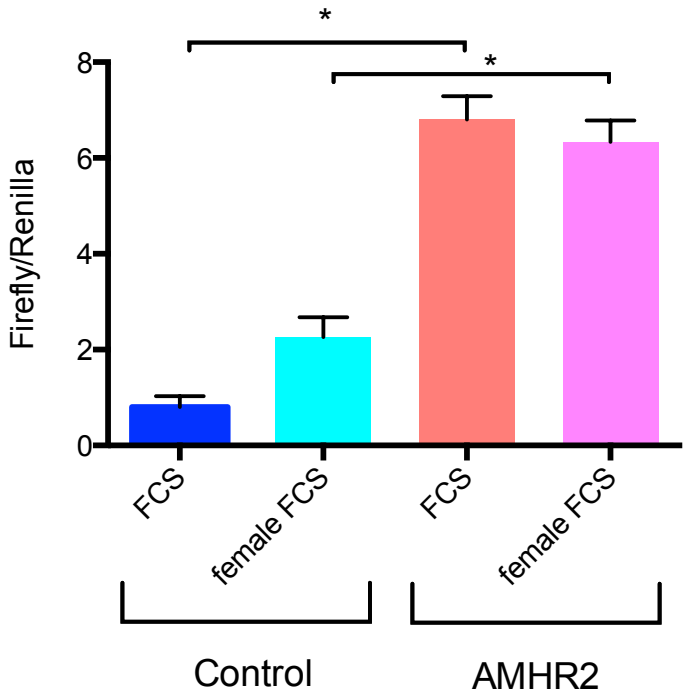

Figure 3-7. AMHR2 transfected cells had a high background

DU145 cells were plated and pre-incubated in culture media supplemented with either 10 % FCS or female FCS for 6 days. The cells were then transfected with or without AMHR2 (0.2 ug/100,000 cells), (BRE)2-Luc (0.2 ug/100,000 cells) and phRL-SV40 (0.002 ug/100,000 cells), and plated at a density of 100,000 cells/well. The cells were incubated in culture media supplemented with 10% FCS or female FCS and incubated for 48 hours. The ratio of the firefly luciferase to *Renilla reniformis* luciferase was calculated and normalized to the ratio obtained after transfection. The bars represent the mean + the standard error of the mean of 3 wells. The groups were significantly different by 2-way ANOVA, with an adjusted p value of $p < 0.0001$. When specific groups were compared by Tukey's multiple comparisons test, the control and AMHR2 treated groups were significantly different ($p < 0.001$) for FCS and for female-FCS. The two control groups ($p < 0.083$) and the two AMHR2 groups were not significantly different from each other.

The length of incubation after transfection and the length of incubation after addition of AMH were varied. Some variation was observed in these experiments, but the best results were obtained with 24 hours for each incubation step (not illustrated). These time periods were used in subsequent experiments, unless indicated otherwise.

At this stage of the assay development, variation from experiment to experiment was a problem, as was the failure of some experiments to yield results. Several key issues were identified. One, the DU145 cells exhibited variable spontaneous differentiation. Two, the LNCaP cells grew slowly and variably. Three, the assay had low sensitivity, and minor variations in procedure were sufficient to invalidate an experiment. For these reasons, work on the DU145 and LNCaP cells was terminated, and development proceeded with a cell line known to have vigorous growth (P19).

3.2.1.4 Expression of TGFβ-superfamily receptors by P19 cells

The expression of TGFβ-superfamily receptors by P19 cells was examined, to assess their suitability for use in an AMH reporter assay. No AMHR2 band was detected in the P19 cells (Figure 3-8). The P19 sample was of good quality, as clear non-degraded rRNA bands were observed (not illustrated) and as a strong β-actin band was detected (Figure 3-9A). The primers for mouse AMHR2 were verified using cDNA from the testes as a positive control. A weak single AMHR2 band of appropriate size was detected in the testes sample. The three AMH type-1 and their co-type-2 receptors: ACVR1 (Figure 3-9B), BMPR1A (Figure 3-9C), BMPR1B (Figure 3-9D), BMPR2 (Figure 3-10A), ACVR2A (Figure 3-10B) and ACVR2B (Figure 3-10C) were also detected in P19 samples. When examined by qPCR (Table 3-1), the level of AMHR2 was not abundant before transfection. Transfection increased the level of AMHR2, but its abundance remained lower than for the other type-2 receptors. The mRNA type-1 receptors were less abundant than the type-2 receptors, with BMPR1A being the most abundant and no significant levels of BMPR1B being detected (Table 3-1).

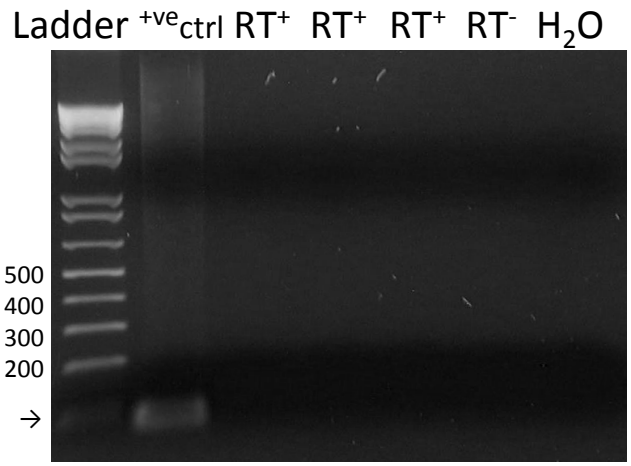

Figure 3-8. Expression of AMHR2 by P19 cells

AMHR2 cDNA was prepared from P19 cells and gene specific primers were used for PCR as described in Chapter 2.2.5. cDNA from mouse testis was used as positive control. H_2O and RT- were used as negative controls. The band size is 89 bp.

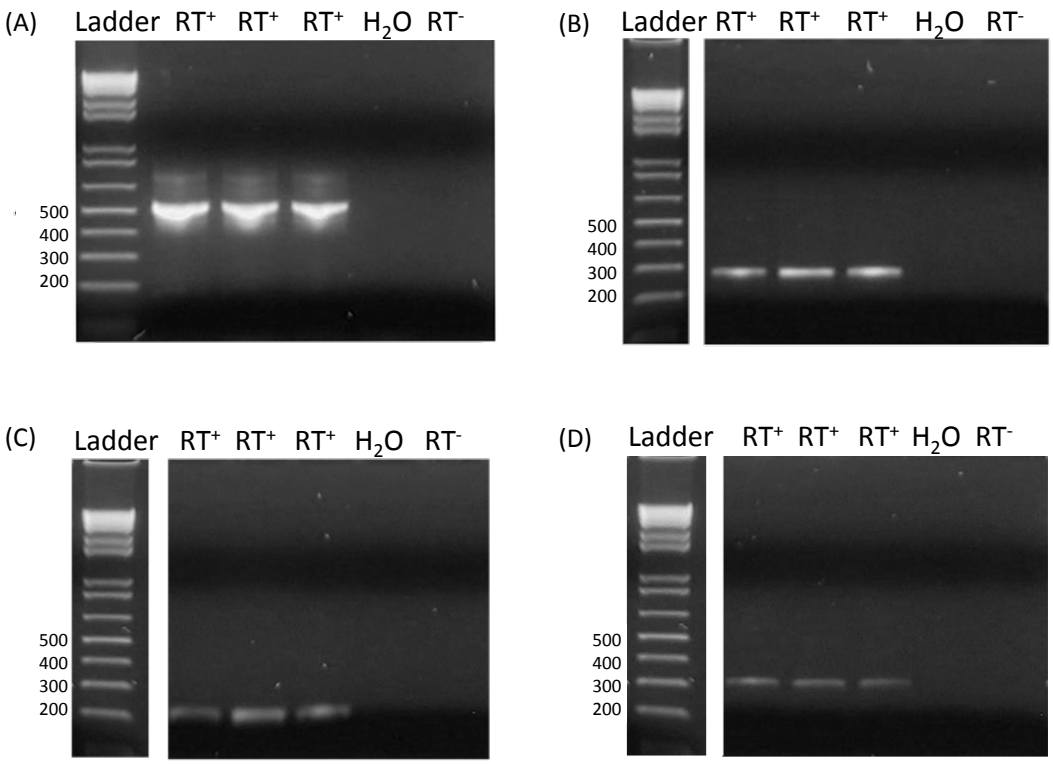

Figure 3-9. Expression of AMH receptors by P19 cells

cDNA was prepared from P19 cells and gene specific primers were used for PCR as described in Chapter 2.2.5. (A) β-actin, (B) ACVR1, (C) BMPR1A, (D) BMPR1B. H_2O and RT- were used as negative controls.

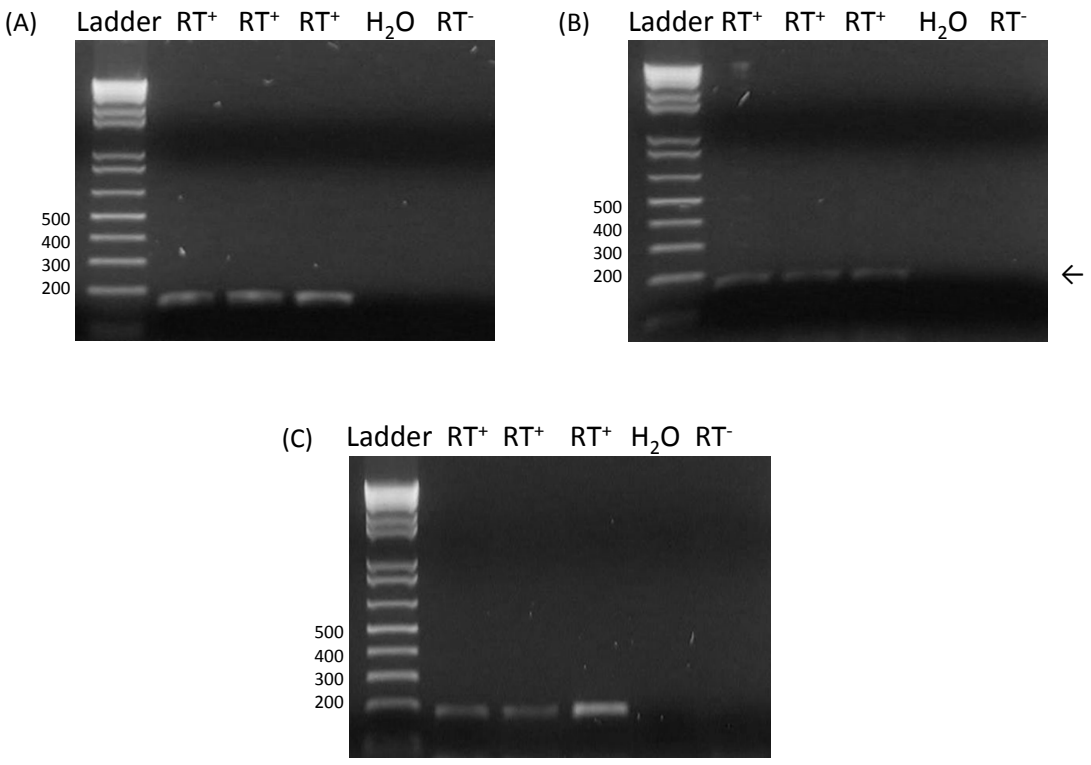

Figure 3-10. Expression of TGFβ type-2 receptors by P19 cells

cDNA was prepared from P19 cells and gene specific primers were used for PCR as described in Chapter 2.2.5. (A) BMPR2, (B) ACVR2A, (C) ACVR2B. H_2O and RT^- were used as negative controls.

Table 3-1. mRNA abundance of P19 cells

Receptor	mRNA abundance in P19 cells
AMHR2	9 ± 0.1
BMPR2	100 ± 0.1
ACVR2A	115 ± 1.7
ACVR2B	136 ± 1.3
hAMHR2 (transfected)	32 ± 3.2
ACVR1	13 ± 1.5
BMPR1A	44 ± 1.6
BMPR1B	0 ± 0.1

The data is the mean ± standard error of the mean of 3 flasks. The copy number for each mRNA species was calculated and is expressed as % of BMPR2 copy number.

3.2.1.5 Do P19-AMHR2 cells respond to AMH?

When AMHR2 non-transfected P19 cells were used, the background reporter activity was similar in FCS and female FCS, and no response to 4.3 nM AMH_C was observed (Figure 3-11). When P19 cells were transfected with AMHR2, the background reporter activity was not significantly increased (Figure 3-12). These observations indicate that the background reporter activity is unlikely to be due to AMH in the medium.

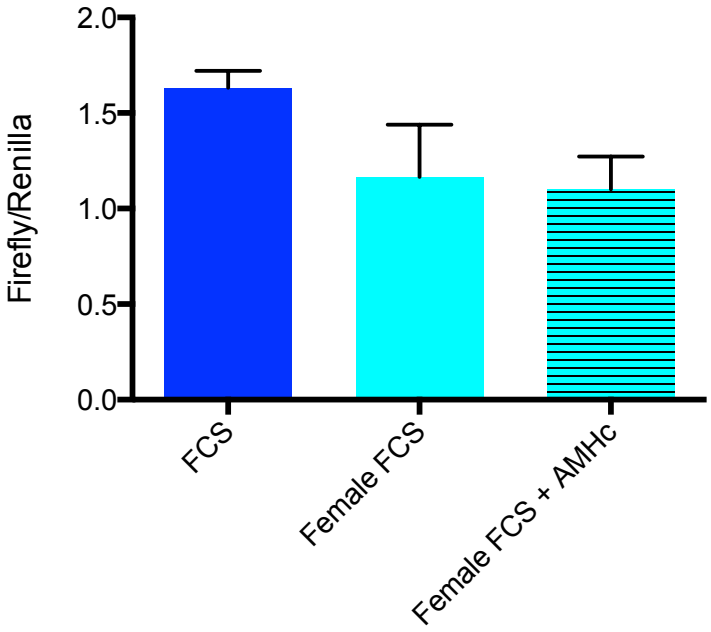

Figure 3-11. AMHR2 non-transfected P19 cells did not respond to AMH_C

P19 cells were transfected with (BRE)2-Luc (0.2 ug/100,000 cells) along with phRL-SV40 (0.02 ug/100,000 cells) and plated at a density of 50,000 cells per well. The cells were incubated in culture media supplemented with 10% FCS, 10% Female FCS, or Female FCS containing 4.3 nM AMH_C for 48 hours. The ratio of the firefly luciferase to *Renilla reniformis* luciferase was calculated and normalized to the ratio obtained after transfection. The bars represent the mean + the standard error of the mean of 3 wells. Neither female FCS nor AMH_C were significant different to FCS, $p > 0.05$, one-way ANOVA.

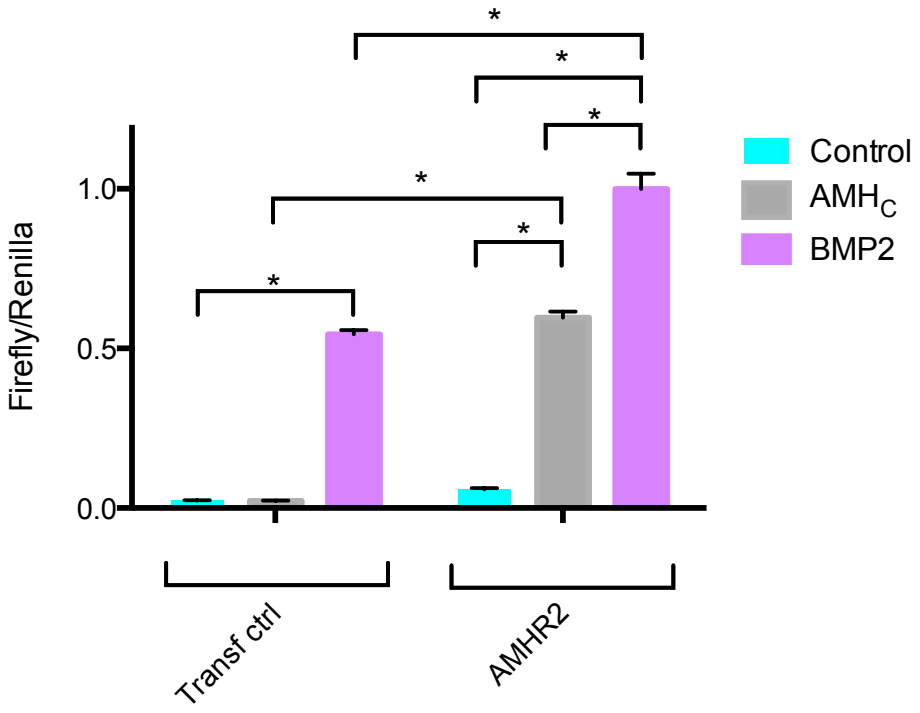

Figure 3-12. Transfection of AMHR2 changes the signal to noise with AMH_C

P19 cells were transfected with or without AMHR2 (0.2 ug/100,000 cells), along with (BRE)2-Luc (0.2 ug/100,000 cells) and phRL-SV40 (0.002 ug/100,000 cells), and plated at a density of 100,000 cells per well. The cells were incubated in culture media supplemented with 10 % female FCS for 24 hours. Half the culture medium was removed and mixed with AMH_C, BMP2 or no additional factor, and the returned to the cells for 24 hours. The final concentration of AMH_C and BMP2 was 4.3 nM and 7.7 nM, respectively. The ratio of the firefly luciferase to *Renilla reniformis* luciferase was calculated and normalized to the ratio obtained after transfection. The data is the combined results from 2 replicate experiments, with a total of 6 wells per group. The bars represent the mean + the standard error of the mean. The * indicate the groups were significantly different from each other, 2-way ANOVA with an adjusted p value of $p < 0.0001$.

When 4.3 nM AMH_C was added to the P19 cells transfected with AMHR2, strong reporter signal was detected. The AMH_C-induced signal was 10 times larger than the background signal, which is markedly different to the small AMH effect observed when DU145 cells were used (Figure 3-6). Importantly, similar results were obtained when this and subsequent experiments were repeated. The effect of AMH_C on the AMHR2 transfected cells varied with the AMH_C concentration, in the expected manner. The reporter activity increased most rapidly when the AMH_C concentration increased from 0 to 0.2 nM, with further increases in AMH_C resulting in lower rises in reporter output. The effect of AMH appeared to be maximal at around 1.0 nM (Figure 3-13).

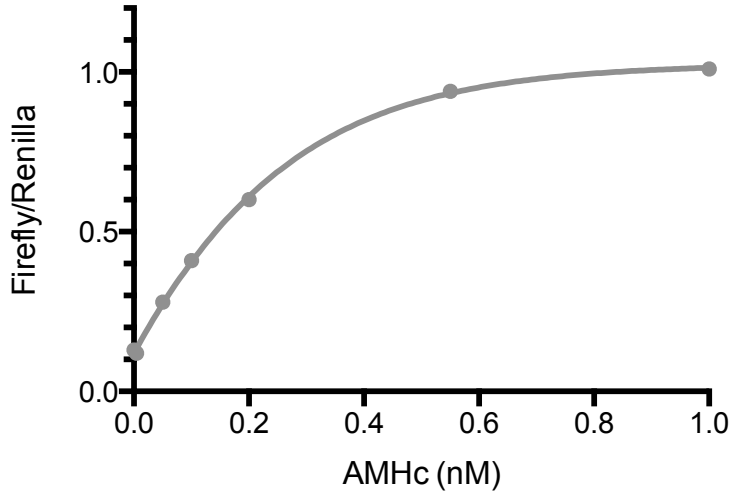

Figure 3-13. AMH_C is dose-responsive in transfected P19 cells

P19 cells were transfected with AMHR2 (0.2 ug/100,000 cells), along with (BRE)2-Luc (0.2 ug/100,000 cells) and phRL-SV40 (0.002 ug/100,000 cells), and plated at a density of 50,000 cells per well. The cells were incubated with culture media supplemented with female 10% FCS for 24 hours. They were then exposed to various concentrations of AMH_C for 24 hours. The ratio of the firefly luciferase to *Renilla reniformis* luciferase was calculated and normalized to the ratio obtained after transfection. The data is a total of 3 wells per group. A dose-response curve was fitted using the "sigmoidal dose-response (variable slope)" function of Prism

The method was established using AMH_C, which is the ligand-binding portion of AMH. However, the physiologically active form of AMH appears to be $AMH_{N,C}$. The Otago AMH Neurobiology Group's supply of $AMH_{N,C}$ is generated by cleavage of proAMH with furin, which will therefore be present in experiments using $AMH_{N,C}$. The potential influence of furin on the reporter assay was determined by whether furin decreases the response produced by AMH_C. No effect of furin was observed (Figure 3-14).

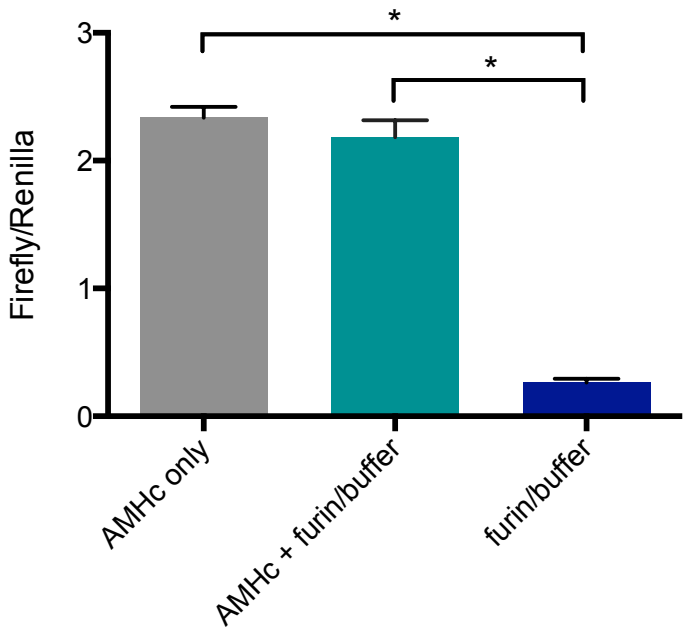

Figure 3-14. Furin does not affect the reporter assay

P19 cells were transfected with AMHR2, along with (BRE)2-Luc and phRL-SV40, and incubated with culture media supplemented with female 10% FCS for 24 hours. They were then incubated in 4 nM AMH_C with 0.02 IU/µl of furin buffer or with 0.02 IU/µl of furin buffer. The ratio of the firefly luciferase to *Renilla reniformis* luciferase was calculated and normalized to the ratio obtained after transfection. The mean of 3 wells for each data point is plotted. The furin-treated group was not significantly different to the control, 1-way ANOVA $p > 0.05$.

The level of reporter activity after the addition of $AMH_{N,C}$ had a clear dose response curve (Figure 3-15). There was a large difference between the maximum response

and the background (zero-added AMH). The maximum reporter activity induced by AMH was similar for both $AMH_{N,C}$ and AMH_C. In this experiment, $AMH_{N,C}$ was more potent than AMH_C. This observation was replicated. However, the response to AMH_C had an atypically shaped dose-response curve compared to previous and subsequent experiments, suggesting that it arose from a technical issue relating to one aliquot of AMH_C (see also Discussion).

(A)

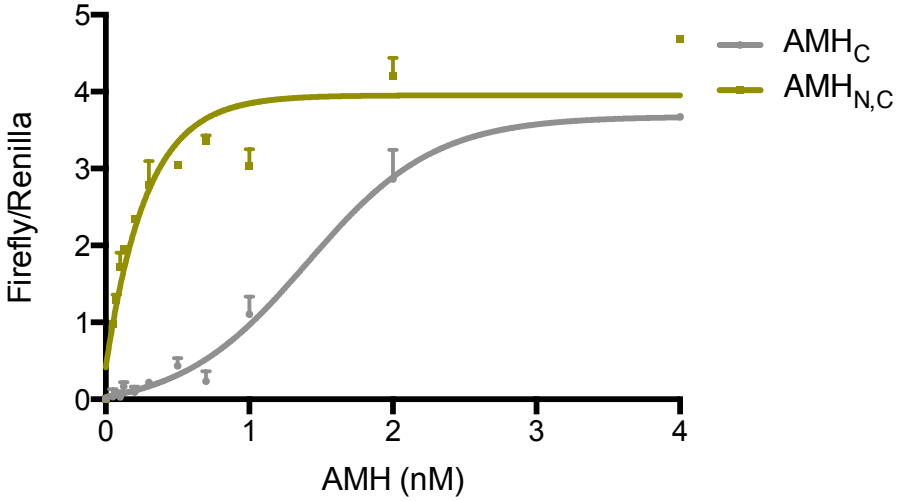

(B)

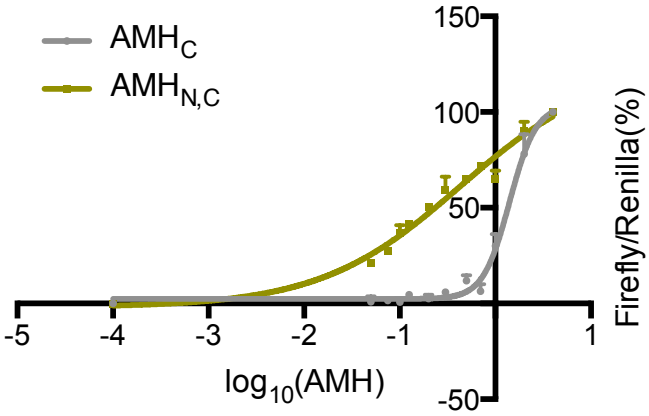

Figure 3-15. AMH$_{N,C}$ is dose-responsive in transfected P19 cells

P19 cells were transfected with AMHR2, along with (BRE)2-Luc and phRL-SV40, and incubated with culture media supplemented with female 10% FCS for 24 hours. They were then exposed to various concentrations of AMH$_C$ and AMH$_{N,C}$ for 24 hours. The ratio of the firefly luciferase to *Renilla reniformis* luciferase was calculated and normalized to the ratio obtained after transfection. Each data point is the mean of 2 wells. The bars represent the mean + the standard error of the mean. (A) A dose-response curve was made using the "sigmoidal dose-response (variable slope)" function of Prism. (B) The data was normalized as a percentage of the maximum concentration of AMH and log transformed in Prism and the two curves compared using the "log (agonist) vs. response - variable slope (four parameters)".

3.2.1.6 Do P19-AMHR2 cells respond to BMP?

The response of the P19 cells to BMP2 was examined as part of the validation of the assay (see Discussion). 7.7 nM of BMP2 induced strong reporter activity in the non-transfected cells (Figure 3-12). Unexpectedly, the reporter activity in response to BMP2 was significantly greater in the AMHR2-transfected cells than in the non-transfected cells (Figure 3-12). Other research groups have previously reported a similar observation using AMHR2-transfected P19 cells and the mouse Leydig tumor cell line (MA-10) [192, 196], with the phenomenon also being evident in the preliminary experiments of this thesis, which used DU145 cells (Figure 3-6). These experiments (Figures 3-6, 3-12) were not designed to specifically examine whether BMP2 can activate AMHR2. Consequently, the control cells were not transfected with a control vector, and therefore had a lower level of transgenic DNA than the AMHR2-transfected cells.

Further experiments were therefore undertaken to verify whether transfection of P19 cells with AMHR2 altered BMP signaling, as the canonical theory of AMH specifies that AMHR2 is AMH specific (Chapter 1.6.6). P19 cells were transfected with the BRE reporter and either AMHR2 or a control vector. The response of P19 control cells to rhBMP2, rhBMP4, rhBMP6 and rhBMP7 were examined in the absence of AMHR2. rhBMP7 produced minimum activation of the P19 cells (not illustrated) and was not further studied. The EC50 (half maximal effective concentration) values for BMP2 and BMP4 were 2.6 and 1.1 nM, respectively (Figure 3-16). Transfection of the P19 cells with AMHR2 did not significantly affect the EC50 or the maximum value for any of the BMPs tested (Figure 3-16). This suggests that BMPs do not signal through AMHR2, although the conclusion is only valid if the signaling components downstream of the type-2 receptor are not already maximal when strong activation of BMPR2 occurs. That is, the assay can be activated above the maximum (top) value of BMP working through BMPR2. Preliminary analysis of this issue is described in the next Section.

(A)

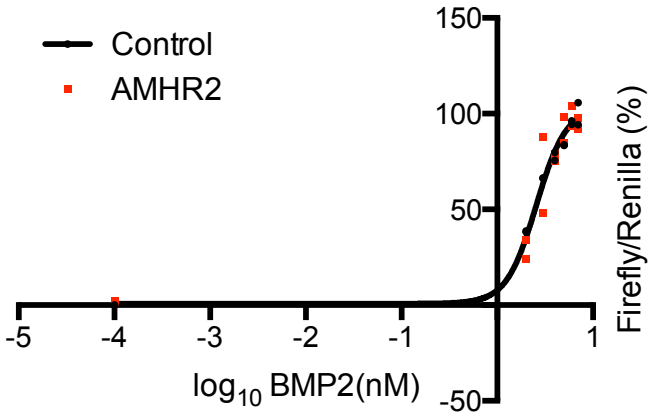

(B)

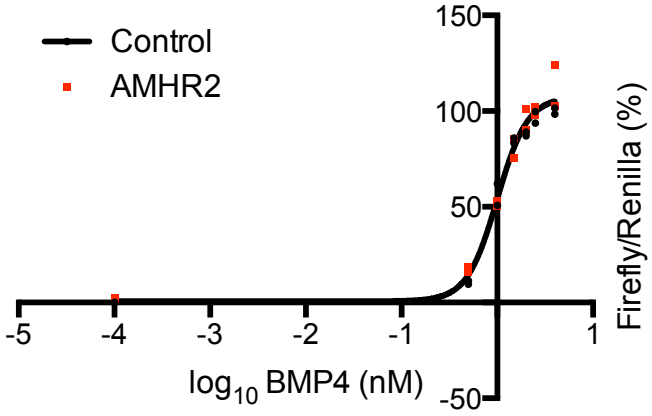

Figure 3-16. BMP is dose-responsive in transfected P19 cells

P19 cells were transfected with AMHR2 or control vector, along with (BRE)2-Luc and phRL-SV40, and incubated with culture media supplemented with female 10% FCS for 24 hours. They were then exposed to various concentrations of (A) BMP2 and (B) BMP4 for 24 hours. The ratio of the firefly luciferase to *Renilla reniformis* luciferase was calculated and normalized to the ratio obtained after transfection. The data is the total of 2 wells per group. The bars represent the mean + the standard error of the mean. The data was first normalized as a percentage of the maximum concentration of BMP. A dose-response curve was made using the "sigmoidal dose-response (variable slope)" function of Prism.

3.2.2. Interactions between BMPs and AMH

The fact that the P19 reporter assay responds to both BMP and AMH does not affect its use as a screening tool to detect AMH BPs. However, the assay has the potential to be used to investigate the interaction between BMP and AMH signaling, which may be a determinant of the magnitude of AMH response produced *in vivo*. Consequently, some preliminary experiments were undertaken to determine how AMH and BMPs interact in the reporter assay.

3.2.2.1 Does AMH inhibits BMP signaling when AMHR2 is absent?

AMH does not activate the P19 reporter cells in the absence of AMHR2. However, this does not exclude the possibility that AMH may associate with its type-1 receptors, and diminish the ability of those receptors to associate with BMPs. Previous work using levels of ligands that were greatly supraphysiological (71.4 nM) suggests that this does not occur [192]. As a first step, this issue was re-examined using physiological levels of ligands. The addition of 1 nM AMH_C to the culture medium did not affect the reporter activity produced by 0.4 nM of BMP2 (Figure 3-17), indicating that AMH is not an inhibitor of BMP signaling, in this assay.

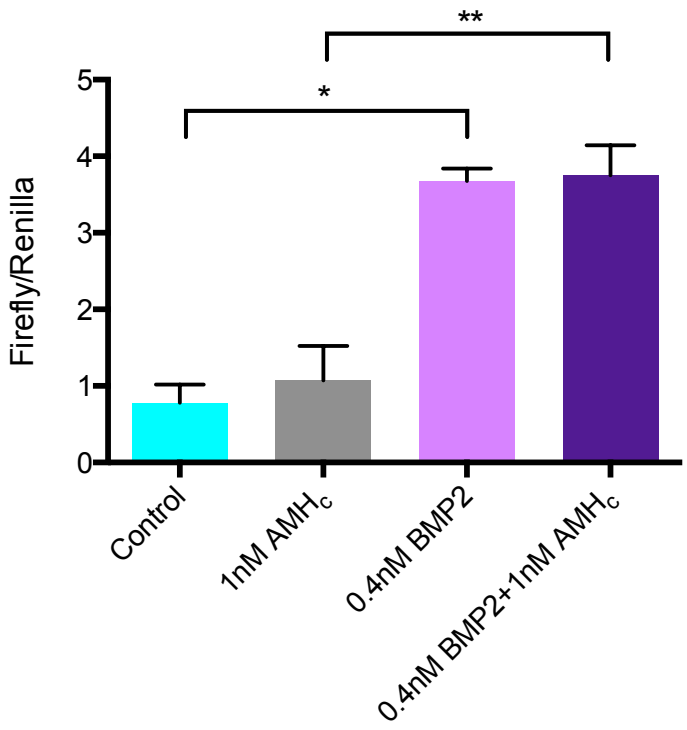

Figure 3-17. AMH does not affect BMP signaling in the absence of AMHR2

P19 cells were transfected with AMHR2 (0.2 ug/100,000 cells), along with (BRE)2-Luc (0.2 ug/100,000 cells) and phRL-SV40 (0.002 ug/100,000 cells), and plated at a density of 50,000 cells per well. The cells were incubated with culture media supplemented with female 10% FCS for 24 hours. They were then exposed to various concentrations of 0.4 nM BMP2 or/and 1nM AMH_C for 24 hours. The ratio of the firefly luciferase to *Renilla reniformis* luciferase was calculated and normalized to the ratio obtained after transfection. The data is a total of 3 wells per group. The * and ** indicate the groups were significantly different from each other, one-way ANOVA with an adjusted p value of $p < 0.0012$ and 0.002, respectively.

3.2.2.2 Do BMP4 and AMH redundantly activate P19 reporter cells?

The interactions between BMPs and AMH_C were also examined by adding different concentrations of BMP and AMH. In the first experiment, 3 nM of AMH_C was used as this maximally activates the P19 assay in previous experiments (e.g. Figure 3-15). As expected, this caused a robust response from the P19 cells (Figure 3-18). 0.6 nM

of BMP4 was also added, which produced a half-maximal response for BMP. The combination of 3 nM AMH_C and 0.6 nM BMP4 did not produce an additive effect, with the activation being not different to that produced by 3 nM of AMH_C alone and only slightly above that produced by 0.6 nM BMP4 alone (Figure 3-18). This suggests that the BMP and AMH signaling are largely redundant when the reporter is strongly activated.

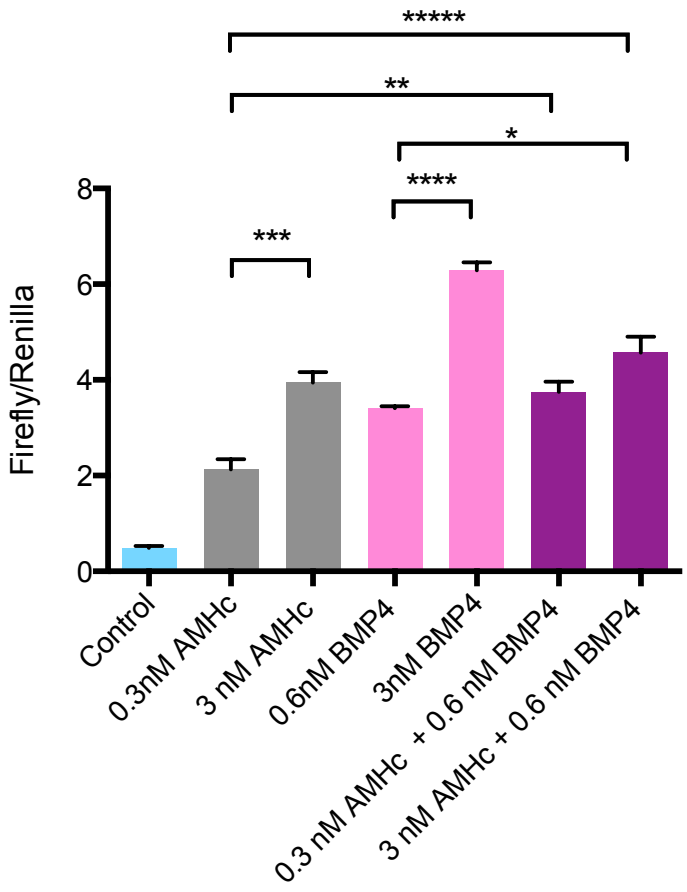

Figure 3-18. When AMH is maximum, BMP is not additive

P19 cells were transfected with AMHR2, along with (BRE)2-Luc and phRL-SV40, and incubated with culture media supplemented with female 10% FCS for 24 hours. The cells were incubated with culture media supplemented with female 10% FCS for 24 hours. They were then exposed to various concentrations of 0.6 nM or 3 nM BMP4 or/and 0.3 nM or 3 nM AMH_C for 24 hours. The ratio of the firefly luciferase to *Renilla reniformis* luciferase was calculated and normalized to the ratio obtained after transfection. The data is a total of 4 wells per group. The *,**,***,and **** indicate the groups were significantly different from each other, one-way ANOVA with an adjusted p value of $p=0.0068$, $p=0.0002$, $p=0.0001$ and $p<0.0001$, respectively. Similar observations were obtained when similar experiments were undertaken using slightly different concentrations of BMP4 (all of which yielded strong activation of the assay).

0.3 nM of AMH_C significantly increased reporter activity when added in combination with 0.6 nM of BMP4. However, the magnitude of the increase was not fully additive, with the observed effect of the combined factors being 3.75 ± 0.20. This was significantly less than sum of the BMP and AMH values (4.94) ($p < 0.011$, one-sample T-test). Figure 3-19 describes the converse experiment, where a sub-optimal dose of AMH is added to a maximum dose of BMP4. The addition of AMH did not increase the response above that of BMP4 alone.

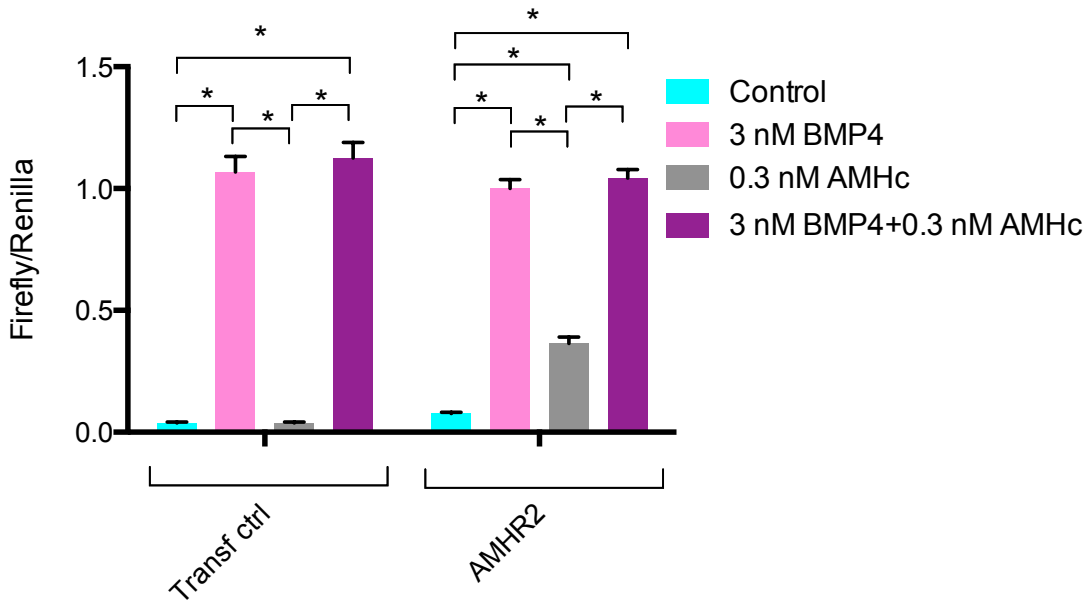

Figure 3-19. When BMP is maximum, AMH is not additive

P19 cells were transfected with AMHR2, along with (BRE)2-Luc and phRL-SV40, and incubated with culture media supplemented with female 10% FCS for 24 hours. The cells were incubated with culture media supplemented with female 10% FCS for 24 hours. They were then exposed to various concentrations of 0.6 nM or 3 nM BMP4 or/and 0.3 nM or 3 nM AMH_C for 24 hours. The ratio of the firefly luciferase to *Renilla reniformis* luciferase was calculated and normalized to the ratio obtained after transfection. The data is the combined results from 3 replicate experiments, with a total of 14 wells per group. The * indicate the groups were significantly different from each other, 2-way ANOVA with an adjusted p value of $p<0.0001$.

3.3 Discussion

3.3.1 An AMH-reporter assay was developed

A highly sensitive AMH reporter assay was developed based on transfected P19 cells. The concentration required to induce half-maximal activation of the reporter was of the order of 0.4 nM of $AMH_{N,C}$, with 1 nM producing near maximal activation. These values are within the physiological range of circulating AMH observed in developing human males (Chapter 1.2.3). The assay produced broadly similar results for $AMH_{N,C}$ and AMH_C (see also Chapter 3.2.1.5).

3.3.1.1 Maximum (top) value

The maximum reporter value induced by AMH was less than that produced by BMP. This indicates that assay is not limited by the downstream components of the assay, including endogenous components such as SMAD 1/5/8 and the (BRE)2-Luc reporter. Consequently, if a BP were to increase the maximal response to AMH, then the assay should be able to detect this.

In the initial experiments, the concentration of AMH and BMP were different, as the purpose of the experiments was not to compare the two ligands. However, the maximum response generated by AMH_C and BMP2 were also different in subsequent experiments (Chapter 3.2.1). The maximum response in AMH-(BRE)2-Luc reporter assays is proportional to the abundance of AMHR2 [163]. At the level of mRNA, the transfected P19 cells have less AMHR2 than BMPR2, which may explain why the AMH-induced maximum is less than for the BMP2-induced maximum. If so, increasing the amount of AMHR2 vector may have increased the maximum response. However, this was not done for several reasons. First, the assay involves transfection of 3 vectors, which risks adverse consequences for the cells. Second, the maximum response needs to be sufficiently low to ensure that the downstream components are never limiting. If AMHR2 were maximized, this may negate the ability to detect BPs whose action increases the efficacy of AMH receptor activation. Third, the assay was sufficiently sensitive for the required purpose. There was no additional benefit to be obtained by further increasing the signal to noise.

The abundance of AMHR2 mRNA in the transfected P19 cells was similar to that of the type-1 receptors, at the level of mRNA. It is unknown whether this corresponds the abundance of the receptor protein. However, this is a further reason to be cautious about raising the level of AMHR2, as signaling requires both type-1 and type-2 receptors. Simply raising AMHR2 levels alone may not substantially increase signaling.

One disadvantage of using AMHR2-transfected cells is that the level of AMHR2 may vary between experiments. This issue also relates to the level of (BRE)2-Luc and phRL-SV40, which may contribute to variation between experiments. The Otago AMH Neurobiology Group examined the possibility of producing stable transfected cells line, with one or all of the vectors and I tested these cell lines. This experimental approach was discontinued as the cell line proved to be unstable. They exhibited poor growth characteristics and the appearance of the cells changed, indicating that spontaneous differentiation was occurring. At that time, the research group was also developing the capacity to produce recombinant AMH, in collaboration with PX' Therapeutics. When AMH expression was optimized, the cells producing it grew more slowly and were less healthy in appearance. This suggests that AMH may have adverse affects on cell growth. Consequently, a decision was made to use transiently transfected cells, as the development of permanent cells might have required prolonged research, and have may not been successful, as the presence of AMHR2 might have adversely affected the maintenance of the cell line.

3.3.1.2 Minimum (bottom) value

The reporter value when no AMH was added appeared to be much lower for P19 cells than for DU145 cells. This was advantageous for the purpose of the reporter assay, as it increased the signal-to-noise ratio and as it minimized the possibility of BPs affecting the assay by interacting with the factors that generate the zero value. The reason for the difference between the cells is unclear, and was not investigated further as it appeared to be outside of the scope of the thesis.

The existence of a low minimum value could have arisen if AMH were present in the control cultures, which had no added AMH. Theoretically, this could be from a low

production of AMH by P19 cells, although the presence of AMH in the added serum is a more likely explanation. The level of serum was restricted to 10% for this reason, and female FCS was used as it was expected to have less endogenous AMH. The observation that the background is low in the absence of added AMH indicates that little or no AMH is being added along with the FCS. This could not be directly tested as the available ELISAs were for human AMH, with the first validated assay for bovine AMH being reported in 2015 [197].

FCS contains BMPs and BPs [198] and these BMPs may be responsible for the zero AMH value in the reporter assay. This was not a significant problem as the level of activation is low. A single batch of FCS was used throughout the entire thesis to ensure the level of added growth factors was constant.

Ideally, it would have been nice to eliminate these BMPs. Consideration was given to use serum-free medium, as a way of achieving this. However, this option was not used for the following reasons. Cells need growth factors to grow and the assay is dependent on the cells being healthy, otherwise the added factors may alter gene expression by affecting the health of the cells, rather than solely by the level SMADs activation. The presence of minimum levels of growth factors is therefore potentially more advantageous than further lowering of the zero-AMH level. Serum-free medium contains growth factors, with the identity and concentration of the factors being a commercial secret. Using serum-free medium therefore does not necessarily eliminate BMPs. On balance, further development of the assay to reduce the small zero-AMH value was not considered to be worth the investment of time and resources.

3.3.1.3 Other factors affecting the P19 reporter assay

The $AMH_{N,C}$ used in the experiment was generated by cleavage of proAMH with furin. Furin is labile and its activity declines during the preparation of $AMH_{N,C}$. Some residual furin activity would therefore have been present in the $AMH_{N,C.}$, creating the possibility that furin would interfere with the assay. However, the addition of furin to control cultures did not affect the growth of the P19 cells, or their response to AMH_C.

The initial results had high variation within and between experiments. This variation was substantially reduced through multiple independent changes, most of which are outlined in Chapter 2, particularly Section 2.1.6.

3.3.1.4 DU145 and LNCaP cells

The initial development of the reporter assay began with DU145 and LNCaP cells. These cell lines were presumed to be natural targets for AMH and had been used by other research groups to develop AMH-reporter assays [169, 193]. A basic reporter assay based on these cell line had been developed by Dr Imhoff, a previous member of the research team [199]. For the reasons outlined below, the replacement of DU145 and LNCaP by P19 cells was the most critical step in developing a robust reporter assay.

A basic reporter response was observed with both the LNCaP and DU145 cells, but refinement was needed as the signal-to-noise ratio was low, and as the variation in the assay was unacceptably high. Further development of an LNCaP-based assay was terminated early in the thesis, principally because the growth characteristics of LNCaP cells were poor. The dependence of LNCaP cells on testosterone was an additional factor in this decision, as it creates unnecessary complexity in the reporter assay. Tran *et al.* had reported that LNCaP cells could survive for four days without testosterone [193]. However, this observation was not corroborated by the initial data from this thesis, which supports the more commonly held view that the growth of LNCaP cells has a requirement for testosterone [169].

The low signal-to-noise ratio with the DU145 cells appeared to be due to the low expression of AMHR2. If so, a sensitive and reliable assay based on DU145 cells would require the cells to be transfected with AMHR2. The need to use transfection meant that there was no advantage in using a putative target cell of AMH, particularly as transfection of DU145 cells with AMHR2 did not substantially improve the signal-to-noise ratio. I therefore elected to test a cell line that had robust growth characteristics, and which also naturally expressed the AMH type-1 receptors. P19 cells were the first cell line tested, and proved superior to the DU145 cells, leading to the discontinuation of research using the DU145 cells.

The minimum value was increased when DU145 cells were transfected with AMHR2, with this phenomenon being previously reported for MA-10 cells [196]. The reason for this is unclear. If this was simply due to AMH in the medium, then this phenomenon should also have been observed in the P19 cells. However, the minimum value for P19 cells was low compared to the DU145 cells, and was not significantly increased after AMHR2 transfection, which is consistent with a previous study [200]. This issue was not further examined, due to the decision to focus the project on advancing the assay based on P19 cells.

3.3.1.5 Technical issues relating to assay development

Some of the initial experiments described in this Chapter were exploratory in nature, and were not fully controlled, as they were not intended to generate publishable data. Most specifically, when cells are transfected with vectors, the vector can alter the growth and/or other characteristics of the cells. For example, when the DU145 cells were transfected with AMHR2 the *Renilla reniformis* luciferase reporter signal was reduced, indicating that the transfection with AMHR2 had decreased cell number. Transfecting the control cells with an empty-vector could have controlled for this. Ideally, this control should have been done, but the absence of this control did not affect the assay development, as the comparison between transfected and non-transfected cells was not a critical issue. For example, in Figure 3-6 the main comparison is within the untransfected cells and within the transfected cells, rather than between the two groups. Control vectors were routinely used when the influence of changing AMHR2 levels was being examined, for example Figure 3-16.

3.3.1.6 Comparison with other reporter assays

The EC50 of the P19 assay is within the physiological range of circulating AMH for boys, but is above the physiological range of circulating levels of AMH in men and females. The adult-like levels of AMH, however, produce detectable levels of activation of the reporter activity. This is in marked contrast to most previous assays, which have reported EC50 values that are supra-physiological (see Chapter 4, Table 4-1). The reasons for this are unclear, and multiple factors may be important, as outlined below.

Visser *et al.* have also used P19 cells [180], suggesting that cell type is a not a critical issue. However, cell lines can accumulate mutations, and the two P19 cell lines are not necessarily identical. Visser *et al.* used a TLX2-Lux promoter [180], which could have a different dose-response curve to the (BRE)2-Luc used in this thesis. However, there are also reports of non-physiological EC50 when (BRE)2-Luc is used with other cell types [189].

One recurring issue with historic studies is that the AMH used was a mixture of proAMH and $AMH_{N,C}$. The rhAMH used by Visser *et al.* appears to be an example of this. They used rhAMH produced by HEK-293S cells transfected with proAMH [180]. The rhAMH produced by the Otago AMH Neurobiology Group is also from HEK cells, and is predominantly proAMH, with only minor levels of $AMH_{N,C}$, indicating that HEK cells have limited capacity to active proAMH. proAMH does not activate AMHR2, and the high EC50 reported by Visser *et al.* may be because their AMH preparation contained little bioactive AMH. The EC50 values reported in this thesis are derived from AMH preparation that is predominantly ($AMH_{N,C}$) or exclusively (AMH_C) bioactive.

3.3.1.7 Summary

In conclusion, Chapter 3 has established a robust AMH reporter assay, which has multiple purposes, within and beyond this Thesis. The chemistry of signaling processes is dependent on concentration. Many of the earlier studies of AMH have used concentrations that are order(s) of magnitude above the concentrations present in humans. The physiological significance of these studies is unclear. Importantly, the P19 assay described in the thesis works at physiologically relevant levels of AMH.
In the process of developing a working reporter assay, some of the results provided preliminary data about the nature of AMH signaling. These issues are outlined in the remaining two Sections of this Discussion.

3.3.2 Does BMPR2 limit AMH signaling?

3.3.2.1 Expression of AMH type-1 receptors

The transfected P19 cells expressed all of the type-1 receptors required for a cell to respond to AMH, which is consistent with previous qualitative studies (for example, [201]). ACVR1 and BMPR1A were the most abundant type-1 receptors, with the limited expression of BMPR1B mRNA by P19 cells. In most of the initial PCR conditions, a BMPR1B band was not detected (data not shown). This was confirmed by qPCR and is consistent with other studies of P19 cells [202]. ACVR1 and BMPR1A mediate the majority of the proven actions of AMH (Chapter 1.6.7). The low level of BMPR1B was therefore not of concern for the validity of the bioassay, and no attempt was made to increase BMPR1B levels.

It is currently unclear whether the rate-limiting step in AMH signaling involves the type-1 or the type-2 receptors. The way receptor complexes are assembled varies within the TGFβ superfamily. For example, the activins and the TGFβ-subfamily ligands bind to their type-2 receptors independently of the type-1 receptors. The type-1 receptors are then recruited to form the full signaling complex. The type-1 receptors cannot bind these ligands in the absence of the type-2 receptors [203].

In contrast, the BMPs can bind to a type-1 receptor or to a pre-formed complex of BMPR2 and a type-1 receptor [204]. Consequently, when BMPR2 is present, some of the type-1 receptors may be bound to it. The binding affinity for the ligand dramatically increases when both type-1 and type-2 receptors are present [205]. This may be due to the ability of BMPR2 and BMP type-1 receptors to form preassembled heterometric receptor complexes, in the absence of a ligand [204].

AMH is thought to bind directly to AMHR2 and not to its type-1 receptors, although this has not been definitively proven. If this is correct, then the abundance of AMHR2 may be more critical than the abundance of the type-1 receptors. The abundance of the type-1 receptor mRNA in the P19 cells was lower than for the type-2 receptors, but despite this the output of the reporter assay was very sensitive to the abundance of AMHR2 (Section 3.3.1.1). This is consistent with the generally accepted scheme for the assembly of the AMH-signaling complex.

3.3.2.2 Competition for type-1 receptors

The maximum reporter activity produced by AMH was consistently lower than the maximum produced by BMP. This may have been because BMPR2 was more abundant than AMHR2, as noted above (Section 3.3.1.1). The BMPR2 being expressed by the P19 is murine, as are the type-1 receptors. The AMHR2 and the AMH are recombinant based on the human sequences. This is advantageous as the BPs used are also human, but it is possible that hAMHR2 is less able to compete for murine type-1 receptors than mouse AMHR2 and mouse BMPR2. If so, the difference in the maximum response between AMHR2 and BMPR2 may be an artifact of using proteins from different species. Alternatively, it could also result from differences in the way that AMHR2 and BMPR2 interact with the type-1 receptors.

BMPR2 can bind type-1 receptors in the absence of ligand [204]. This potentially limits the ability of the initial AMH-AMHR2 complex to recruit type-1 receptor and thus form a complete signaling complex. The extent to which this might occur will depend on the Kd of the type-2 receptors for the type-1 receptors, and their distributions within the cell membrane. If AMH-AMHR2 cannot strip all of the type-1 receptor from BMPR2, then this should result in a lower maximum activation by AMH relative to BMP.

The dose-response curve for BMPs was not significantly altered by transfection of AMHR2. This suggests that AMHR2 does not inhibit BMP signaling by competing with BMPR2 for the type-1 receptors. However, the experiments reported in this Chapter were not designed to specifically test this, and it is not possible to fully exclude that this mechanism might be important when BMP levels are low. That is, when the concentration of BMP-BMPR2 is low.

3.3.3 Can AMH and BMP signaling be redundant?

At the beginning of this thesis, there was a consensus that AMH was a classical hormone, with only one function. AMH was considered to signal in isolation of other regulators, as it had its own unique receptor, AMHR2. The Otago AMH Neurobiology Group has progressively challenged this, arguing that AMH conforms

to the pattern of TGFβ signaling, where the influence of a ligand is contextual [10, 206]. The characteristics of the P19 reporter assay are relevant to this debate.

The activation of the P19 reporter cells was dose-dependent when AMH was the only ligand in the medium. This form of signaling is consistent with that of a classical hormone, and may model the mechanism that occurs during the regression of the Müllerian duct. However, when the reporter assay was strongly stimulated by a BMP, the addition of AMH had little or no effect on reporter activity. Hence, in this model system, the AMH pathway is not independent of the BMP pathway. AMH here is a redundant ligand that has little or no activity unless BMP levels are physiologically low. Similarly, when a dose of AMH close to its EC50 was added with a dose of BMP4 close to its EC50, then the combined increase in reporter activity was significantly less than the sum of the reporter activity of AMH alone plus BMP4 alone. This is consistent with AMH and BMP4 signaling via a common sigmoidal dose-response curve, where doubling the EC50 dose does not lead to doubling of output. AMH and BMP4 have different top (maximum values) and further experimentation is required to define what the precise dose-response curve of combinations of AMH and BMPs are. This was beyond the scope of the thesis, and was therefore not investigated further.

Most immature neurons in mice express AMHR2, and AMH is present in the blood of developing male mice. However, the numbers of neurons are only sexually dimorphic in a minority of brain nuclei. This could arise if most neurons are exposed to BMPs from sources that are common to males and females, during the period of natural cell death. In these neurons, the presence of AMH in males would not have an affect as the SMAD 1/5/8 pathway is strongly activate by BMPs. In brain nuclei with low levels of endogenous BMPs (or the absence of BMPR2), then SMAD 1/5/8-induced survival of neurons would become strongly regulated by AMH, creating a male bias. This is an early stage hypothesis that requires substantial further evidence to be proved.

The above argument illustrates that the P19 reporter assay has uses that are independent of its use as a vehicle to identify AMH BPs. At the beginning of the thesis, one of the options available was to further investigate the interactions between

AMH and BMPs. Whilst this was an attractive option, it was not possible to examine this option and to simultaneously search for AMH BPs. For this reason, further work was not undertaken on the interaction between AMH and other TGFβ-superfamily members. As noted in the next Chapter, the study of BPs is potentially informative about BMP and AMH interactions, as well as putatively being central to the understanding why AMH appears to be able to signal at diverse concentrations.

Chapter 4: Do AMH binding proteins exist?

4.1 Introduction

AMH is a member of the TGFβ superfamily, whose actions are pleiotrophic and context dependent (Chapter 1.5.1). The complexity of signaling is generated through shared receptors, and shared BPs. AMH has historically been viewed as being outside of this framework, so that the role of BPs as modulators of AMH biology has not been examined. One reason to suspect that BPs influences AMH signaling is that different dose curves for AMH have been described and because the Kd of AMH binding to its specific receptor is outside of the biological range of AMH levels, as discussed below.

4.1.1 Kd and EC50

The understanding of a hormone/cytokine includes knowledge of the range of concentrations that it affects the behavior of cells. One component of this is the ability of the cytokine to bind to its receptor, which is most directly measured by the Kd. AMH putatively binds directly to AMHR2, with the type-1 receptors then being recruited to bind with the AMH-AMHR2 complex [140]. If this is correct, then the Kd of AMHR2 for AMH is an important determinant of the dose-response curve of cells to AMH.

Another measure of the response of a cell to a cytokine is the EC50. The EC50 of a sigmoidal dose-response curve represents the concentration of a compound that causes an effect that is half way between the baseline (Bottom) and maximum response (Top). The EC50 can differ from the Kd for multiple reasons. First, and most importantly for this thesis, the binding of AMH to AMHR2 may be modulated by BPs. BPs might sequester AMH. If so, a higher concentration of AMH would be needed to affect the cells, leading to a change in the EC50 without a change in Kd of AMH for AMHR2. Alternatively, a BP might facilitate the binding of AMH to AMHR2, thus lowering the effective Kd and the EC50. Second, the intracellular

cascade may modulate the dose-response curve, through feedback mechanisms and intracellular BPs. In this thesis, EC50 has been used as the initial screen for BPs as EC50 can detect BPs acting by diverse mechanisms. Nevertheless, the Kd of AMHR2 for AMH is relevant to the understanding of an EC50, and is therefore outlined in the next section.

4.1.2 Paradox of AMH concentration and Kd for AMHR2

4.1.2.1 Müllerian duct

The level of AMH in the blood of male embryos is highly variable [23]. However, males almost invariably lack a uterus, indicating that the removal of the Müllerian duct is insensitive to the concentration of AMH. This could occur if the lowest concentration of AMH found in male embryos (200-300 pM) were sufficient to produce a strong activation of the AMHR2. This would require the Kd of AMHR2 for AMH to be around 200 pM, or possibly less. However, the reported Kd for AMHR2 varies between 2.5 and 20 nM (Table 4-1), which is orders of magnitude above the highest level of AMH recorded in the circulation of a male. This creates the paradox where AMH is leading to invariant loss of the Müllerian duct, despite insufficient AMH levels to cause significant direct activation of its receptor.

Table 4-1. Estimates of the affinity of AMHR2 for AMH

Test system	nM	reference
COS cells with transfected hAMHR2	2.5 (Kd, iodinated $AMH_{N,C}$)	[158] – note 1
human epidermoid carcinoma cell line (A431)	5.8 (Kd,iodinated $AMH_{N,C}$)	[207] – note 1
human ovarian carcinoma cell line (OVCAR5)	10 (Kd, biotinylated proAMH and $AMH_{N,C}$ mixture)flow cytometory	[208] – note 1
AMHR2-antibody hybrid used as the capture reagent	10 (Kd, AMH_C, $AMH_{N,C}$, ELISA)	[140]
human ovarian carcinoma cell line (OVCAR8)	12 (Kd, biotinylated proAMH and $AMH_{N,C}$ mixture)flow cytometory	[209]
Leydig cells	15(Kd, biotinylated proAMH and $AMH_{N,C}$ mixture) flow cytometory	[12]
transfected P19 cells	18 (EC50, proAMH and $AMH_{N,C}$ mixture)	[180]
duct regression in vitro	15-20 (EC50, proAMH and $AMH_{N,C}$ mixture)	[152] – note 2

Note 1. The $AMH_{N,C}$ was generated by plasmin cleavage of proAMH, which generates $AMH_{N,C}$ and an alternative cleavage form, whose ability to bind to AMHR2 is unknown [153]. Hence, the Kd may be an over-estimate as a proportion of the AMH may lack the ability to bind to AMHR2.

Note 2. As the duct regression assay is an organ culture, the estimation of the effective dose of AMH may be affected by the ability of AMH to diffuse into the Müllerian duct. This provides some insight into the amount of AMH needed to trigger the regression of the Müllerian duct in vivo, but is a less accurate estimate of the ability of AMH to bind to AMHR2 than the direct measures of Kd, using tagged AMH.

There are several possible resolutions of this paradox. First, a BP may modulate the binding of AMH to AMHR2, in a manner analogous to the way that betaglycan modules the binding of TGFβ2 to TβR2 (Chapter 1.5.4.1). The influence of the BP would need to be large, probably shifting the EC50 by one or two orders of magnitude. Second, the local concentration of AMH adjacent to the Müllerian duct may be orders of magnitude higher than in the circulation of male embryos. This would require that the diffusion of AMH away from the Müllerian duct is limited. This could be achieved by the presence of BPs around the Müllerian duct, which act to concentrate AMH around the AMHR2-expressing cells. Third, AMH induces regression of the Müllerian duct by triggering the release of an apoptotic factor by the cells surrounding the duct. This could act as an amplifying mechanism where a low level of activation of AMHR2 leads to a large release of apoptotic factor via various methods.

4.1.2.2 Circulating AMH

The putative endocrine roles of AMH appear to be dose-dependent within the physiological range. The signaling mechanism here, may therefore be different to what is occurring during the removal of the Müllerian duct, depending on which mechanism creates the dose-insensitivity of this phenomenon (see previous Section).

Immature neurons express AMH receptors, and AMH contributes to generation of male biases in the brain [17, 30]. Heterozygous male mice that carry a null mutation of AMH ($AMH^{+/-}$) exhibit a neural phenotype that is intermediate between $AMH^{-/-}$ and $AMH^{+/+}$ littermates. In marked contrast to the brain, $AMH^{+/-}$ male mice lack Müllerian ducts, illustrating the difference dose-dependencies between the brain and the Müllerian duct. $AMH^{+/-}$ mice have half the level of AMH mRNA [30], suggesting that the influence of AMH on immature neurons is dose-dependent at physiological concentrations of AMH. A similar situation appears to be occurring during human development, as the circulating level of a boy's AMH correlates with a measure of his maturity [28], and with the severity of his symptoms, if he has an autistic spectrum disorder [210]. These observations also suggest that AMH produces a dose-dependent effect, at physiological concentrations. The physiological concentration of AMH in developing human males (approximately 0.3 - 2 nM [21, 28]) is lower than the reported Kd of AMHR2 for AMH, and much lower than the various estimates of

EC50 for AMH, using cell lines (Table 4-1). This indicates that the canonical mechanism for AMH signaling does not fully explain the observed dose-response curves in living individuals.

Men and women have an order of magnitude less circulating AMH than boys (Chapter 1.3.4). Consequently, if the difference between the Kd for AMHR2 and the level of AMH in boys makes AMH signaling paradoxical, then it is even less clear that the AMH in the circulation of adults is sufficient to produce meaningful activation of AMH receptors. For this reason, the possibility that AMH is a hormone in adults has not been seriously considered until recently. AMH levels in men and female rhesus monkeys correlate with various cardiovascular traits [32], but there is currently no evidence that the observed correlations are due to causal regulation by AMH in adults. If this were occurring, then AMH would need to signal with a different dose-response curve in boys and adults. Consistent with this, the observed dose-response curve to AMH_C in Chapter 3 (Figure 3-13) included activation of the AMH reporter at adult-like levels of AMH, with the top of the curve being reached at the lower range of boy-levels. Again, one possible resolution of this issue is that AMH signaling in adults and boys is facilitated by different BPs. Alternatively, AMH may signal through a receptor other than AMHR2 in adult peripheral tissues, as there is currently no proof that the putative adult functions of AMH are AMHR2-dependent.

4.1.2.3 Ovarian follicular AMH

Extremely high levels of AMH exist within the gonads, with this being most comprehensively documented in females. The level of AMH in the follicular fluid of small antral follicles is of the order of 8 nM [55] (Chapter 1.3.3). At first sight, this level of AMH is sufficient to produce significant activation of AMHR2, based on some but not all of the reported EC50 values (Table 4-1). However, most of the AMH in the follicular fluid is the uncleaved precursor, proAMH [211], which does not bind to AMHR2 [140]. The level of $AMH_{N,C}$ in the follicular fluid thus appears to be too low to produce substantial activation of AMHR2, unless a BP or some other mechanism is altering the response of granulosa cells to AMH.

4.1.2.4 In vitro studies using embryonic neurons

The influence of AMH on cells isolated from tissues outside of the reproductive tract has rarely been studied, as AMH was not expected to affect such cells until recently. The first such study by our research group used embryonic motoneurons isolated from mouse embryos. Embryonic motoneurons *in vitro* die in the absence of an exogenous survival factor. When AMH is added to embryonic motoneurons, the observed dose-response curve was log dose – linear output. Consequently, significant survival of neurons was observed at both adult human-like and boy-like levels of AMH [17]. The effect of AMH was maximal at concentration of 360 - 710 pM, with higher concentrations of AMH being inhibitory [17]. Prof. Donahoe (Harvard) provided the AMH used in this study, and the observed sensitivity of motoneurons to this AMH was orders of magnitude greater than obtained by the gifting laboratory in their assays using cancer cell lines [12, 209]. The data from the embryonic motoneurons provides a basis for postulating that the AMH in the circulation is functional. However, it is unknown why embryonic neurons are more sensitive to AMH than cell lines, or why the dose-response curve for neurons is log-linear in vitro when the limited data suggests that it is linear-linear *in vivo* (Chapter 4.1.2.2). Again, the existence of AMH BPs is a possible explanation.

4.1.3 Forms of AMH for the assay

The initial experiments in this Chapter used rhAMH$_{C,}$ as the identity of the AMH species in the circulation were unknown, and historically, most of the AMH experiments have used rhAMH$_C$. Furthermore, a source of recombinant AMH$_{N,C}$ was not available at the beginning of the thesis. Additional experiments using AMH$_{N,C}$ were undertaken later in this thesis, after the presence of AMH$_{N,C}$ was discovered in serum [140]. Theoretically, AMH$_C$ and AMH$_{N,C}$ could have different affinities for BPs, as the presence of the N-terminal domain of AMH could create or disrupt binding sites for BPs. The glycosylation of AMH is predominantly associated with the N-terminal domain [139]. AMH$_C$ and AMH$_{N,C}$ may thus differ in the extent of glycosylation as well as in the amino acid portion of AMH. Additionally, the use of AMH$_{N,C}$ makes the tests more physiological as the existence of free AMH$_C$ has not been demonstrated in natural fluids. One minor limitation to the use of AMH$_{N,C}$ is

that it had to be produced from proAMH *in vitro* by our research group. Consequently, the $AMH_{N,C}$ preparation contains traces of furin (see Chapter 3.3.1.3) and traces of proAMH. The latter may cause the EC50 values to be slightly under-estimated as a proportion of the AMH is not AMHR2-competent. The concentration of $AMH_{N,C}$, and the extent of any proAMH contamination, will vary from batch to batch, which limits the ability to compare experiments undertaken with different batches of $AMH_{N,C}$. For this reason, a single large batch of $AMH_{N,C}$ was prepared for the experiments in this Chapter.

The ability of BPs to affect proAMH will be discussed in Chapter 5.

4.1.4 Soluble binding proteins

The initial test of the BPs used soluble versions of the BPs. If any of the BPs bound AMH, then addition of them to the culture medium was expected to decrease AMH reporter activity by preventing AMH reaching the receptor. That is, they were expected to act as a sink for AMH as the total number of BP molecules in the medium was expected to be large relative to the number of BPs on the surface of the P19 cells. This scenario is modeled on the known actions of soluble betaglycan that inhibits TGFβ signaling (Chapter 1.5.4.1) and soluble FS that acts as a ligand trap of activin [79]. The development of a sensitive bioassay (Chapter 3) was important for this strategy, as the accurate detection of inhibition required a clear positive control in the absence of the inhibitor. This strategy was not designed to test the mode of action of the BPs *in vivo*, which requires different types of experiments.

The P19 cells may produce BPs and there may be low levels of BPs in the culture medium. These BPs are only likely to influence the reporter assay if they were membrane bound or bound to the extracellular matrix, as the culture medium was changed at the start of the assay. If such BPs exists they may compete with the BPs added as part the experiment. In order to minimize this, the concentration of the BPs used in the screens described in this Chapter was high (Table 4-2). The fact that the volume of the medium is large relative to the P19 cells, is a further safe-guard as it

ensures that the molar number of the test BP will be very large relative to the number of endogenously occurring BPs.

Table 4-2. Binding proteins and the concentrations used in this Chapter

Binding protein	Dose curves	Figures 4-4, 4-5	ELISA
	[BP nM] x replicates	(nM)	(nM)
Betaglycan	5 x 1, 10 x 2	10	-
Brorin	30 x 1, 20 x 2	20	-
Chordin	10 x 3	10	20
Chordin-like1	20 x 3	20	20
Chordin-like 2	20 x 3	20	-
DAN	106 x 1, 20 x 2	20	-
Decorin	53 x 1, 20 x 2	20	-
Endoglin	8.2 x 1, 10 x 2, 10 x 3 ($AMH_{N,C}$)	10	20
FS288	7.9 x 3 (AMH_{C}), 20 x 3 ($AMH_{N,C}$)	20	20
FS315	10 x 3	10	20
FS-like1	28 x 1, 20 x 2	20	-
FS-like3 (FLRG)	20 x 3	20	20
FS-like 4	10 x 3	10	-
Noggin	20 x 3	20	-
α2-macroglobulin	10 x 3	10	-

Note. Dose-curve experiments were conducted as three independent replicates. At the beginning of the thesis, the concentrations of BPs were calculated in ng/ml. This limits the ability to compare the potency of BPs, as they were added in different molar concentrations. Subsequently, the BPs were used at either 10 or 20 nM, depending on the availability of the BP. Consequently, some of the replicate experiments had variation in the concentration of the BP. For example, two of the curves for decorin used 20 nM and the other 53 nM. In all cases, the BPs were in a large excess, and the

results of the three experiments were comparable, enabling them to be combined. Ideally, each replicate should have been identical.

4.1.5 Objectives of Chapter 4

A priori, AMH signaling may be modulated by multiple BPs, which act at one or multiple sites (Müllerian duct, gonads, or endocrine target cells). In this Chapter, I have used the assay established in Chapter 3 to examine whether 15 of the known TGFβ-superfamily BPs can bind to AMH, leading to a change in the AMH dose-response curve of the P19 reporter activity. The methods used in this Chapter were described in Chapter 2 and 3.

4.2 Results

4.2.1 Binding proteins with AMH

4.2.1.1 Dose curve and EC50

The response of transfected P19 cells to AMH_C (Figure 3-13) was re-examined with an extended dose curve, to more accurately define the EC50 (Figure 4-1). The EC50 of AMH_C was calculated to be approximately 0.5 nM, with near-maximal response occurring at concentrations greater than 1 nM (Figure 4-1). Figure 4-1A illustrates that the dose-response curve was sigmoidal. The EC50, top, and bottom values of the sigmoidal dose curve were calculated from the log of the AMH concentration, and the log dose-response curve is shown in Figure 4-1B. The log dose curves illustrate the influence of BPs more clearly than the simple dose-response curve, and subsequent data is presented as log dose curves for this reason. The AMH_C dose-response curve was broadly similar between experiments (c.f. Figure 4-1 and Figure 4-2).

(A)

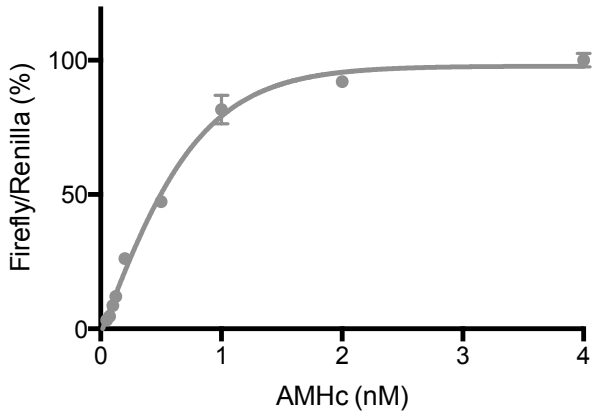

(B)

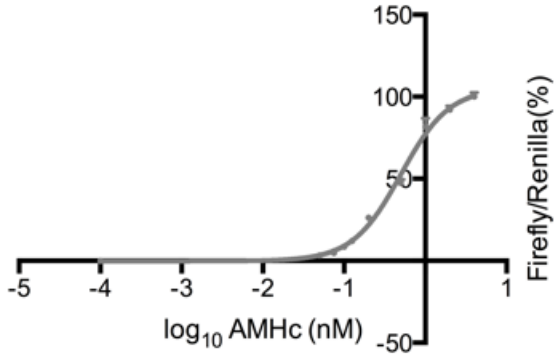

Figure 4-1. Definition of the dose-response curve for AMH_C

(A) A dose-response curve was fitted using the "sigmoidal dose-response (variable slope)" function of Prism. (B) The data were log transformed in Prism and the two curves compared using the "log (agonist) vs. response - variable slope (four parameters)". The data is the mean plus and minus the standard error, with six wells for each concentration point.

4.2.1.2 AMH and binding proteins

The known TGFβ-superfamily BPs were sequentially studied, using two screens. The effect of each BP on the AMH dose-response curve was examined using AMH_C. The EC50, the top, and bottom values were examined. When a supply of $AMH_{N,C}$ became available, the effect of the BPs was re-examined at 0.16 nM of $AMH_{N,C}$. Among the first 14 of the BPs tested, 8 had no effect in the AMH_C screen, with the other 5 producing only a small change. The 15th of the BPs tested (FS288) produced a larger effect. The results of the 8 BPs that did not affect AMH signaling in the reporter assay are present in Figure 4-2 (A-H). These BPs did not alter the EC50, or the top or bottom values of the AMH dose-response curve (Table 4-3).

(A)

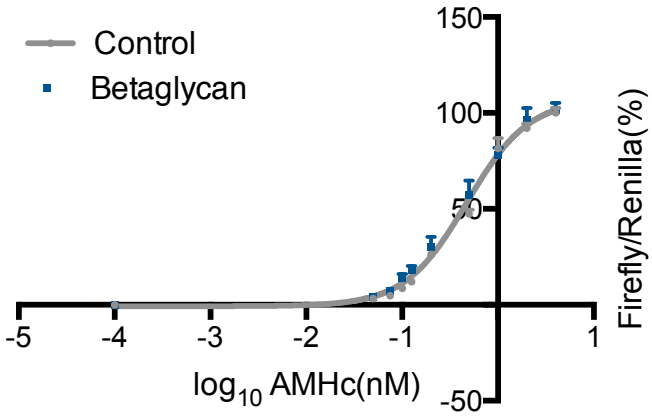
Control
Betaglycan
150
100
50
-50
-5
-4
-3
-2
-1
1
log10 AMHc(nM)
Firefly/Renilla(%)

(B)

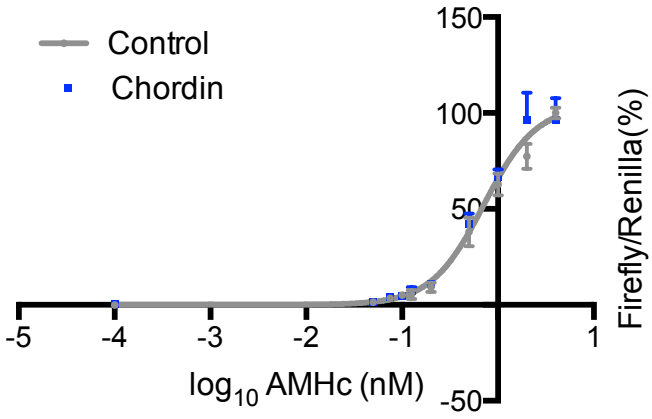
Control
Chordin
150
100
50
-50
-5
-4
-3
-2
-1
1
log10 AMHc (nM)
Firefly/Renilla(%)

(C)

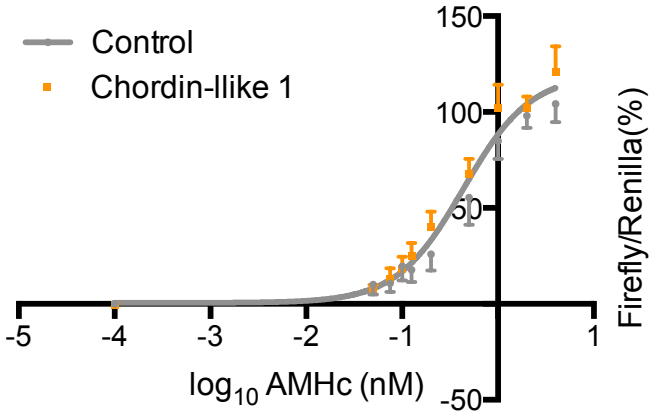
Control
Chordin-llike 1
150
100
50
-50
-5
-4
-3
-2
-1
1
log10 AMHc (nM)
Firefly/Renilla(%)

(D)

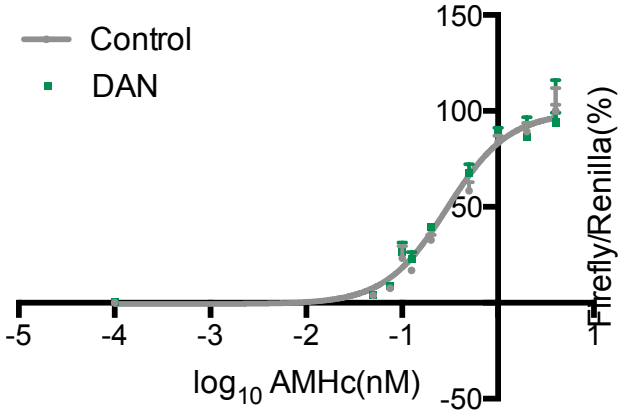
Control
DAN
150
100
50
-50
-5
-4
-3
-2
-1
1
log10 AMHc(nM)
Firefly/Renilla(%)

(E)

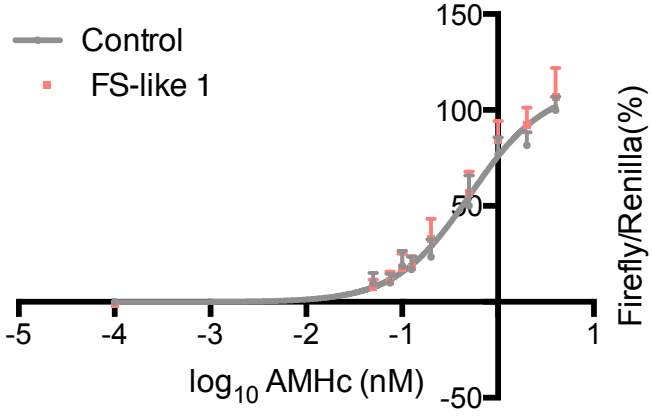
Control
FS-like 1
150
100
50
-50
-5
-4
-3
-2
-1
1
log10 AMHc (nM)
Firefly/Renilla(%)

(F)

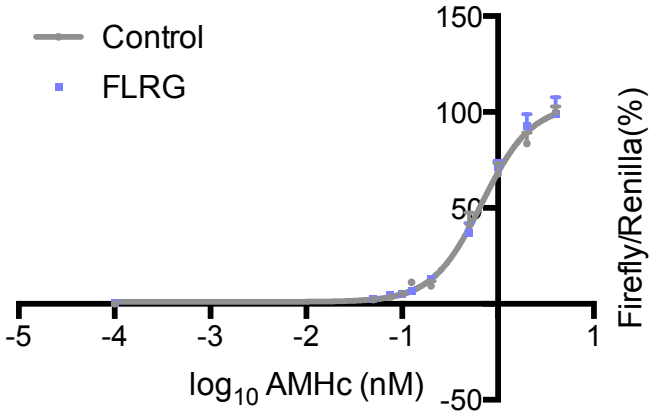
Control
FLRG
150
100
50
-50
-5
-4
-3
-2
-1
1
log10 AMHc (nM)
Firefly/Renilla(%)

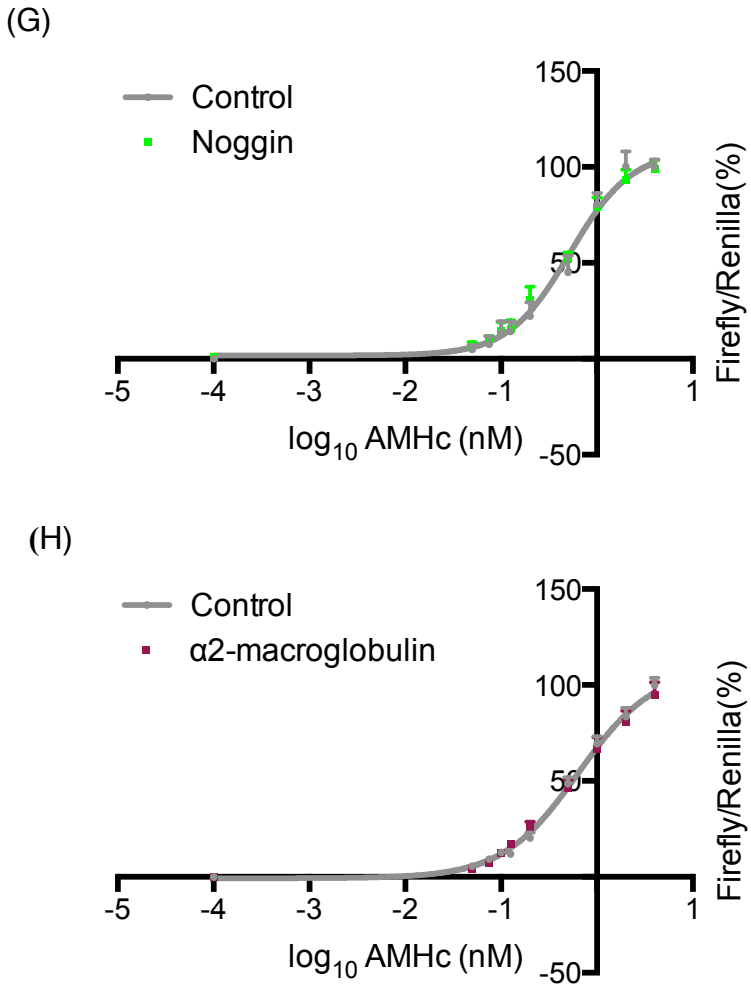

Figure 4-2. Influence of BPs on the dose-response curve to AMH_C

The influence of eight BPs on the response of the P19 reporter cells to AMH_C is illustrated. (A) Betaglycan, (B) Chordin, (C) Chordin-like 1, (D) DAN, (E) FS-like 1, (F) FLRG, (G) Noggin, (H) α2-macroglobulin. The BPs were added in a large molar excess relative to the maximum concentration of AMH_C (Table 4-2). The data is illustrated as the mean plus the standard error of the mean of 6 wells for each concentration point, in both the control and BP-treated curves. The statistical analysis of each curve was from the 60 data points, as described in Section 2.1.5.

The dose-response curve to AMH_C in the presence of 20 nM or 30 nM of brorin was significantly different to the control curve (p=0.0025), although the magnitude of the change was relatively small (Figure 4-3A). With the addition of 20 nM of brorin, the EC50 for AMH_C decreased from 0.50 nM to 0.40 nM, with no apparent change in either the top or bottom value (Table 4-3). Although statistically significant, a change in the EC50 of 0.1 nM is within the noise of the assay and insufficient to explain the phenomena described in the Introduction to this Chapter. A second screen was therefore used to verify whether the small changes were robust. When brorin was added to a single dose of AMH_C near the EC50 (0.5 nM), there was no significant change in the reporter activity of the P19 cells (figure 4-4B). Similarly, when 20 nM of brorin was added to a single dose of $AMH_{N,C}$ near the EC50 (0.16 nM, Figure 3-15), there was no significant change in the reporter activity of the P19 cells (Figure 4-5B). This indicates that if brorin has an effect on AMH signaling, the magnitude of the effect is near the limits of detection of the assay.

(A)

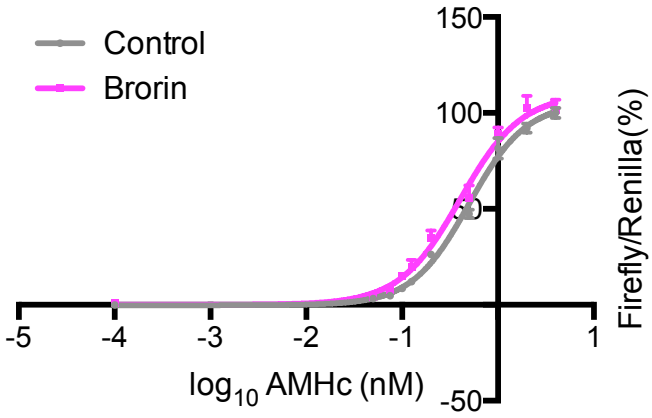
Control
Brorin
150
100
50
-50
-5
-4
-3
-2
-1
1
log10 AMHc (nM)
Firefly/Renilla(%)

(B)

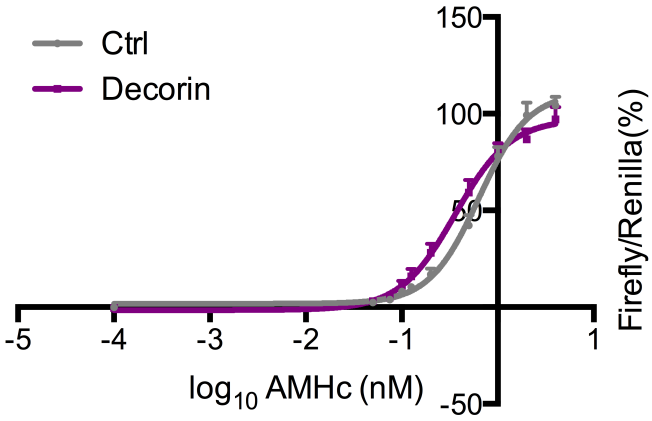
Ctrl
Decorin
150
100
50
-50
-5
-4
-3
-2
-1
1
log10 AMHc (nM)
Firefly/Renilla(%)

(C)

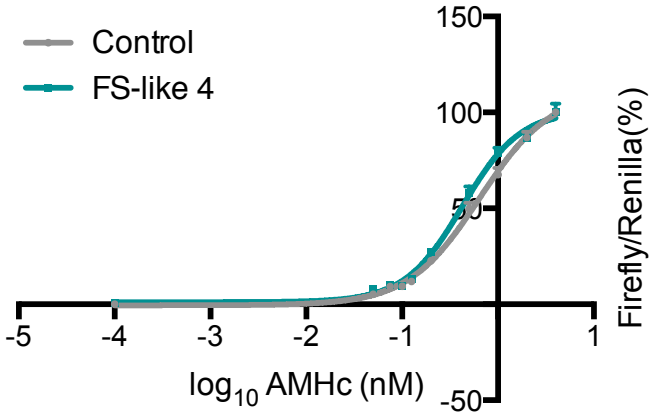
Control
FS-like 4
150
100
50
-50
-5
-4
-3
-2
-1
1
log10 AMHc (nM)
Firefly/Renilla(%)

Figure 4-3. Brorin, Decorin and FS-like 4 affect AMH_C signaling

The influence of brorin, decorin and FS-like 4 on the response of the P19 reporter cells to AMH_C is illustrated. (A) Brorin, (B) Decorin, (C) FS-like 4. The BPs were added in a large molar excess relative to the maximum concentration of AMH_C (Table 4-2). The data is illustrated as the mean plus the standard error of the mean of 6 wells for each concentration point, in both the control and BP-treated curves. The statistical analysis of each curve was from the 60 data points, as described in Section 2.1.5.
(A)-(C) were significantly different from control with (A) p=0.0025, (B) p=0.0003, (B) p=0.0006.

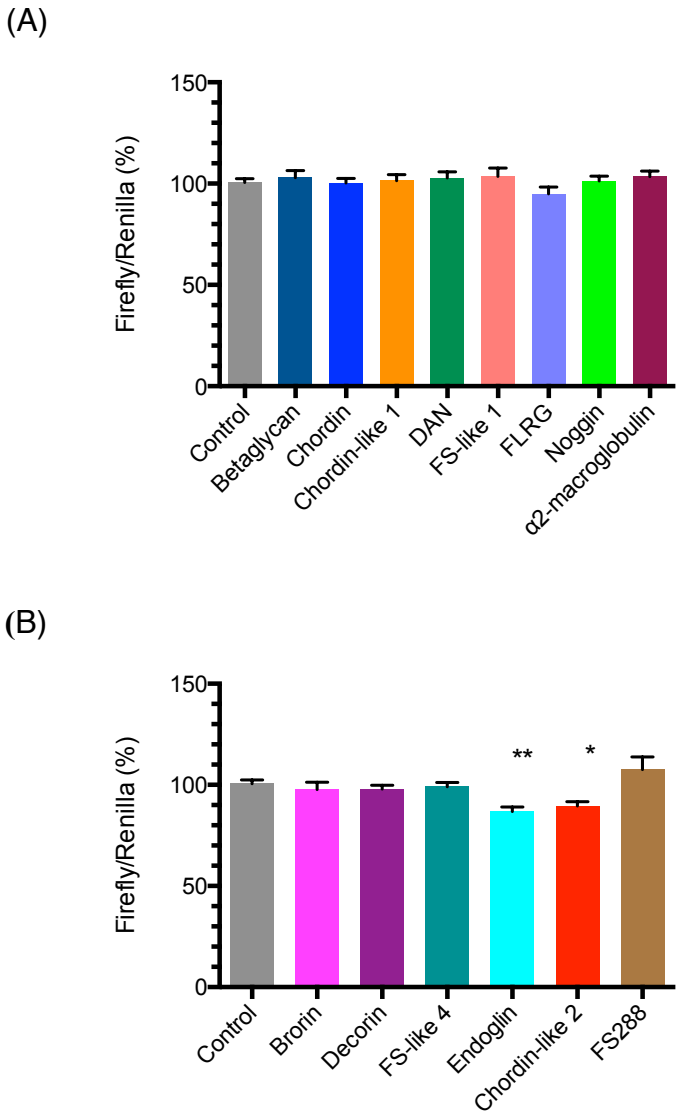

Figure 4-4. The effect of binding proteins on 0.5 nM AMH_C

The influence of 14 BPs on the reporter activity generated by an EC50-like concentration of AMH_C is illustrated. Panel (A) illustrates the BPs which had no effect on the AMH_C dose-response curve (Figure 4-2), whereas panel (B) illustrates the BPs which affected the dose-response curve (Figure 4-3, 4-7, 4-10, 4-12). The concentration of BPs used is recorded in Table 4-2. The BPs in panels A and B were tested in the same experiment. The bars represent the mean + the standard error of the mean of 9 wells. There was a statistically significant effect of group for the entire experiment (General Linear Model, $p<0.0005$). Bonferroni post-hoc tests indicated that endoglin (**, $p=0.003$) and chordin-like 2 (*, $p=0.04$) were significantly different to the control group.

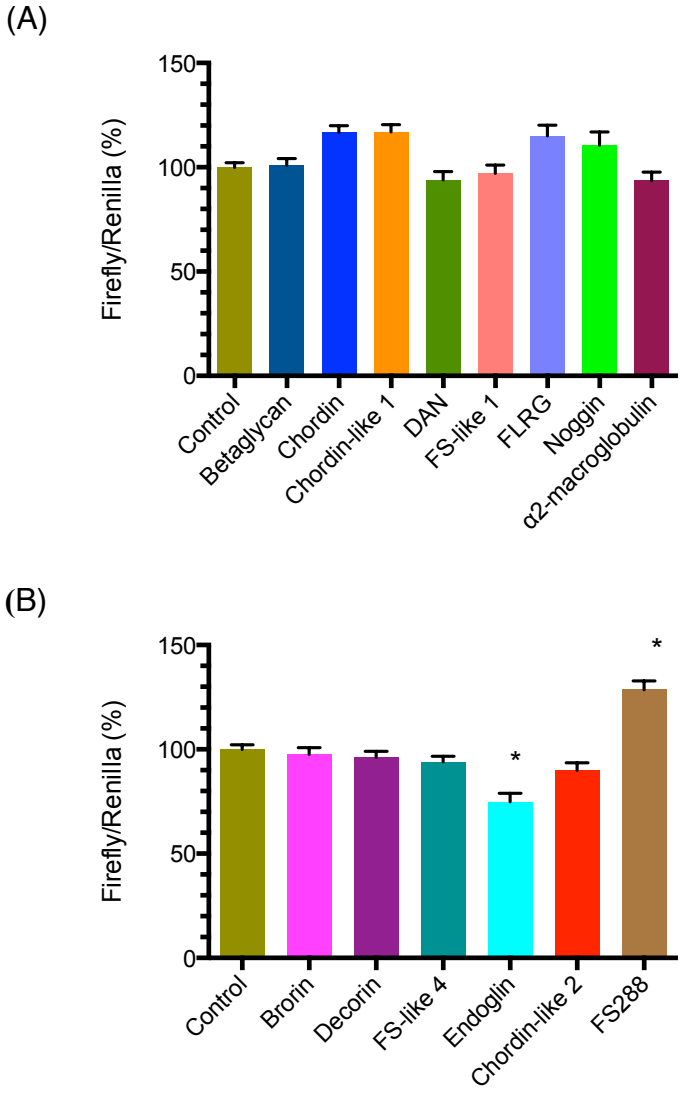

Figure 4-5. The effect of binding proteins on 0.16 nM $AMH_{N,C}$

The influence of 14 BPs on the reporter activity generated by an EC50-like concentration of $AMH_{N,C}$ is illustrated. Panel (A) illustrates the BPs which had no effect on the AMH_C dose-response curve (Figure 4-2), whereas panel (B) illustrates the BPs which affected the dose-response curve (Figure 4-3, 4-7, 4-10, 4-12). The concentration of BPs used is recorded in Table 4-2. The BPs in panels A and B were tested in the same experiment. The bars represent the mean + the standard error of the mean of 8 wells. There was a significant effect of group for the entire experiment (General Linear Model, $p<0.0005$). Bonferroni's post-hoc test indicated that endoglin and FS288 were significant different to the control group (*, $p<0.0005$).

Similarly, the addition of 20 nM or 53 nM of decorin caused a small but statistically significant change to the dose-response curve (p=0.0003) (Figure 4-3B). The EC50 changed from 0.64 nM to 0.36 nM, with no apparent change in either the top or bottom values (Table 4-3). However, 20 nM of decorin did not cause a significant increase in the second screen, using single doses of AMH_C (Figure 4-4B) and $AMH_{N,C}$ (Figure 4-5B) near their EC50.

The effect of 10 nM of FS-like 4 was similar to that of decorin and brorin. The EC50 changed from 0.64 nM to 0.43 nM (Figure 4-3C, p=0.0006), with no apparent change in either the top or bottom value (Table 4-3). No change was observed in the second screen using either AMH_C (Figure 4-4B) or $AMH_{N,C}$ (Figure 4-5B).

Table 4-3. Change of top, bottom and EC50 value with binding proteins

Binding protein	Top		Bottom		EC50	
	Control	with BP	Control	with BP	Control	with BP
Betaglycan	105	109	-0.18	-1.2	0.50	0.45
Chordin	110	103	-1.4	1.1	0.84	0.65
Chordin-like1	113	124	2.8	-1.3	0.50	0.38
DAN	105	95	-0.71	-0.49	0.37	0.24
FS-like1	109	115	1.2	-1.4	0.57	0.47
FLRG	105	103	0	2.1	0.70	0.68
Noggin	109	107	3.4	0.89	0.57	0.48
α2-macroglobulin	110	107	0.1	-1.5	0.66	0.61
Brorin	105	110	-0.18	0.04	0.50	0.40
Decorin	111	97	1.8	-1.5	0.64	0.36
FS-like 4	111	101	-0.52	1.1	0.64	0.43
Endoglin(AMH_C)	106	98	1.3	-5.3	0.58	0.53
Endoglin($AMH_{N,C}$)	109	99	-0.69	-0.19	0.37	0.40
Chordin-like 2	108	92	-0.64	-2.2	0.60	0.49
FS288 (AMH_C)	102	103	-1.7	1.48	0.37	0.22
FS288 ($AMH_{N,C}$)	104	106	-3.5	-0.16	0.54	0
FS315(AMH_C)	114	110	-1.6	2.3	0.84	0.65

The data are the top (maximum), bottom (minimum) and EC50 values from the curves illustrated in Figures 4- 2,3,7,8,10,11,12,15. All values are the % of the top value in the absence of a BP.

The differences in the results between the first and second screens for brorin, decorin and FS-like 4 could be due to random fluctuation in the assays, as the magnitude of the observed effects were small. Alternatively, they could be produced if the effect of the BPs were limited to the lower or upper portions of the dose-response curve. This requires additional experimentation to prove, but indicative results can be obtained by comparing the ratio of the reporter activity in the presence and absence of the BP for each concentration of AMH. The enhancement of AMH_C signaling produced by

brorin (Figure 4-6A) and decorin (Figure 4-6B) were limited to the lower doses of $AMH_{C,}$ corresponding to adult-like circulating levels of AMH. The effect of FS-like 4 was also restricted to the low concentrations, but the magnitude of the FS-like 4-induced change is small and is mainly generated from a single data point (Figure 4-6C). This type of limited post-hoc analysis is only valid when a statistically significant effect has been detected in the dose-response curve. Similar analyses for the 9 BPs that had no significant effect on the dose-response curve (Figure 4-2) were therefore not reported.

(A)

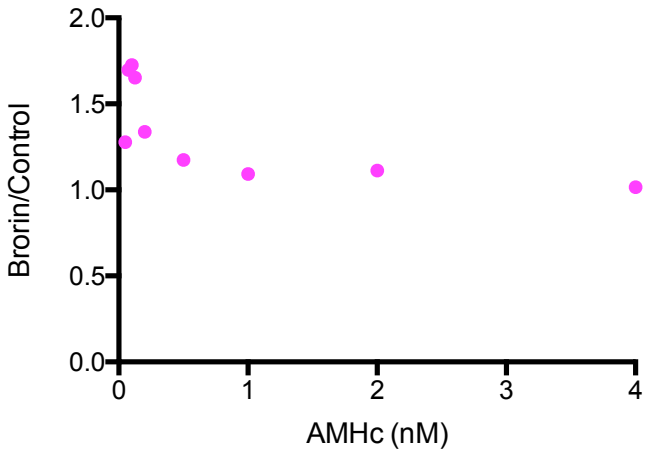
Brorin/Control
2.0
1.5
1.0
0.5
0.0
0
1
2
3
4
AMHc (nM)

(B)

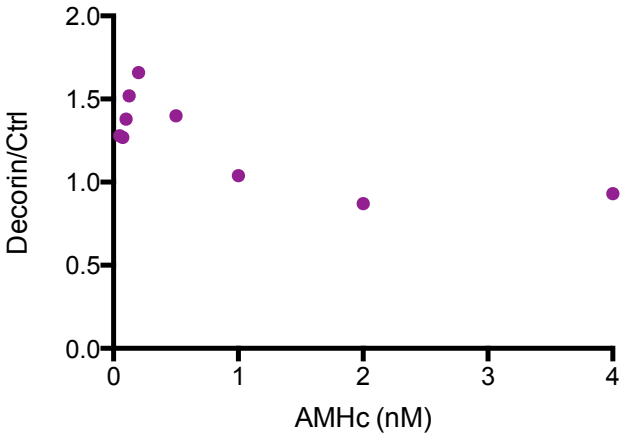
Decorin/Ctrl
2.0
1.5
1.0
0.5
0.0
0
1
2
3
4
AMHc (nM)

(C)

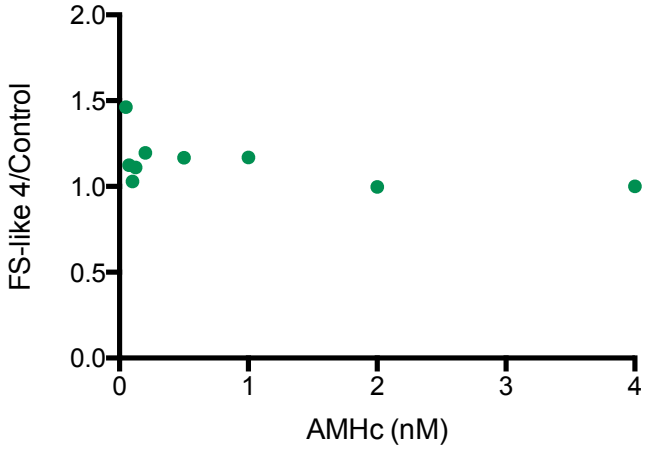
FS-like 4/Control
2.0
1.5
1.0
0.5
0.0
0
1
2
3
4
AMHc (nM)

Figure 4-6. The effect of brorin, decorin and FS-like 4 may vary depending on the concentration of AMH

The illustrated experiment examined whether the effect of (A) Brorin, (B) Decorin and (C) FS-like 4 varied depending on the concentration of AMH_C. The ratio of reporter activity in the presence and absence of the BP was calculated for each concentration of AMH_C, and is plotted against the concentration of AMH_C. Values above 1 indicate enhanced signaling. The data are from Figure 4-3. Each BP had a significant effect on the AMH-dose curve as a whole (legend Figure 4-3). Robust post-hoc analysis of individual concentrations is not possible, as each illustrated point is the ratio of mean values, and is therefore n=1. In this type of analysis, variation will be greatest at the low dose as the ratio of two small numbers is being calculated. Conclusions should therefore only be reached if there is a consistent pattern to the data.

4.2.1.3 Endoglin and chordin-like 2 reduce the signaling of AMH

8.2 nM or 10 nM of Endoglin reproducibly decreased the response to AMH. The reporter activity was lower at each dose of AMH_C in the dose-response curve (Figure 4-7B) and the response to the EC50 dose of AMH_C ($p=0.003$, Figure 4-4B) was also lower, with high statistical certainty. The shape of the dose-response curve was not altered (Figure 4-7A). The log dose-response curve had a calculated bottom value below zero. This suggests that the endoglin affected the dose curve by decreasing the basal activity of the reporter assay. When the entire plus endoglin curve was shifted such that the zero value was aligned to the minus endoglin (control) curve, then there was no difference to the AMH_C signaling with and without endoglin (Figure 4-7C).

(A)

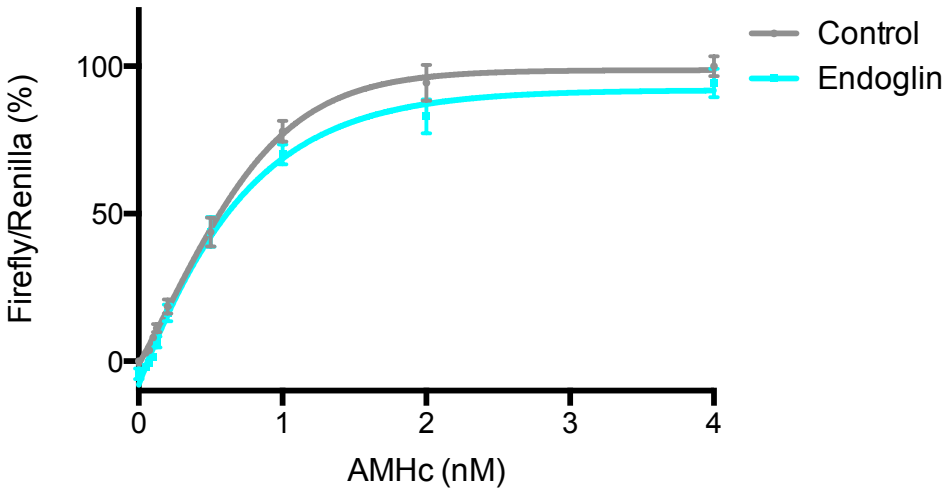
Control
Endoglin
Firefly/Renilla (%)
100
50
0
0
1
2
3
4
AMHc (nM)

(B)

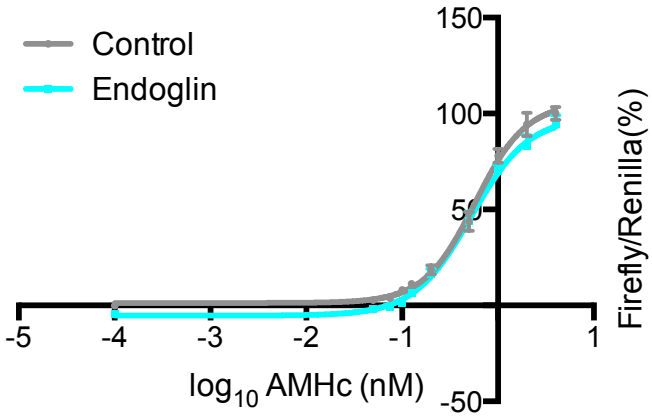
Control
Endoglin
150
100
50
-50
-5
-4
-3
-2
-1
1
log10 AMHc (nM)
Firefly/Renilla(%)

(C)

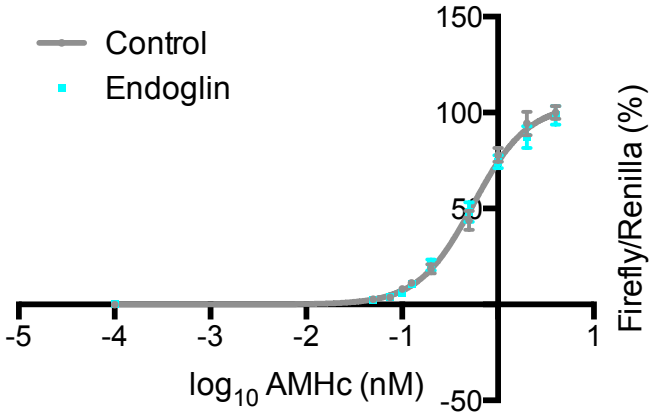
Control
Endoglin
150
100
50
-50
-5
-4
-3
-2
-1
1
log10 AMHc (nM)
Firefly/Renilla (%)

Figure 4-7. Endoglin reduces reporter activity, independent of AMH_C

The influence of endoglin on the response of the P19 reporter cells to AMH_C is illustrated. Endoglin was added in a large molar excess relative to the maximum concentration of AMH_C (Table 4-2). The data is illustrated as the mean plus the standard error of the mean of 6 wells for each concentration point, in both the control and endoglin-treated curves. The statistical analysis of each curve was from the 60 data points, as described in Section 2.1.5. (A) A dose-response curve was fitted using the "sigmoidal dose-response (variable slope)" function of Prism. (B) The data were log transformed in Prism and the two curves compared using the "log (agonist) vs. response - variable slope (four parameters)". The groups were significantly different from each other with p=0.0041. (C) Separate no AMH values were calculated for the control and the endoglin curves (no AMH, plus endoglin) and the curves re-plotted as described for (B).

Similar results were obtained when 10 nM of endoglin was added to $AMH_{N,C}$. All values were lower on the dose-response (Figure 4-8), and the response produced by 0.16 nM of $AMH_{N,C}$ was lower when endoglin was present ($p<0.0005$, Figure 4-5B). When the base line was corrected for the observed effect of endoglin, the endoglin dose-response curve was still significantly different to the control dose curve (p=0.0008, Figure 4-8B). The difference was small, and was present across the entire dose-response curve (Figure 4-8C). However, there was no significant effect of dose when the concentration of endoglin was varied between 1 and 10 nM and the concentration of $AMH_{N,C}$ held constant at a high level (2nM) (Figure 4-9). The zero dose point for endoglin in this curve was statistically significant to the wells that had endoglin added to them ($p<0.001$, Figure 4-9), but the magnitude of the effect was small, consistent with the previous experiments (Figure 4-8). This suggests that the effect of endoglin is maximal at 1 nM.

(A)

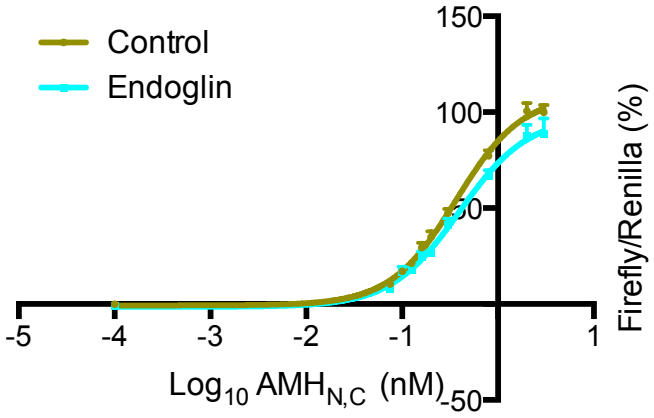
Control
Endoglin
150
100
50
-50
-5
-4
-3
-2
-1
1
Log10 AMHN,C (nM)
Firefly/Renilla (%)

(B)

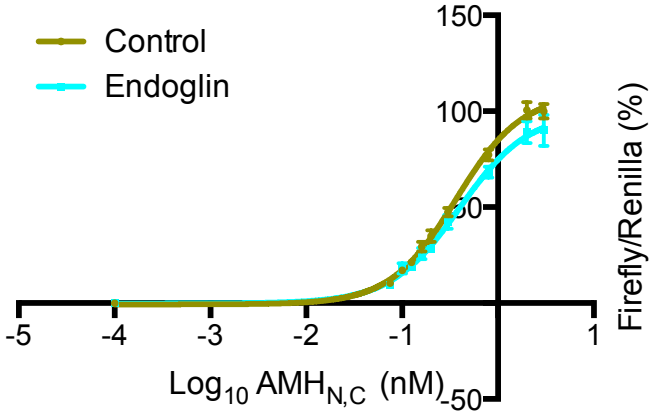
Control
Endoglin
150
100
50
-50
-5
-4
-3
-2
-1
1
Log10 AMHN,C (nM)
Firefly/Renilla (%)

(C)

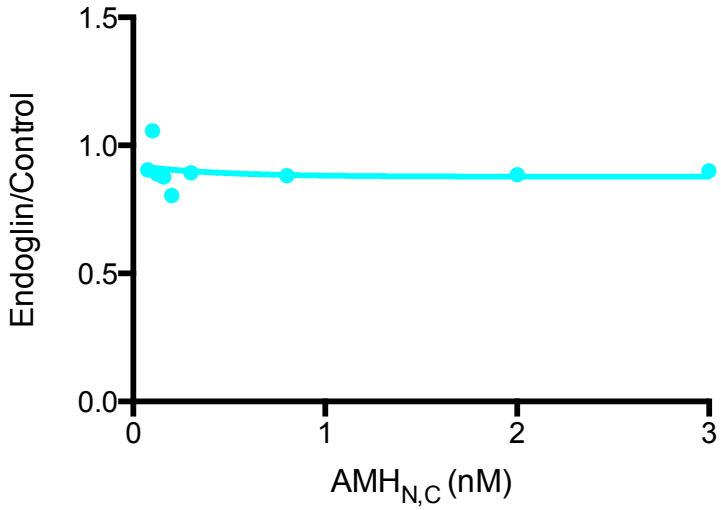
1.5
1.0
0.5
0.0
0
1
2
3
Endoglin/Control
AMHN,C (nM)

Figure 4-8. Endoglin reduces reporter activity, independent of $AMH_{N,C}$

The influence of endoglin on the response of the P19 reporter cells to $AMH_{N,C}$ is illustrated. Endoglin was added in a large molar excess relative to the maximum concentration of $AMH_{N,C}$ (Table 4-2). The data is illustrated as the mean plus the standard error of the mean of 6 wells for each concentration point, in both the control and endoglin-treated curves. The statistical analysis of each curve was from the 60 data points, as described in Section 2.1.5. (A) and (B) The data were log transformed in Prism and the two curves compared using the "log (agonist) vs. response - variable slope (four parameters)". The curve illustrated in (B) has been corrected for the influence of endoglin on the basal activity of the reporter assay. The curves in (A) and (B) were significantly different from each other with $p<0.0001$. (C) The possibility that the effect of endoglin varies with the concentration of $AMH_{N,C}$ was examined using the method described in Figure 4-6.

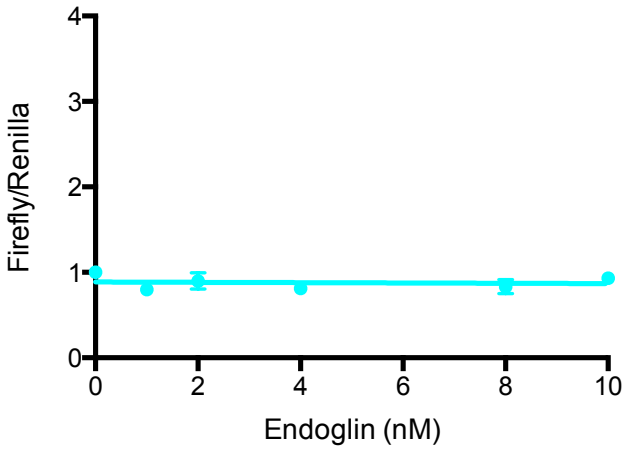

Figure 4-9. The influence of endoglin on $AMH_{N,C}$ did not vary with concentration

The influence of endoglin on the reporter activity generated by 2 nM $AMH_{N,C}$ is illustrated. Each data point is the mean ± the standard error of the mean of 6 wells. The zero endoglin point was significantly different to all other points ($p<0.001$).

Similarly to endoglin, 20 nM of chordin-like 2 reproducibly decreased the response to AMH_C. The reporter activity was lower at each dose of AMH_C in the dose-response curve ($p=0.026$, Figure 4-10B) and the response to the EC50 dose of AMH_C (Figure 4-B) was also significantly lower ($p=0.04$). However, this effect was smaller than for endoglin. The shape of the dose-response curve was not altered (Figure 4-10A). The log dose-response curve had a calculated bottom value below zero. This suggests that the chordin-like 2 affected the dose curve by decreasing the basal activity of the reporter assay similarly to endoglin. When the zero-value was reset to the calculated bottom of the dose-response curve, then the dose response curves to AMH_C with and without chordin-like 2 were identical (Figure 4-10C). However, this effect of chordin-like 2 was not observed with $AMH_{N,C}$ (Figure 4-5B).

(A)

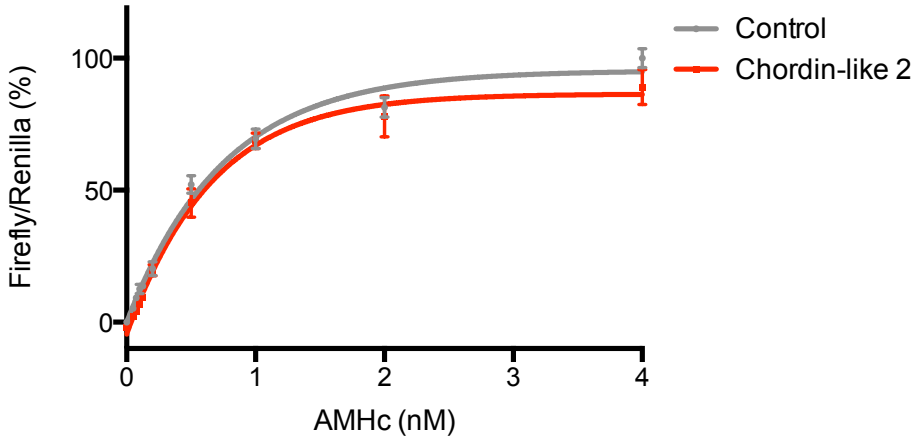
Control
Chordin-like 2
Firefly/Renilla (%)
100
50
0
0
1
2
3
4
AMHc (nM)

(B)

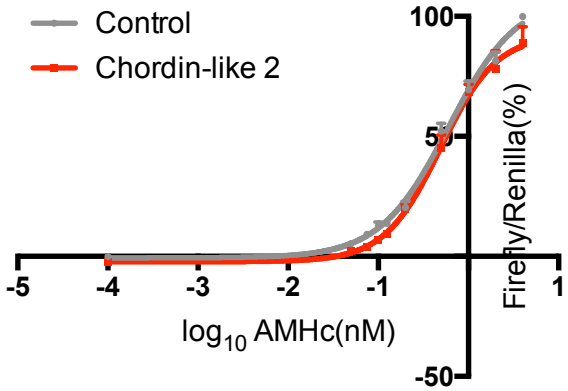
Control
Chordin-like 2
100
50
-50
-5
-4
-3
-2
-1
1
log10 AMHc(nM)
Firefly/Renilla(%)

(C)

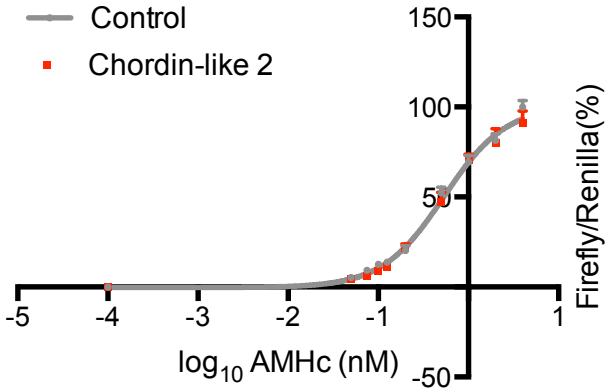
Control
Chordin-like 2
150
100
50
-50
-5
-4
-3
-2
-1
1
log10 AMHc (nM)
Firefly/Renilla(%)

Figure 4-10. Chordin-like 2 reduces reporter activity, independent of AMH_C

The influence of chordin-like 2 on the response of the P19 reporter cells to AMH_C is illustrated. Chordin-like 2 was added in a large molar excess relative to the maximum concentration of AMH_C (Table 4-2). The data is illustrated as the mean plus the standard error of the mean of 6 wells for each concentration point, in both the control and chordin-like 2-treated curves. The statistical analysis of each curve was from the 60 data points, as described in Section 2.1.5. (A) A dose-response curve was fitted using the "sigmoidal dose-response (variable slope)" function of Prism. (B) The data were log transformed in Prism and the two curves compared using the "log (agonist) vs. response - variable slope (four parameters)". The groups were significantly different from each other with p=0.026. (C) Separate no AMH values were calculated for the control and the chordin-like 2 curves (no AMH, plus chordin-like 2) and the curves re-plotted as described for (B).

4.2.1.4 Follistatin 288 increased the signal to dose of AMH_C

FS288 reproducibly increased the response to AMH. The dose response curve was shifted to the left, with the EC50 in the presence of 7.9 nM of FS288 being 0.22 nM compared to 0.37 nM for the control ($p<0.0001$, Figure 4-11A,B). The top and the bottom of the curve were not altered (Figure 4-11B). Consequently, the relative effect of FS288 was largest when AMH concentrations were low, with little or no effect when AMH levels were sufficient to produce a near maximal response (1 nM) (Figure 4-11C). The reporter activity produced from 0.5 nM AMH_C was 108% of the control when 20 nM of FS288 was present, which was not significantly different (Figure 4-4B). This result is consistent with the original screen (Figure 4-11C) (see 4.3.2).

(A)

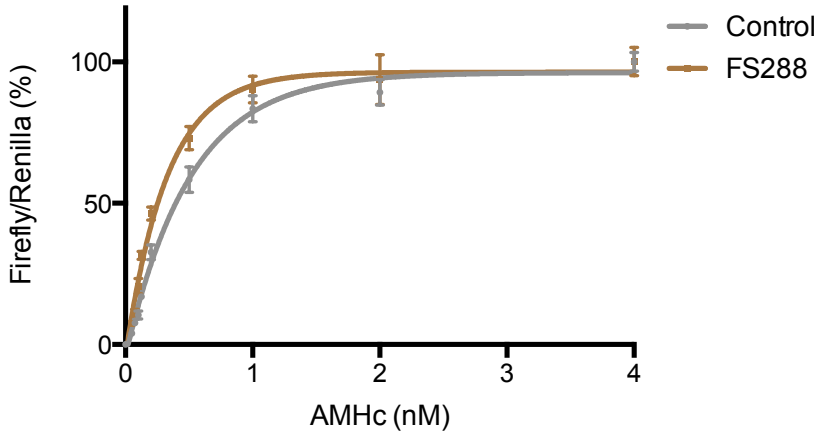
Control
FS288
Firefly/Renilla (%)
100
50
0
0
1
2
3
4
AMHc (nM)

(B)

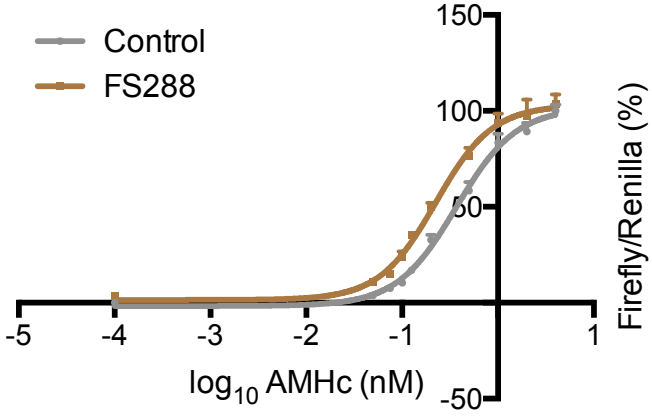
Control
FS288
150
100
50
-50
-5
-4
-3
-2
-1
1
log10 AMHc (nM)
Firefly/Renilla (%)

(C)

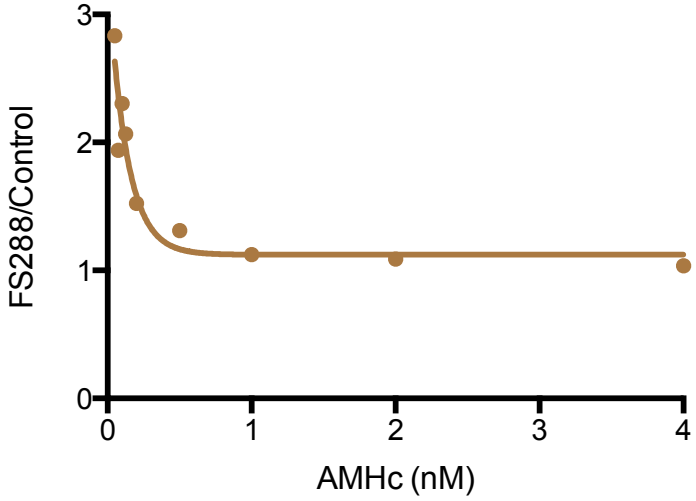
FS288/Control
3
2
1
0
0
1
2
3
4
AMHc (nM)

Figure 4-11. Follistatin 288 altered the EC50 for AMH_C

The influence of FS288 on the response of the P19 reporter cells to AMH_C is illustrated. FS288 was added in a large molar excess relative to the maximum concentration of AMH_C (Table 4-2). The data is illustrated as the mean plus the standard error of the mean of 6 wells for each concentration point, in both the control and FS288-treated curves. The statistical analysis of each curve was from the 60 data points, as described in Section 2.1.5. (A) A dose-response curve was fitted using the "sigmoidal dose-response (variable slope)" function of Prism. (B) The data were log transformed in Prism and the two curves compared using the "log (agonist) vs. response - variable slope (four parameters)". The groups were significantly different from each other with $p<0.0001$. (C) This panel illustrates the effect of FS288 varies with the concentration of AMH_C. The data was calculated as described in Figure 4-6.

When 20 nM of FS288 was added to a dose-response curve for $AMH_{N,C}$, the curve was significantly different to control ($p<0.0001$), with a lowered EC50 (Figure 4-12A). However, the dose-response curve did not exhibit a typical sigmoidal shape, raising the possibility that an error had occurred. The experiment was therefore repeated. FS288 again shifted the dose-response curve to the left ($p<0.0001$), with the EC50 decreasing from 0.54 nM to 0.28 nM (Figure 4-12B). The curve had a normal sigmoidal shape (Figure 4-12B). FS288 did not significantly increase the maximum response produced by $AMH_{N,C}$ (Figure 4-12B and Figure 4-13B). In the second screen, 20 nM of FS288 increased the reporter response to 0.16 nM of $AMH_{N,C}$ by 29% ($p<0.0005$) (Figure 4-5B). The post-hoc analysis was examined by calculating the ratio of the reporter activity in the presence and absence of the BP for each concentration of AMH. Values greater than 1 were observed with low doses of AMH_C with FS288 (Figures 4-12C). The effect of FS288 was dose-dependent across a range spanning 0.1 to 5 nM, when the concentration of $AMH_{N,C}$ was 0.2 nM (Figure 4-14A).

(A)

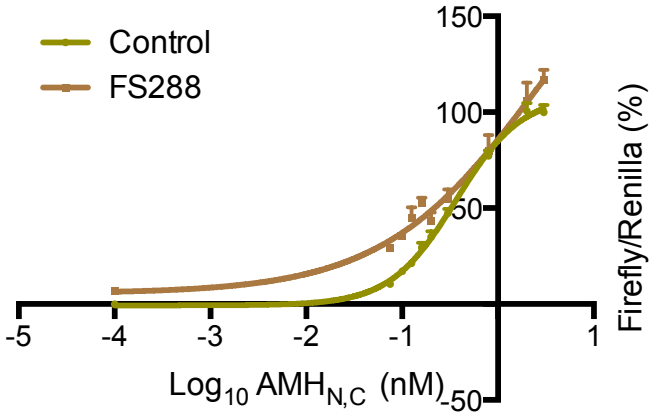
Control
FS288
150
100
50
-50
-5
-4
-3
-2
-1
1
Log10 AMHN,C (nM)
Firefly/Renilla (%)

(B)

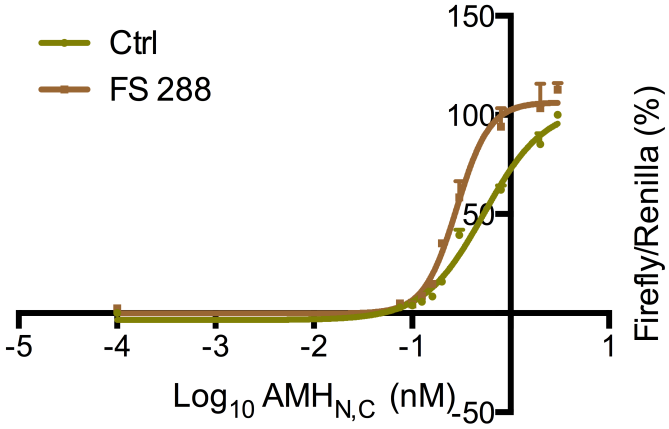
Ctrl
FS 288
150
100
50
-50
-5
-4
-3
-2
-1
1
Log10 AMHN,C (nM)
Firefly/Renilla (%)

(C)

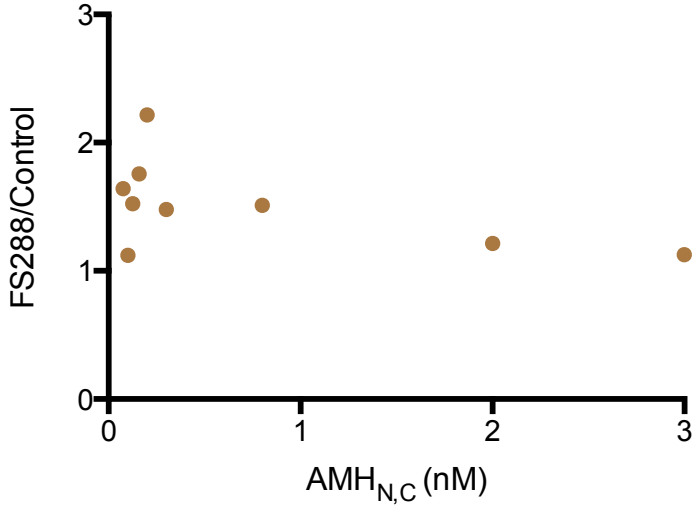
3
2
1
0
0
1
2
3
FS288/Control
AMHN,C (nM)

Figure 4-12. Follistatin 288 altered the EC50 for $AMH_{N,C}$

The influence of FS288 on the response of the P19 reporter cells to $AMH_{N,C}$ is illustrated. FS288 was added in a large molar excess relative to the maximum concentration of $AMH_{N,C}$ (Table 4-2). The data is illustrated as the mean plus the standard error of the mean of 6 wells for each concentration point, in both the control and FS288-treated curves. The statistical analysis of each curve was from the 60 data points, as described in Section 2.1.5. (A) and (B) illustrate two replicate experiments The data were log transformed in Prism and the two curves compared using the "log (agonist) vs. response - variable slope (four parameters)". The curves in (A) and (B) were significantly different from each other with $p<0.0001$. (C) The possibility that the effect of FS288 varies with the concentration of $AMH_{N,C}$ was examined using the method described in Figure 4-6.

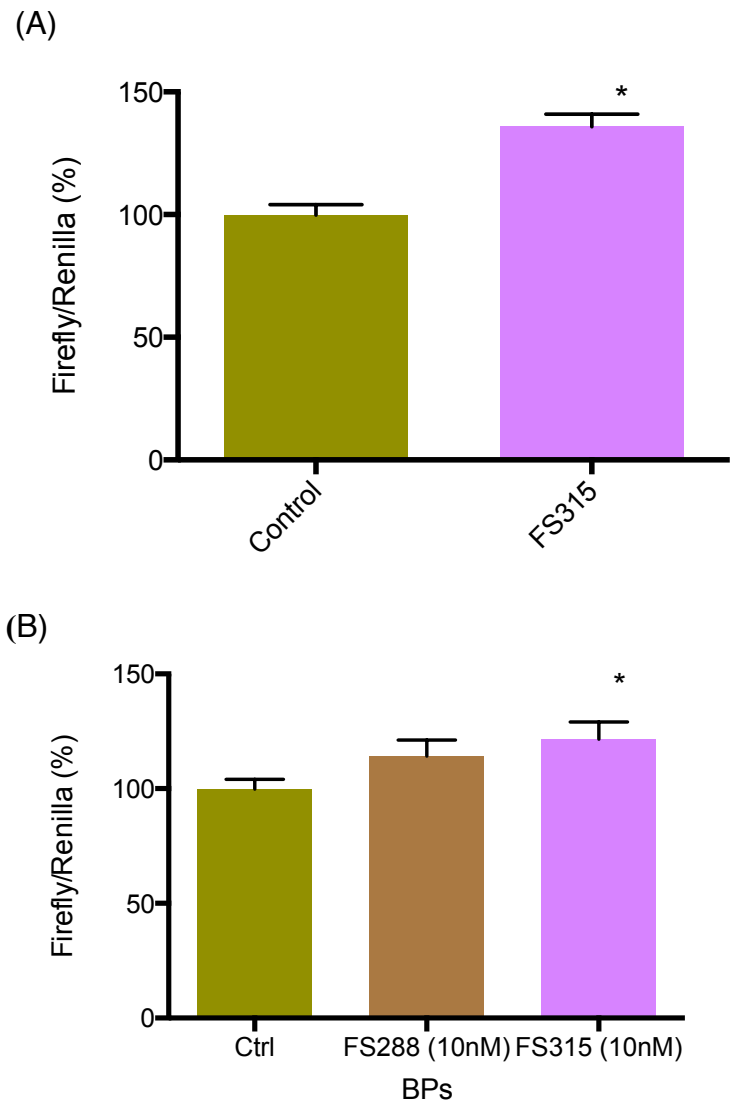

Figure 4-13. The follistatins affect AMH signaling at moderate and high $AMH_{N,C}$ concentrations

(A) The effect of FS315 on the reporter activity produced by an EC50-like concentration of $AMH_{N,C}$ (0.16 nM). The bars represent the mean + the standard error of the mean with an n of 8 wells. The * indicates that the groups were significantly different from each other, one-way ANOVA with p value of p=0.0005. (B) The effect of FS288 and FS315 on the reporter activity produced by 3nM $AMH_{N,C}$. The bars represent the mean + the standard error of the mean, with an n of 8 wells. The * indicate the groups were significantly different from each other, one-way ANOVA with a p value adjusted for multiple tests, p=0.029.

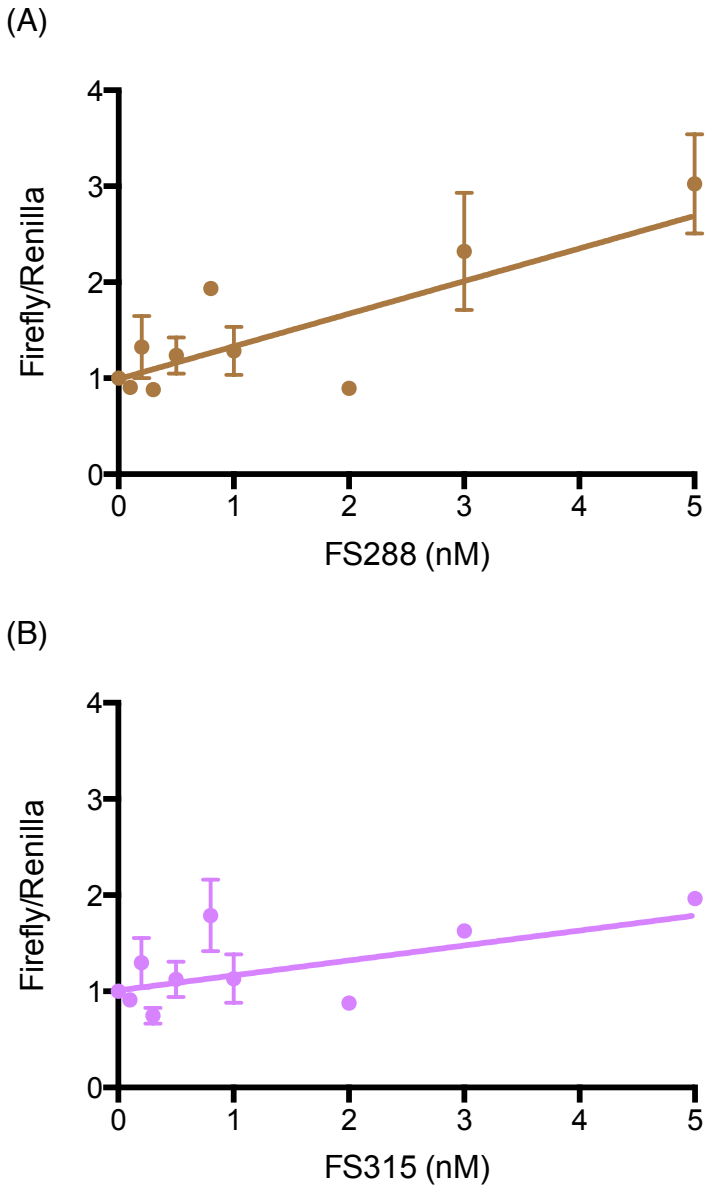

Figure 4-14. The follistatins have a dose-dependent effect on 0.2 nM $AMH_{N,C}$.

The influence of (A) FS288 and (B) FS315 on the reporter activity generated by 0.2 nM $AMH_{N,C}$ is illustrated. Each data point is the mean ± the standard error of the mean of 6 wells. The data were significantly different to zero, linear regression (A) $p<0.0001$, (B) $p=0.01$.

4.2.1.5 Follistatin 315 may differentially affect AMH_C and $AMH_{N,C}$

FS288 and FS315 are splice variants. FS315 was added to the screen for BPs at a late stage of the thesis, after the FS288 data was obtained. Ten nM FS315 did not significantly affect the dose-response curve of the P19 reporter cells to AMH_C (Figure 4-15). FS315 was not included in either of the secondary screens using AMH_C (Figure 4-4) or $AMH_{N,C}$ (Figure 4-5) as FS315 was only obtained after these screens had been completed.

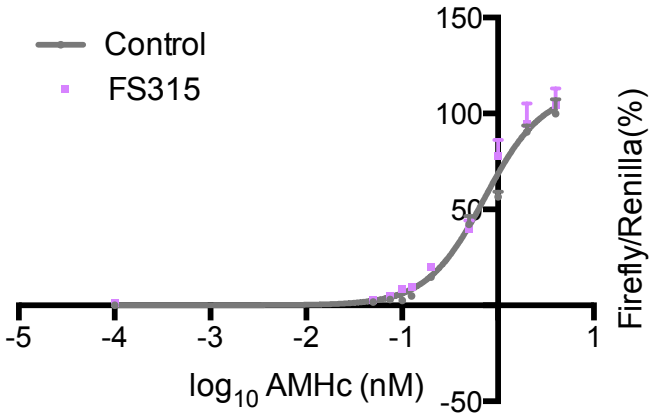

Figure 4-15. Follistatin 315 did not influence the dose-response curve to AMH_C

The influence of FS315 on the response of the P19 reporter cells to AMH_C is illustrated. FS315 was added in a large molar excess relative to the maximum concentration of AMH_C (Table 4-2). The data is illustrated as the mean plus the standard error of the mean of 6 wells for each concentration point, in both the control and FS315-treated curves. The statistical analysis of each curve was from the 60 data points, as described in Section 2.1.5. The data were log transformed in Prism and the two curves compared using the "log (agonist) vs. response - variable slope (four parameters)".

FS315 was also examined with $AMH_{N,C}$, despite the negative result obtained with AMH_C, to enable the activities of FS288 and FS315 to be compared. In contrast to the results obtained with AMH_C, 10 nM of FS315 significantly increased the reporter activity produced by 0.16 nM of $AMH_{N,C}$ ($p=0.0005$) (Figure 4-13A). There was also a small but significant increase in the reporter activity when a high concentration (3 nM) of $AMH_{N,C}$ was used ($p=0.029$) (Figure 4-13B). These experiments were undertaken in preference to a dose curve as there was insufficient $AMH_{N,C}$ available. The FS315-induced amplification of the effect of 0.2 nM $AMH_{N,C}$ was dose-dependent (Figure 4-14B), although the potency of FS315 was less than that of FS288 (compare Figure 4-14A and 4-14B).

4.2.2 Activin and the reporter assay

The classical action of FS is to block the actions of activin, although this is not its only function (Chapter 1.5.4). The first step towards understanding how FS may affect the AMH reporter assay was therefore to determine whether the observed affect of FS was secondary to an effect on activin. Activin A did not activate the $(BRE)_2$-Luc reporter construct, irrespective of whether the P19 cells were transfected with AMHR2 or a control vector (Figure 4-16). This is consistent with the generally accepted pathway for activin signaling, which involves SMAD2/3 rather than SMAD1/5/8. However, this does not exclude the possibility that activation of the SMAD2/3 pathway affects signaling via SMAD1/5/8. If this occurs, then the dose-response curves to AMH would change when activin A was present. 10 nM of activin A caused a small but statistically significant change to the dose response curve, involving an increase in the maximum (top) value ($p=0.0012$, Figure 4-17A). There was no clear effect of activin A at lower doses of AMH_C, or around the EC50 concentration (Figure 4-17B).

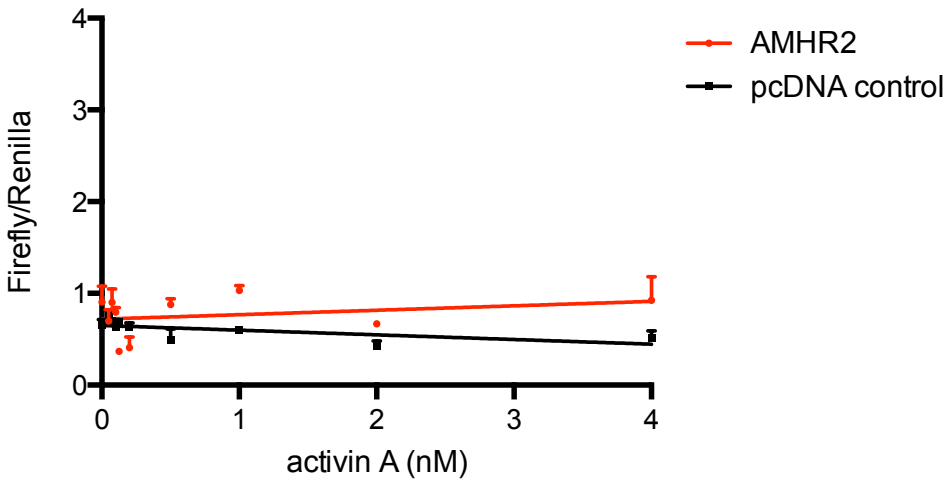

Figure 4-16. Activin A does not have a dose-dependent effect on reporter activity

P19 cells were transfected with AMHR2 or pcDNA3.1(+), along with (BRE)2-Luc and phRL-SV40. Each data point is the mean + standard error of 3 wells. A dose-response curve was fitted using the "sigmoidal dose-response" function of Prism.

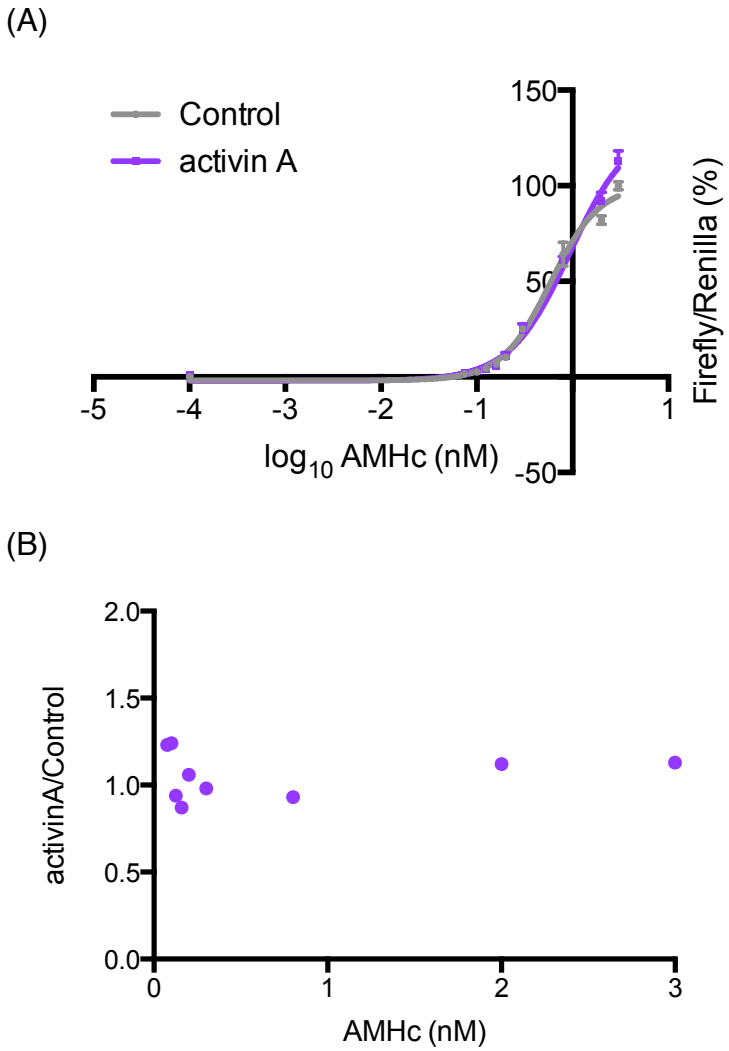

Figure 4-17. Activin A does not inhibit AMH_C signaling at low concentrations

The influence of Activin A on the response of the P19 reporter cells to AMH_C is illustrated. Activin A was added in a large molar excess relative to the maximum concentration of AMH_C (10 nM). The data is illustrated as the mean plus the standard error of the mean of 6 wells for each concentration point, in both the control and Acticin A -treated curves. The statistical analysis of each curve was from the 60 data points, as described in Section 2.1.5. (A) The data were log transformed in Prism and the two curves compared using the "log (agonist) vs. response - variable slope (four parameters)". The two curves were significantly different ($p=0.0012$), due to an elevated top value for the activin A treated group. When the high concentrations of AMH ($\geq$ 2 nM) were omitted, the two curves were not different. (B) The relative effect of activin A at difference concentrations of AMH_C is illustrated (see legend of Figure 4-6 for a description of the method).

4.2.3 Do binding proteins influence an AMH ELISA?

FS288 is a serum protein [212]. Consequently, the results reported above raise the possibility that part or all of the AMH in the circulation may be bound to FS288. If so, then FS288 may prevent anti-AMH antibodies binding to AMH in immunoprecipitation experiments and in immunoassays, such as ELISAs. A similar argument can be made in reference to the study of the gonadal functions of AMH, as FS288 and other BPs are present in the gonads, including ovarian follicular fluid [56, 213, 214]. The effect of selected BPs on the detection of AMH in the Beckman Coulter Gen II ELISA were therefore examined, with the dual purpose of determining whether BPs have the potential to confound the ELISA and as a first test of whether the BPs that influence the EC50 of AMH in the reporter assay bind directly to AMH.

None of the BPs that affected the $AMH_{N,C}$ EC50 of the P19 reporter assay (Section 4.2.1) altered the quantitation of 29 pM of $rhAMH_{N,C}$ (Figure 4-18).

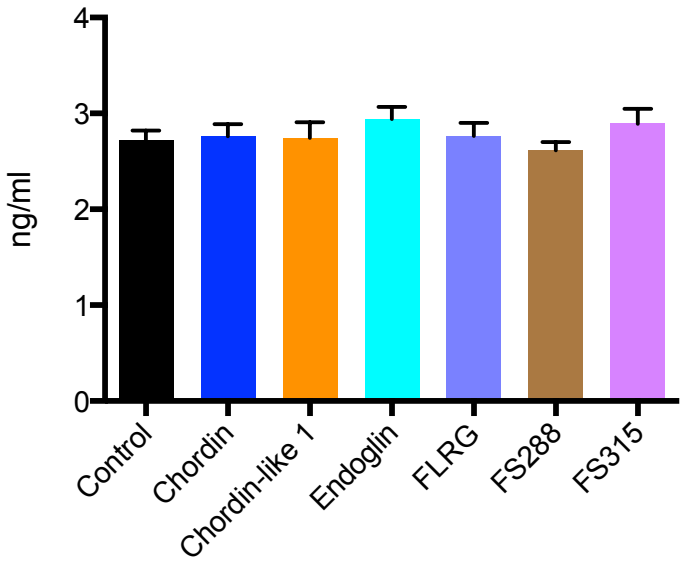

Figure 4-18. Binding proteins do not interfere with an AMH ELISA

The BPs which affected AMH signaling in previous experiments were tested to determine whether they altered the detection of AMH in the Gen II AMH ELISA.
20 nM of either chordin, chordin-like1, endoglin, FLRG, FS288 or FS315 were added to 29 pM of rh-$AMH_{N,C}$, and the level of AMH measured in triplicate, using an ELISA. The bars represent the mean + the standard error of the mean. The data were first normalized as a percentage of the control, in the absence of any added BP. There was no significant effect in the experiment as a whole (one-way ANOVA).

4.3 Discussion

4.3.1 Overview

This Chapter has examined the ability of the 15 known TGFβ-superfamily BPs to influence AMH signaling, using a broad screen. The BPs that had the greatest influence on AMH signaling were the FSs, which ironically were amongst the last of the BPs to be tested. This discussion therefore begins with an overview of FS, and the possible relevance of FS to the understanding of AMH biology. Three BPs (brorin, decorin and FS-like 4) had small effects and are discussed together. Similarly, the two BPs (endoglin and chordin-like 2) that depressed the bottom of the AMH dose curve are discussed together. The Chapter ends with a discussion of the biological relevance of identifying which BPs do not influence AMH signaling. The aims of this Chapter were to undertake the first exploration of AMH BPs and consequently there is no prior literature relating to AMH and BPs to discuss.

4.3.2 Follistatin appeared to increase AMH signaling

FS288 had the strongest effect on the dose-response curve for AMH_C, and was therefore selected for additional examination (Table 4-4). A significant effect was also observed with the first $AMH_{N,C}$ dose-response curve, but the shape of the curve was atypical. When replicated, the effect was again strongly significant and a normal-shaped curve was observed. The effect of FS288 was greatest at lower concentrations of AMH, but was also detectable at concentrations around the EC50. A significant effect was observed when FS288 was added to 0.16 nM $AMH_{N,C}$. FS288 caused a non-significant ($p=0.078$) elevation of the effect of 0.5 nM of AMH_C. The magnitude of the effect of FS288 in this experiment was similar to that produced by 0.5 nM of AMH_C in the dose-response experiment. This suggests that the experiment was underpowered rather than a clear negative result, as the effect of FS288 was examined at a concentration where its effect on AMH signaling is small. Collectively, the data as a whole shows a robust effect of FS288 on AMH signaling.

FS315 and FS288 are splicing variants of the same gene [215-217]. FS315 was examined because a clear result was obtained with FS288. FS315 had a similar effect to FS288 in experiments using $AMH_{N,C}$, but no effect of FS315 was observed on the dose-response curve to AMH_C (Table 4-4). These results were obtained at the end of the thesis, and further experimentation is needed to prove whether FS315 regulates AMH signaling in a manner similar to FS288.

Table 4-4. Summary of FS288 and FS315

	AMH_C		**$AMH_{N,C}$**		
BPs	**0.5 nM**	**Dose curve**	**0.16 nM**	**Dose curve**	**0.2 nM $AMH_{N,C}$ and FS dose**
FS288	N.S.*	Increase	increase	increase top no change	dose-responsive
FS315	-	N.S.	increase	- (top increase)	dose-responsive (less effective than FS288)

* Note this experiment showed a non-significant increase in reporter activity (p=0.075), with the magnitude of the observed effect being consistent with that expected with the dose curve.

FS was a low priority to test at the beginning of the thesis, as its classical action is inhibitory, and the primary objective was to identify BPs that might enhance AMH activity. The canonical action of FS is to inhibit the binding of activin to the activin receptors [218, 219]. The effects of FS observed in the thesis are not secondary to an indirect effect of FS on endogenous activins. If this were happening, the putative

endogenous activins would need to be suppressing AMH signaling. However, the addition of activin A to the medium had a slight positive effect on AMH signaling.

The screen for BPs was designed to detect inhibition of AMH signaling, as the addition of a BP to the medium was expected to bind to the AMH in the medium, thus limiting its ability to bind to the AMH receptors. This presumption was based on the actions of betaglycan, which enhances signaling when membrane-bound and inhibits signaling when in its soluble form (Chapter 1.5.4.1). The observed effects of the FSs were thus in the opposite direction to the initial expectation. This issue appears to have arisen because the molecular mechanism of FS action is not modeled by betaglycan.

The FSs do not have a transmembrane domain, in contrast to betaglycan. The FS are secreted as soluble proteins, but then associate with the cell membrane by binding to heparan sulfate [118, 214]. Consequently, when FS is added to the medium, it would be expected to bind to the cell surface of the P19 cells, provided they express significant levels of heparin-sulfate proteoglycans. FS binds BMPR1A [220]. This creates the following testable hypothesis; FS binds AMH, and concentrates it at the surface of the cell, through its ability to bind to heparan sulfate. The ability of FS to bind to BMPR1A, would then bring AMH into close association with BMPR1A. BMPR2 can bind to BMPR1A in the absence of ligand [204]. It is not known whether AMHR2 can also do this. If it does, then FS would act to concentrate AMH, BMPR1A and AMHR2 at one site. This may decrease the EC50 for an AMH response by creating a local concentration of AMH near its receptor. Equally, AMH bound to FS may have a lower Kd for its receptors than AMH alone, in a manner analogous to the way that betaglycan facilitates the binding of TGFβ2 and inhibin to receptors.

The FS isoforms differ markedly in their ability to bind to heparan sulfate [118, 214]. FS288 has the highest affinity for heparan sulfate, and is a putative autocrine /paracrine regulator which is thought to have limited ability to diffuse from its site of synthesis. FS315, in contrast, is a serum protein and therefore has a low affinity for heparan sulfate. Consequently, FS315 would be expected to be less potent that FS288 as an enhancer of AMH signaling, if the heparan sulfate binding is important for this

activity. Further experimentation is required to test this, but the limited data discussed above is consistent with this (see Figure 4-14).

The TGFβ-superfamily binding site on FS is on the N-terminal portion of FS, which is common to FS288 and FS315 [221-223]. This binding site appears to be relatively non-specific, as FSs binds BMPs 2,4,6,7,11,15, inhibin and myostatin (GDF8), as well as activin [101, 220, 223, 224]. The binding of activin to FS occurs with high affinity and with limited spontaneous dissociation of the FS-activin complex [101, 222, 225]. In contrast, the BMPs bind to FS with a Kd that is between 1 and 10% of that of activin A [101, 116], with the FS-BMP complex being unstable [116]. This type of binding would facilitate FS-mediated activation but not inhibition, as any FS-mediated activation requires transfer of the ligand from FS to the signaling receptors, which requires FS to dissociate from the ligand. [226, 227]Furthermore, structural analysis of FS has revealed similarities between the activin binding sites on FS and ACVR1 [222, 223]. ACVR1 is a type-1 receptor for AMH (Chapter 1.6.7). Consequently, it is plausible that the FS-induced enhancement of AMH signaling involves a direct interaction between AMH and FS. The direct testing of this is an important next step in analyzing the relationship between FS and AMH.

In summary, FS288 and possibly FS315 are putatively AMH BPs. The concentrations of FS vary with the physiological context, and can be extremely high in some pathologies [226, 228]. The experiments reported in this Chapter used concentrations of FS that are within the natural range of FS in vivo. The current experiments were designed to detect BPs, and are not instructive of what the actions of the BPs may be in vivo. The possible physiological importance of FS-AMH interactions is discussed in Chapter 6.

4.3.3 Brorin, decorin, and follistatin-like 4 appeared to increase AMH signaling on dose curves

Three of the 13 BPs, brorin, decorin, and FS-like 4 caused a statistically significant change in the dose-response curve. The effect of these BPs were small and were only evident when the concentration of AMH was low. There was little or no effect at concentrations of AMH that were near or above the EC50, either in the dose curve (see Figure 4-3) or in the experiments using a single concentration of AMH. Overall, the data strongly suggested that brorin, decorin and FS-like 4 are unlikely to regulate the activity of AMH either in the gonads or in the circulation of boys.

The data does not exclude the possibility that brorin, decorin and/or FS-like 4 influence the effect of circulating AMH in adults. However, each of the BPs was added in supra-physiological concentrations and only produced a moderate amplification of AMH signaling. This suggests that these BPs would only have a minor or no effect of AMH signaling in vivo. These BPs are worthy of further study. However, the priority for this thesis was to detect more potent BPs, and a decision was made to examine further candidates, rather than to study brorin, decorin and/or FS-like 4 more intensely.

4.3.4 Endoglin and chordin-like 2 may inhibit endogenous cytokines

Endoglin and chordin-like 2 reduced the bottom (zero AMH) of the dose-response curve, but did not affect the reporter activity produced by AMH. This suggests that they are not regulators of AMH, and that their effect on the reporter assay is unrelated to AMH. Endoglin and chordin-like 2 inhibit the activity of multiple TGFβ-superfamily ligands [109, 229, 230] and their effect on the assay is presumably related to inhibition of TGFβ-superfamily ligands present in the medium and/or produced by P19 cells (see Chapter 3.3.1.2 and Chapter 4.1.4). The identity and source of the ligands was not investigated as this issue is outside of the scope of the thesis.

4.3.5 BPs and the quantitation of AMH

The detection of AMH within an ELISA is dependent on the antibody binding sites on AMH being accessible. AMH BPs in biological fluids could potentially interfere with the detection of AMH, by blocking the binding of AMH to either capture or the detection antibody of the ELISA. For this reason, the affect of FSs, and other putative AMH BPs, on the Beckman Coulter AMH Gen II ELISA was briefly examined. No interference was detected, suggesting that current AMH ELISAs are not confounded by endogenous BPs.

4.3.6 Most of the TGFβ-superfamily binding proteins did not affect AMH signaling

Eight of the BPs tested appeared to have little or no effect on either the EC50 or the top of the AMH dose curve. Putatively, BPs may affect AMH signaling at the low end of the curve (adult-circulating-like levels), the middle of the curve (boy-circulating-like levels) or the top of the curve (gonadal/paracrine-like levels). Consequently, the absence of a clear effect of a BP on the dose-response curve is relatively strong evidence that the BP does not affect AMH signaling in any context.

One limitation of the experiment is that the molecular context of the BP may not be appropriate. All BPs were added to the culture medium. This mimics the *in vivo* action of the soluble forms of the BP. However, many of the BPs can also be attached to the cell membrane and/or the extracellular matrix. With BPs such as betaglycan, this alters the way a cell responds to a ligand (Chapter 1.5.4.1), but it does not alter the ability of the ligand to bind to the BP. This suggests that the current tests have a sound basis, but it is not possible to be completely certain that the association between AMH and BPs will conform to the proven actions of the well-studied BP-ligand interactions.

Another limitation of the experiments is that the biological activity of the BPs was not directly tested. The BPs were verified as active by the manufacturer, but this does not exclude the possibility that the product degraded during transport. The BPs were added to the cultures at a concentration that was at least an order of magnitude greater

the EC50 concentration of AMH. This was done to maximize the chance of observing an effect, but this would also have provided some protection against partial degradation of the BP. The BPs would have been expected to have observable effects at the low end of the AMH dose curve, even if greater than 90% of the bioactivity had been lost. The above not withstanding, in an ideal world the activity of each BP would have been verified, with this being an acknowledged weakness in the data. This was not initially done, as the normal tests of the bioactivity of the BPs would have required new assays to be established. At the time, I elected to test other BPs rather than to establish a new assay for each BP. However, with the benefit of hindsight, the current assay could have been used to test the BMP-related BPs, by including a BMP positive control, with and without the BP being tested.

One reason for being certain that a BP does not regulate AMH is that the inability of certain BPs to influence AMH signaling may be biologically important. AMH and BMPs share a common downstream pathway, and *in vivo* many cell types may be co-regulated by AMH and BMP. If a BP affects BMP signaling, without also effecting AMH signaling, then it may alter the relative influence of AMH and BMP on the SMAD1/5/8 pathway. This requires experimental verification, but the possible importance of this is illustrated by the following hypothesis. AMH is male-specific during early development, while the BMPs are common to males and females. If the BMPs and AMH have equal effect on the SMAD1/5/8 pathway, the activation of the SMAD1/5/8 pathway would be approximately twice as large in males as in females. If a BMP BP is added, the BMP activation would be reduced. If the reduction was 50%, then female activation of SMAD1/5/8 reduces by half, but the male signaling will only reduce by 25%. Consequently, the magnitude of the difference between male and female activation would increase. If this is correct, then the extent of AMH-induced sexual dimorphism would vary from site-to-site in a male, depending on the relative suppression/activation of BMP and AMH signaling (Figure 4-19).

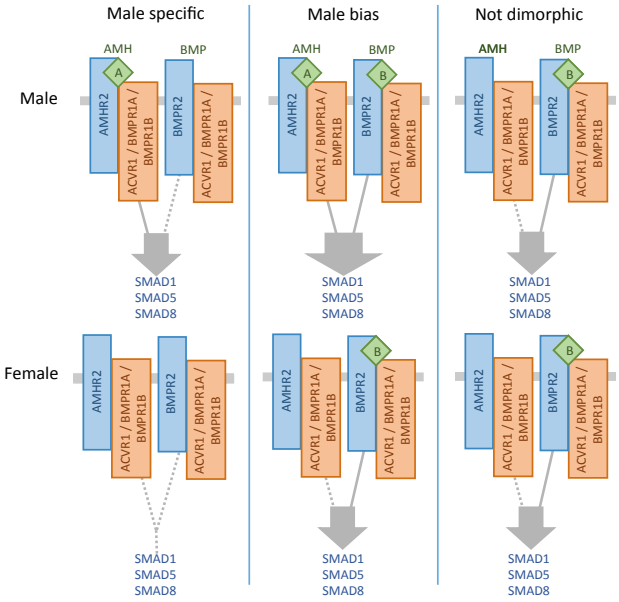

Figure 4-19. The combination of AMH and BMP produces sex differences

If AMH signaling only, the SMAD1/5/8 pathway can create male specific pathway. If both AMH and BMP signal, the SMAD 1/5/8 pathway can create a male bias. If BMP signaling only, the SMAD1/5/8 pathway is not sexual dimorphic.

4.3.7 Gremlins

The BMP inhibitors, gremlin1 or 2, have recently been reported to inhibit the effect of AMH_C on the transition of primordial follicles to the primary follicle in ovarian organ cultures [231]. An antibody to gremilin 2 co-immunoprecipitated AMH_C, suggesting that the gremilins are AMH BPs [231]. These experiments used 0.36 nM of AMH_C, which corresponds to the range of AMH in the circulation of boys. It would be interesting to test the influence of gremlins across the full range of physiological levels, with the reporter assay developed in this thesis being an appropriate first test of this.

4.3.8 Conclusion

At the beginning of the thesis, AMH signaling was thought to occur without any modulation by BPs, in marked contrast to mode of action of the TGFβ superfamily. This Chapter presents the first evidence that several of the known TGFβ-superfamily BPs may influence AMH signaling. The strongest evidence is for FS288, but other BPs such as FS315, brorin, decorin and FS-like 4 need further study. The current experiments are principally an indirect test of chemistry, a test of whether AMH binds to the putative BP in solution. The next step is to test whether any of the putative BPs are relevant to physiological or pathological contexts. This is beyond the time constraints of this thesis to experimentally examine this question, but the possible importance of AMH BPs *in vivo* is discussed in Chapter 6. The next Chapter, discusses a further screen for AMH BPs.

Chapter 5: Do binding proteins regulate the activation of AMH?

5.1 Introduction

5.1.1 The cleavage of proAMH is variable

Recombinant forms of AMH that were generated from the full coding region of the gene contain a mixture of proAMH and $AMH_{N,C}$, with proAMH being the major species ([153] see also Figure 5-3). Similarly, the AMH secreted from cultured testes contains a high proportion of proAMH [152]. Both of these observations suggest that proAMH may be inefficiently cleaved but the significance of this has been generally overlooked. Hence, many studies of AMH signaling have used preparations that contain high levels of proAMH, which does not bind to AMHR2. This has lead to misleading data, such as EC50 for AMH that are outside of the physiological range (Chapter 4, Table 4-1).

During the early stages of this thesis, the Otago AMH Neurobiology Group undertook the first qualitative study of the form of AMH in normal human circulation. Their results showed that AMH in the circulation is a mixture of proAMH and $AMH_{N,C}$ [141]. This issue could not initially be advanced, as existing ELISAs detected both forms [151]. The Otago AMH Neurobiology Group therefore invented a proAMH-specific ELISA [190] and undertook the initial quantitative studies of the form of AMH in the human circulation. The group's unpublished results showed that AMH is inefficiently cleaved by boys and girls, with the result that proAMH is more abundant than $AMH_{N,C}$ in the circulation of preadolescent males. The extent that proAMH was cleaved to $AMH_{N,C}$ varied between similarly aged individuals of the same sex. Unpublished data from the group also showed that the $AMH_{N,C}$ in the serum was cleaved within the gonad, before release. These observations provide the first evidence that biological activity of the AMH in the circulation is partially regulated by the extent to which proAMH is cleaved within the gonad.

The fate of proAMH in the circulation is currently unknown. The Müllerian duct is thought to be able to cleave AMH in vitro [10, 142], but it is unknown whether some tissues (other than the gonads) are able to cleave proAMH. If they do, the cleaved AMH does not return to the circulation.

5.1.2 Function of proAMH

The function of proAMH is unknown. Some procytokines have functions that are unrelated to the biological activities of the cleaved forms. For example, proNGF and NGF each produce distinct biological actions through distinct receptors, which work in co-operation with a shared receptor. This leads to context dependent biology, where the effect of proNGF released by one neuron is dependent on whether the target neuron can cleave the proNGF to NGF [10, 232-234]. To my knowledge, this type of phenomenon has not been described to date for the TGFβ superfamily.

The bioactivity of some TGFβ-superfamily members is regulated in part by whether the proform is cleaved. The uncleaved proTGFβ can be targeted for degradation, thus reducing bioactivity without reducing the initial synthesis of the cytokine [235]. It is unclear whether proAMH is an example of this, as proAMH is released to the circulation rather than being degraded within the gonads.

5.1.3 The cleavage of TGFβ proforms can be regulated by binding proteins

The cleavage of proTGFβs typically occurs intracellularly, during protein synthesis, with all proprotein molecules being cleaved. However, some TGFβ ligands can be secreted as proTGFβs, with extracellular activation of the proforms. The extent of cleavage of some proTGFβs is actively regulated, with BPs being part of this mechanism. For example, the cleavage of proTGFβ1 is controlled intracellularly by HtrA serine peptidase 1a (htra1A) [236], whereas cysteine-rich transmembrane BMP regulator 1 (CRIM1) regulates the cleavage of some BMPs intracellularly [237].

5.1.4 Cleavage of proAMH

AMH is synthesized as a proprotein and the first 24 amino acids are then removed to create proAMH. ProAMH does not activate AMH receptors, and the bioactivity of AMH through AMHR2 is thus dependent on cleavage proAMH (Chapter 1.6.5). The cleavage site for AMH is Arg-Ala-Gln-Arg [139, 146] (Figure 5-1), which is different to the proTGFβ site, which is Arg-His-Arg-Arg [152]. A wider ranger of enzymes cleaves the Arg-Ala-Gln-Arg than the Arg-His-Arg-Arg motif, with the result that multiple enzymes, including furin, are able to cleave proAMH *in vitro* (Chapter 1.6.5). These enzymes are expressed in the gonads and other tissues, with a complex pattern of expression [206]. Consequently, the variation in the extent of proAMH in blood in the population could in part be due to differing levels of cleavage enzymes. However, this does not exclude the possibility that cleavage of proAMH is also regulated by other factors, including BPs that act in a manner analogous to CRIM1 or htr1a.

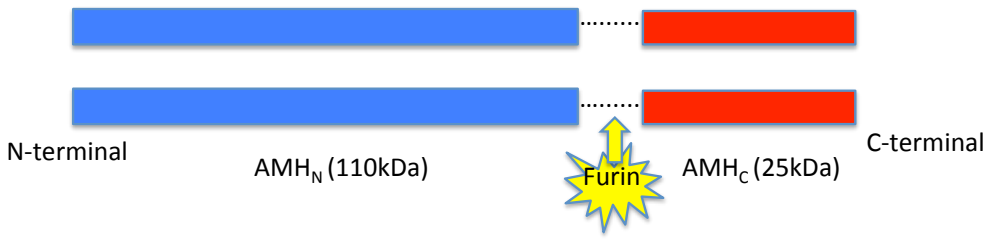

Figure 5-1. Furin cleaves proAMH

ProAMH can be cleaved by furin at an Arg-X-X-Arg site between 120 kDa AMH$_N$ and 25 kDa AMH$_C$.

5.1.5 Aims of Chapter 5

The objective of this Chapter was to determine whether any of the BPs examined in Chapter 4 were able to enhance or inhibit the activation of proAMH by influencing the ability of furin to cleave it.

5.2 Results

5.2.1 Optimizing the incubation time and the concentration of proAMH

BPs putatively could activate or inhibit the cleavage of proAMH. Consequently, the initial screen was done under conditions where approximately half of the proAMH had been cleaved. The precise conditions to achieve this were not known, although previous experience by the Otago AMH Neurobiology Group had provided some indicative data. The effect of a 4- and 8-hour incubation of a 1.2 nM solution of proAMH with furin was therefore examined, with two concentrations of proAMH (1.2 and 6.0 nM) being tested at 8 hours (Figure 5-2). The longer incubation only increased the extent of cleavage from 60% to 74%, suggesting that the activity of furin was diminishing with time. A 4-hour incubation time was therefore used in subsequent experiments. The higher concentration of proAMH (6 nM) gave brighter bands, but clear data was obtained from the lower concentration (1.2 nM), after densitometry readings. The lower concentration was therefore used, to conserve stocks of proAMH and to ensure that the BPs could be added in molar excess to the amount of proAMH.

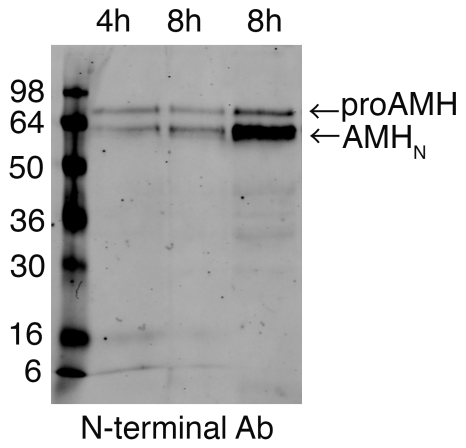

Figure 5-2. Four hours incubation cleaved half of proAMH

ProAMH (1.2nM and 6 nM) were incubated with furin for 4 hours and 8 hours. ProAMH and $AMH_{N,C}$ were detected by a Western blot consisting of samples of proAMH incubated with furin to demonstrate the relative quantities of proAMH and AMH_N present. The N-terminal antibody detects proAMH and AMH_N bands as indicated by the labeled arrows. Lane 1 is the molecular weight marker. Lane 2 (1.2 nM), 3 (1.2 nM), 4 (6 nM) had 4 hours, 8 hours, and 8 hours incubation time, respectively. The densitometry was measured by ImageJ and the data was normalized as a percentage of cleavage. Lane 2 had 40% proAMH and 60% $AMH_{N,C}$, Lane 3 had 26% proAMH and 74% $AMH_{N,C}$, Lane 4 had 20% proAMH and 80% $AMH_{N,C}$.

5.2.2 Do binding proteins affect cleavage of AMH?

The influence of 14 BPs (10-20 nM, Table 5-1) on furin-mediated cleavage of 1.2 nM of proAMH was tested, in replicated experiments. Half of the BPs were tested in three replicates, with the other half being tested twice, due to limitations in the availability of the batch of proAMH. This experiment was undertaken before FS288 was known to increase AMH signaling (Chapter 4). FS315 was therefore not

included in this experiment, as FS315 was only added to the BPs being tested after significant results were obtained with FS288.

The intensity of each band on the western blot was measured by densitometry (Figure 5-3). A small amount of the $AMH_{N,C}$ band was detected in the uncleaved proAMH, which was a normal feature of proAMH preparations [152] (Figure 5-3). None of the BPs tested caused a significant change to the intensity of the proAMH and $AMH_{N,C}$ bands, indicating that they did not affect the rate of furin-induced cleavage of proAMH.

Table 5-1. Binding proteins and the concentration used in this Chapter

Binding proteins	nM
Betaglycan	10
Brorin	20
Chordin	10
Chordin-like1	20
Chordin-like 2	20
DAN	20
Decorin	20
Endoglin	10
FS288	20
FS315	10
FS-like1	20
FS-like3 (FLRG)	20
FS-like 4	10
Noggin	20
α2-macroglobulin	10

The Table lists the concentration of the TGFβ BPs used in the experiments described in this Chapter.

(A1)

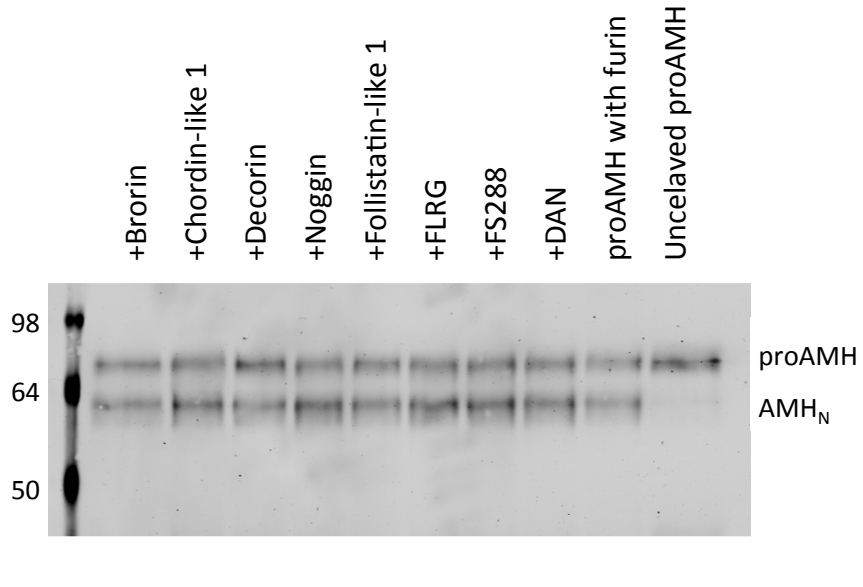
+Brorin
+Chordin-like 1
+Decorin
+Noggin
+Follistatin-like 1
+FLRG
+FS288
+DAN
proAMH with furin
Uncelaved proAMH
98
64
50
proAMH
AMH$_N$

(A2)

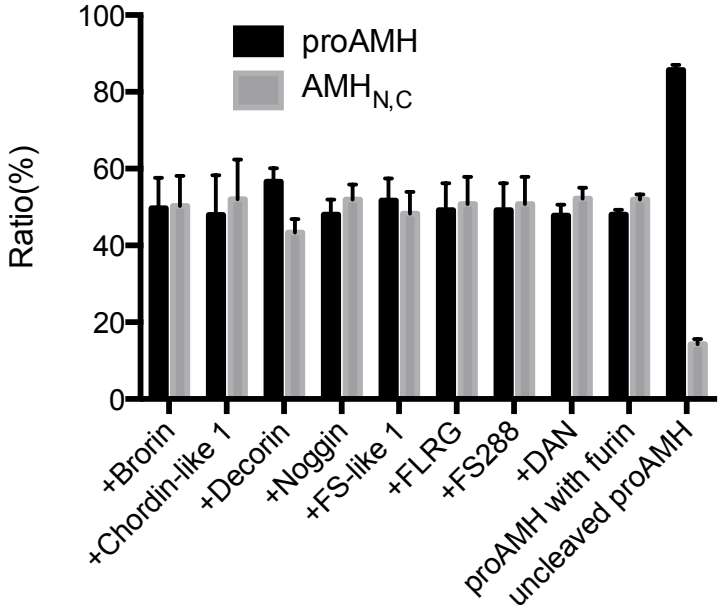
100
80
60
40
20
0
Ratio(%)
proAMH
AMH$_{N,C}$
+Brorin
+Chordin-like 1
+Decorin
+Noggin
+FS-like 1
+FLRG
+FS288
+DAN
proAMH with furin
uncleaved proAMH

(B1)

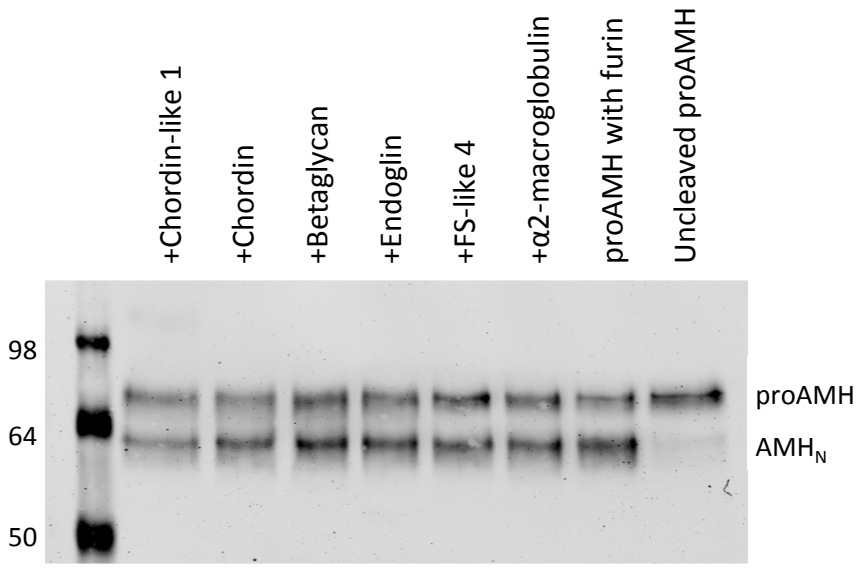

(B2)

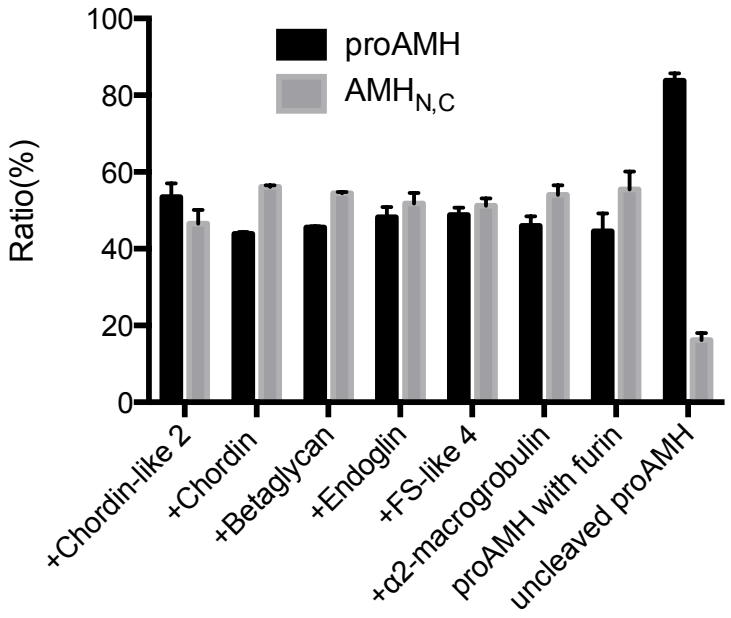

Figure 5-3. Binding proteins did not affect the cleavage of proAMH

ProAMH (1.2 nM) and furin were incubated with 14 BPs (10-20 nM) for 4 hours. An uncleaved proAMH sample was included to indicate the form of the starting material. The BPs were tested in two groups of 8 BPs (A) or 6 BPs (B). Representative Western blots are shown in A1 and B1. The relative abundance of proAMH and $AMH_{N,C}$ were calculated as described in Figure 5-2. Panels A2 and B2 illustrate the results obtained by combining replicate experiments. No statistical analysis was undertaken as the N value is only 2 or 3.

5.3 Discussion

5.3.1 Is proAMH cleavage regulated by binding proteins?

AMH is activated by the cleavage of proAMH, which occurs in the gonads, and putative elsewhere in the body, before the binding to the AMH receptors. However, locations, mechanism and regulation of the cleavage are unknown. One possibility is that the regulation is dependent on BPs. However, the TGFβ superfamily BPs tested in Chapter 5 did not affect the cleavage of proAMH by furin.

There are multiple enzymes that cleave proAMH in vitro, with these enzymes being widely expressed throughout the body [10]. To date, the physiological relevance of these enzymes for the cleavage of proAMH has not been tested. It is possible, that the ability of BPs to regulate the cleavage of proAMH is dependent on which enzymes are present. Consequently, one limitation of the current experiment is that it only relates to furin. The data does not exclude the possibility that the tested BPs regulate proAMH cleavage by other enzymes. Other enzymes were not tested, as they are not generally available, and the time commitment needed to generate them could not be justified, when the relevance of the enzymes to normal physiology is unproven.

5.3.2 Limitations of the experimental approach

The $AMH_{N,C}$ bands were slightly diminished in the presence of decorin and chordin-like 2, but no conclusion can be reached from these observations. The experiments described in this Chapter were designed to detect substantial inhibition, as the BPs known to regulate proTGFβ cleavage are potent. Furthermore, proAMH is abundant in fluids *in vivo*, suggesting that proAMH cleavage *in vivo* may be subject to significant inhibition. Western blots provide qualitative evidence, with multiple replicates needed to obtain even semi-quantitative estimates. The current data therefore does not exclude the possibility that one or more of the BPs slightly reduced the rate of cleavage. The detection of small or moderate inhibition of proAMH cleavage would require a quantitative test, such as a proAMH- and/or $AMH_{N,C}$-

specific ELISA. The Otago AMH Neurobiology Group has developed such ELISAs, but they were not available at the time when the work in this Chapter was conducted.

5.3.3 Conclusion

In summary, this Chapter describes a small exploratory extension from the main objective of this thesis (Chapter 3 & 4). The results obtained were negative, and this avenue of investigation was therefore stopped.

Chapter 6: Final conclusions and future research directions

6.1. Final conclusions

The concentration of AMH varies by orders of magnitude. Circulating levels of AMH in adults are low compared to those in boys, whereas the level of AMH in the serum of boys is low compared to levels within the gonads (Chapter 1.2.3, 1.3.4). This raised the issue of whether AMH signaling varied from context to context, under the influence of BPs. The putative BP was expected to change the EC50 of AMH by an order of magnitude but none of the tested BPs exhibited an effect of this magnitude. There are multiple reasons why a potent BP was not detected. First, and foremost, AMH signaling may not be subject to strong regulation by a BP. Second, 15 BPs were tested, but many other TGFβ-superfamily BPs exist. One of these untested BPs may be a potent regulator of AMH. Third, AMH has a unique type-2 receptor, and may therefore have a unique BP, that is not shared with other TGFβ-superfamily ligands. If so, a different strategy will be needed to discover it.

Although a potent regulator of AMH was not found, lesser effects were observed with some BPs. FS288 was the most significant of these, with a three-fold increase in AMH signaling being observed when the concentration of AMH was at adult-like levels. This may be particularly important for women whose levels of AMH decline as their ovarian reserve declines (Chapter 1.3.5). Signaling in the TGFβ superfamily is context dependent and broad conclusions cannot be made from the study of one context. For example, the interaction between FS288 and AMH signaling putatively involves proteoglycans, whose expression varies between cell types. Similarly, FS288 may combine with other BPs to produce stronger or weaker amplification of AMH signaling.

The forms of AMH in biological fluids have only recently been described and the regulation of the activation of proAMH by cleavage is incompletely described. The

effective concentration of AMH surrounding its receptors *in vivo* is therefore uncertain. Consequently, the understanding of when and where proAMH becomes cleaved is a critical issue to be resolved. A pilot study in Chapter 5 did not reveal any effect of BPs. However, definitive research into the regulation of cleavage cannot occur until the physiological sites and physiologically important enzymes have been identified.

The AMH reporter assay described in Chapter 3 can be used for multiple unrelated studies of AMH. It has been used in Chapter 4 to screen for AMH BPs. It can also be used to examine the interaction between AMH and other TGFβ superfamily ligands that activate the SMAD1/5/8 pathway. The interaction between AMH and BMPs was briefly examined in Chapter 3. The data is consistent with AMH and BMPs having convergent signaling, although further work is needed to prove this. This issue is biologically important, as AMH was originally thought to be an independent regulator of male sexual development, as AMH is the sole inducer of the Müllerian duct regression. Elsewhere in the body, AMH may produce sex biases by interacting with BMPs in developing tissues [10]. If so, the BPs, which inhibits BMPs but not AMH, may influence the magnitude of AMH-induced sexual dimorphism.

My Master of Science thesis related to the role of hormones in generating sexual dimorphism in fish. Therefore, at the beginning of the thesis, my interest related to the male-specific aspects of AMH. However, my experiments and reading about BPs, shifted my interest to the mechanism of the regulation of AMH. I have become especially interested in ovarian folliculogenesis, and the possibility that AMH, BMP and FS may interact to regulate it. This will be discussed in the next section.

6.2 Future direction

FS is a gonadal protein, which was originally discovered due to its ability to inhibit FSH [238]. AMH is also known to inhibit FSH and this prevents it from facilitating small antral follicles maturing into antral follicles (Figure 6-1). Furthermore, AMH blocks the recruitment of primordial follicles by decreasing the responsiveness of follicles to FSH (Chapter1.3.2). These ideas suggest that AMH and FS may interact with ovarian follicles. The combination of these local growth-regulating factors may have roles to regulate the individual follicles.

Similarly to AMH, BMPs are an important factors in folliculogenesis. In contrast to AMH, BMPs are positive regulators of primordial follicles developing into primary follicles. The expression of FS mRNA has not been reported in the stage between primordial follicles and preantral follicles. However, similar to AMH, FS may be expressed and secreted from the follicles in later stages, which may then affect the early stage follicles interacting with AMH or BMP. Therefore, the combined action of AMH, BMP, and (or) FS with FSH could be examined for preantral follicle growth on ovarian follicle development by using *in vitro* follicle culture system. This work could be expanded *in vivo* by using AMH deficient female mice or conditional knockout of these genes. Alternatively, the direct binding of AMH and FS could be also tested by immunoprecipitation or two-hybrid technique.

This Thesis showed FS increased AMH signaling with low AMH concentration, which may be important for ovarian reserve. Finding of the regulation mechanism of folliculogenesis by these proteins may eventually improve the infertility treatment such as IVF.

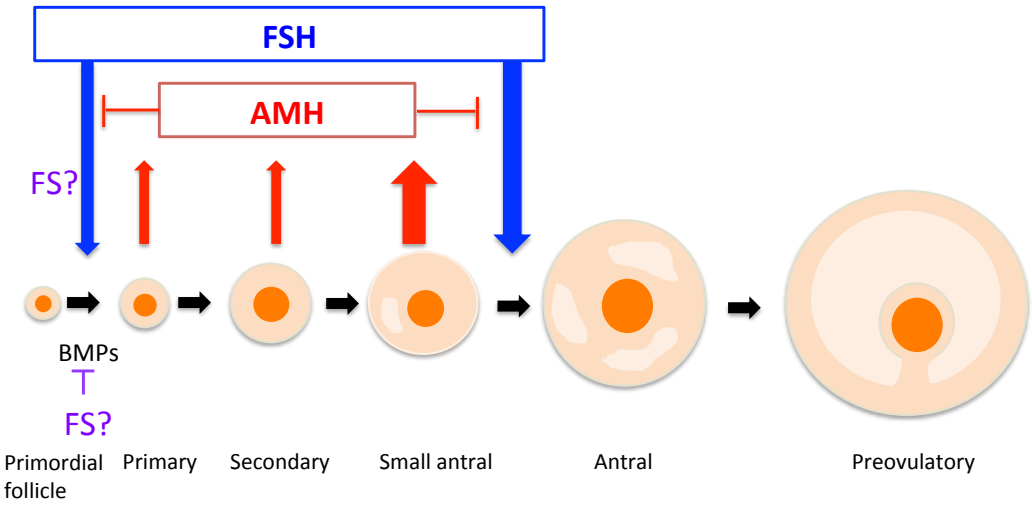

Figure 6-1. Schematic model of the actions of AMH and BMP in folliculogenesis.

AMH is produced by the small growing follicles. AMH inhibits initial follicle recruitment and inhibits FSH-dependent growth and selection of follicles. BMPs has been shown to stimulate the transition from primordial to primary follicle. FS may interact AMH and BMP and regulate these growth.

References

1. **Orvis GD, Jamin SP, Kwan KM, Mishina Y, Kaartinen VM, Huang S, Roberts AB, Umans L, Huylebroeck D, Zwijsen A, Wang D, Martin JF, Behringer RR** 2008 Functional redundancy of TGF-beta family type I receptors and receptor-Smads in mediating anti-Mullerian hormone-induced Mullerian duct regression in the mouse. Biol Reprod 78:994-1001
2. **Taguchi O, Cunha GR, Lawrence WD, Robboy SJ** 1984 Timing and irreversibility of Mullerian duct inhibition in the embryonic reproductive tract of the human male. Dev Biol 106:394-398
3. **Jirasek JE** 1971 Genital ducts and external genitalia: development and anomalies. Birth Defects Orig Artic Ser 7:131-139
4. **Teixeira J, Maheswaran S, Donahoe PK** 2001 Mullerian inhibiting substance: an instructive developmental hormone with diagnostic and possible therapeutic applications. Endocr Rev 22:657-674
5. **MacLaughlin DT, Donahoe PK** 2004 Sex determination and differentiation. N Engl J Med 350:367-378
6. **Lee MM, Donahoe PK** 1993 Mullerian inhibiting substance: a gonadal hormone with multiple functions. Endocr Rev 14:152-164
7. **Josso N, Picard JY** 1986 Anti-Mullerian hormone. Physiol Rev 66:1038-1090
8. **Imbeaud S, Carre-Eusebe D, Rey R, Belville C, Josso N, Picard JY** 1994 Molecular genetics of the persistent mullerian duct syndrome: a study of 19 families. Hum Mol Genet 3:125-131
9. **Belville C, Josso N, Picard JY** 1999 Persistence of Mullerian derivatives in males. Am J Med Genet 89:218-223
10. **McLennan IS, Pankhurst MW** 2015 Anti-Mullerian hormone is a gonadal cytokine with two circulating forms and cryptic actions. J Endocrinol 226:R45-57
11. **Teixeira J, He WW, Shah PC, Morikawa N, Lee MM, Catlin EA, Hudson PL, Wing J, Maclaughlin DT, Donahoe PK** 1996 Developmental expression of a candidate müllerian inhibiting substance type II receptor. Endocrinology 137:160-165
12. **Lee MM, Seah CC, Masiakos PT, Sottas CM, Preffer FI, Donahoe PK, MacLaughlin DT, Hardy MP** 1999 Müllerian-Inhibiting Substance Type II Receptor Expression and Function in Purified Rat Leydig Cells. Endocrinology 140:2819-2827
13. **Teixeira J, Fynn-Thompson E, Payne AH, Donahoe PK** 1999 Mullerian-inhibiting substance regulates androgen synthesis at the transcriptional level. Endocrinology 140:4732-4738
14. **Wu X, Arumugam R, Baker SP, Lee MM** 2005 Pubertal and adult Leydig cell function in Mullerian inhibiting substance-deficient mice. Endocrinology 146:589-595
15. **Lillie FR** 1916 The Theory of the Free-Martin. Science 43:611-613
16. **Vigier B, Tran D, Legeai L, Bezard J, Josso N** 1984 Origin of anti-Mullerian hormone in bovine freemartin fetuses. J Reprod Fertil 70:473-479
17. **Wang PY, Koishi K, McGeachie AB, Kimber M, Maclaughlin DT, Donahoe PK, McLennan IS** 2005 Mullerian inhibiting substance acts as a motor neuron survival factor in vitro. Proc Natl Acad Sci U S A 102:16421-16425

18. **Krishnan AV, Moreno J, Nonn L, Malloy P, Swami S, Peng L, Peehl DM, Feldman D** 2007 Novel pathways that contribute to the anti-proliferative and chemopreventive activities of calcitriol in prostate cancer. J Steroid Biochem Mol Biol 103:694-702
19. **Wang J, Dicken C, Lustbader JW, Tortoriello DV** 2009 Evidence for a Mullerian-inhibiting substance autocrine/paracrine system in adult human endometrium. Fertil Steril 91:1195-1203
20. **Long WQ, Ranchin V, Pautier P, Belville C, Denizot P, Cailla H, Lhomme C, Picard JY, Bidart JM, Rey R** 2000 Detection of minimal levels of serum anti-Mullerian hormone during follow-up of patients with ovarian granulosa cell tumor by means of a highly sensitive enzyme-linked immunosorbent assay. J Clin Endocrinol Metab 85:540-544
21. **Aksglaede L, Sorensen K, Boas M, Mouritsen A, Hagen CP, Jensen RB, Petersen JH, Linneberg A, Andersson AM, Main KM, Skakkebaek NE, Juul A** 2010 Changes in anti-Mullerian hormone (AMH) throughout the life span: a population-based study of 1027 healthy males from birth (cord blood) to the age of 69 years. J Clin Endocrinol Metab 95:5357-5364
22. **Lebeurrier N, Launay S, Macrez R, Maubert E, Legros H, Leclerc A, Jamin SP, Picard JY, Marret S, Laudenbach V, Berger P, Sonderegger P, Ali C, di Clemente N, Vivien D** 2008 Anti-Mullerian-hormone-dependent regulation of the brain serine-protease inhibitor neuroserpin. J Cell Sci 121:3357-3365
23. **Lutterodt M, Byskov AG, Skouby SO, Tabor A, Yding Andersen C** 2009 Anti-Mullerian hormone in pregnant women in relation to other hormones, fetal sex and in circulation of second trimester fetuses. Reprod Biomed Online 18:694-699
24. **Josso N, Lamarre I, Picard JY, Berta P, Davies N, Morichon N, Peschanski M, Jeny R** 1993 Anti-mullerian hormone in early human development. Early Hum Dev 33:91-99
25. **Lee MM, Donahoe PK, Hasegawa T, Silverman B, Crist GB, Best S, Hasegawa Y, Noto RA, Schoenfeld D, MacLaughlin DT** 1996 Mullerian inhibiting substance in humans: normal levels from infancy to adulthood. J Clin Endocrinol Metab 81:571-576
26. **Chong YH, Dennis NA, Connolly MJ, Teh R, Jones GT, van Rij AM, Farrand S, Campbell AJ, McLennan IS** 2013 Elderly men have low levels of anti-Mullerian hormone and inhibin B, but with high interpersonal variation: a cross-sectional study of the sertoli cell hormones in 615 community-dwelling men. PLoS One 8:e70967
27. **Guibourdenche J, Lucidarme N, Chevenne D, Rigal O, Nicolas M, Luton D, Léger J, Porquet D, Noël M** 2003 Anti-Müllerian hormone levels in serum from human foetuses and children: pattern and clinical interest. Mol Cell Endocrinol 211:55-63
28. **Morgan K, Dennis NA, Ruffman T, Bilkey DK, McLennan IS** 2011 The stature of boys is inversely correlated to the levels of their sertoli cell hormones: do the testes restrain the maturation of boys? PLoS One 6:e20533
29. **Carey MA, Card JW, Voltz JW, Germolec DR, Korach KS, Zeldin DC** 2007 The impact of sex and sex hormones on lung physiology and disease: lessons from animal studies. Am J Physiol Lung Cell Mol Physiol 293:L272-278
30. **Wang PY, Protheroe A, Clarkson AN, Imhoff F, Koishi K, McLennan IS** 2009 Mullerian inhibiting substance contributes to sex-linked biases in the brain and behavior. Proc Natl Acad Sci U S A 106:7203-7208

31. **Morgan K, Meredith J, Kuo JYA, Bilkey DK, McLennan IS** 2011 The sex bias in novelty preference of preadolescent mouse pups may require testicular Müllerian inhibiting substance. Behav Brain Res 221:304-306
32. **Dennis NA, Jones GT, Chong YH, van Rij AM, McLennan IS** 2013 Serum anti-Mullerian hormone (AMH) levels correlate with infrarenal aortic diameter in healthy older men: is AMH a cardiovascular hormone? J Endocrinol 219:13-20
33. **Appt SE, Chen H, Clarkson TB, Kaplan JR** 2012 Premenopausal antimullerian hormone concentration is associated with subsequent atherosclerosis. Menopause 19:1353-1359
34. **Fallat ME, Siow Y, Belker AM, Boyd JK, Yoffe S, MacLaughlin DT** 1996 The presence of mullerian inhibiting substance in human seminal plasma. Hum Reprod 11:2165-2169
35. **Al-Qahtani A, Muttukrishna S, Appasamy M, Johns J, Cranfield M, Visser JA, Themmen AP, Groome NP** 2005 Development of a sensitive enzyme immunoassay for anti-Mullerian hormone and the evaluation of potential clinical applications in males and females. Clin Endocrinol (Oxf) 63:267-273
36. **Fujisawa M, Yamasaki T, Okada H, Kamidono S** 2002 The significance of anti-Mullerian hormone concentration in seminal plasma for spermatogenesis. Hum Reprod 17:968-970
37. **Fenichel P, Rey R, Poggioli S, Donzeau M, Chevallier D, Pointis G** 1999 Anti-Mullerian hormone as a seminal marker for spermatogenesis in non-obstructive azoospermia. Hum Reprod 14:2020-2024
38. **Siow Y, Fallat ME, Amin FA, Belker AM** 1998 Mullerian inhibiting substance improves longevity of motility and viability of fresh and cryopreserved sperm. J Androl 19:568-572
39. **Fallat ME, Siow Y, Klar EA, Belker AM, MacLaughlin DT** 1998 The presence of Mullerian inhibiting substance binding sites in human sperm. J Urol 159:2210-2214
40. **Faddy MJ, Gosden RG, Gougeon A, Richardson SJ, Nelson JF** 1992 Accelerated disappearance of ovarian follicles in mid-life: implications for forecasting menopause. Hum Reprod 7:1342-1346
41. **Wallace WH, Kelsey TW** 2010 Human ovarian reserve from conception to the menopause. PLoS One 5:e8772
42. **McGee EA, Hsueh AJ** 2000 Initial and cyclic recruitment of ovarian follicles. Endocr Rev 21:200-214
43. **Hutt KJ, Albertini DF** 2007 An oocentric view of folliculogenesis and embryogenesis. Reprod Biomed Online 14:758-764
44. **Halpin DM, Charlton HM, Faddy MJ** 1986 Effects of gonadotrophin deficiency on follicular development in hypogonadal (hpg) mice. J Reprod Fertil 78:119-125
45. **te Velde ER, Scheffer GJ, Dorland M, Broekmans FJ, Fauser BC** 1998 Developmental and endocrine aspects of normal ovarian aging. Mol Cell Endocrinol 145:67-73
46. **Visser JA, Schipper I, Laven JS, Themmen AP** 2012 Anti-Mullerian hormone: an ovarian reserve marker in primary ovarian insufficiency. Nat Rev Endocrinol 8:331-341
47. **Kaipia A, Hsueh AJ** 1997 Regulation of ovarian follicle atresia. Annu Rev Physiol 59:349-363
48. **Weenen C, Laven JS, Von Bergh AR, Cranfield M, Groome NP, Visser JA, Kramer P, Fauser BC, Themmen AP** 2004 Anti-Mullerian hormone

expression pattern in the human ovary: potential implications for initial and cyclic follicle recruitment. Mol Hum Reprod 10:77-83

49. **La Marca A, Broekmans FJ, Volpe A, Fauser BC, Macklon NS, Table ESIGfRE--AR** 2009 Anti-Mullerian hormone (AMH): what do we still need to know? Hum Reprod 24:2264-2275
50. **Visser JA, de Jong FH, Laven JS, Themmen AP** 2006 Anti-Mullerian hormone: a new marker for ovarian function. Reproduction 131:1-9
51. **Durlinger AL, Kramer P, Karels B, de Jong FH, Uilenbroek JT, Grootegoed JA, Themmen AP** 1999 Control of primordial follicle recruitment by anti-Mullerian hormone in the mouse ovary. Endocrinology 140:5789-5796
52. **Durlinger AL, Gruijters MJ, Kramer P, Karels B, Kumar TR, Matzuk MM, Rose UM, de Jong FH, Uilenbroek JT, Grootegoed JA, Themmen AP** 2001 Anti-Mullerian hormone attenuates the effects of FSH on follicle development in the mouse ovary. Endocrinology 142:4891-4899
53. **Visser JA, Themmen AP** 2005 Anti-Mullerian hormone and folliculogenesis. Mol Cell Endocrinol 234:81-86
54. **Braem MG, Voorhuis M, van der Schouw YT, Peeters PH, Schouten LJ, Eijkemans MJ, Broekmans FJ, Onland-Moret NC** 2013 Interactions between genetic variants in AMH and AMHR2 may modify age at natural menopause. PLoS One 8:e59819
55. **Andersen CY, Schmidt KT, Kristensen SG, Rosendahl M, Byskov AG, Ernst E** 2010 Concentrations of AMH and inhibin-B in relation to follicular diameter in normal human small antral follicles. Hum Reprod 25:1282-1287
56. **Yding Andersen C, Rosendahl M, Byskov AG** 2008 Concentration of anti-Mullerian hormone and inhibin-B in relation to steroids and age in follicular fluid from small antral human follicles. J Clin Endocrinol Metab 93:2344-2349
57. **Jeppesen JV, Anderson RA, Kelsey TW, Christiansen SL, Kristensen SG, Jayaprakasan K, Raine-Fenning N, Campbell BK, Yding Andersen C** 2013 Which follicles make the most anti-Mullerian hormone in humans? Evidence for an abrupt decline in AMH production at the time of follicle selection. Mol Hum Reprod 19:519-527
58. **Richmond JR, Deshpande N, Lyall H, Yates RW, Fleming R** 2005 Follicular diameters in conception cycles with and without multiple pregnancy after stimulated ovulation induction. Hum Reprod 20:756-760
59. **Durlinger AL, Gruijters MJ, Kramer P, Karels B, Ingraham HA, Nachtigal MW, Uilenbroek JT, Grootegoed JA, Themmen AP** 2002 Anti-Mullerian hormone inhibits initiation of primordial follicle growth in the mouse ovary. Endocrinology 143:1076-1084
60. **Rajpert-De Meyts E, Jorgensen N, Graem N, Muller J, Cate RL, Skakkebaek NE** 1999 Expression of anti-Mullerian hormone during normal and pathological gonadal development: Association with differentiation of Sertoli and granulosa cells. Journal of Clinical Endocrinology & Metabolism 84:3836-3844
61. **Guibourdenche J, Lucidarme N, Chevenne D, Rigal O, Nicolas M, Luton D, Leger J, Porquet D, Noel M** 2003 Anti-Mullerian hormone levels in serum from human foetuses and children: pattern and clinical interest. Mol Cell Endocrinol 211:55-63
62. **Hagen CP, Aksglaede L, Sorensen K, Main KM, Boas M, Cleemann L, Holm K, Gravholt CH, Andersson AM, Pedersen AT, Petersen JH, Linneberg A, Kjaergaard S, Juul A** 2010 Serum levels of anti-Mullerian hormone as a marker of ovarian function in 926 healthy females from birth to

adulthood and in 172 Turner syndrome patients. J Clin Endocrinol Metab 95:5003-5010
63. **Kelsey TW, Wright P, Nelson SM, Anderson RA, Wallace WH** 2011 A validated model of serum anti-mullerian hormone from conception to menopause. PLoS One 6:e22024
64. **Seifer DB, Baker VL, Leader B** 2011 Age-specific serum anti-Mullerian hormone values for 17,120 women presenting to fertility centers within the United States. Fertil Steril 95:747-750
65. **Chong YH, Campbell AJ, Farrand S, McLennan IS** 2012 Anti-Mullerian hormone level in older women: detection of granulosa cell tumor recurrence. Int J Gynecol Cancer 22:1497-1499
66. **Robertson DM, Hale GE, Fraser IS, Hughes CL, Burger HG** 2008 A proposed classification system for menstrual cycles in the menopause transition based on changes in serum hormone profiles. Menopause 15:1139-1144
67. **de Vet A, Laven JS, de Jong FH, Themmen AP, Fauser BC** 2002 Antimullerian hormone serum levels: a putative marker for ovarian aging. Fertil Steril 77:357-362
68. **Hansen KR, Knowlton NS, Thyer AC, Charleston JS, Soules MR, Klein NA** 2008 A new model of reproductive aging: the decline in ovarian non-growing follicle number from birth to menopause. Hum Reprod 23:699-708
69. **Tsepelidis S, Devreker F, Demeestere I, Flahaut A, Gervy C, Englert Y** 2007 Stable serum levels of anti-Mullerian hormone during the menstrual cycle: a prospective study in normo-ovulatory women. Hum Reprod 22:1837-1840
70. **Eldar-Geva T, Ben-Chetrit A, Spitz IM, Rabinowitz R, Markowitz E, Mimoni T, Gal M, Zylber-Haran E, Margalioth EJ** 2005 Dynamic assays of inhibin B, anti-Mullerian hormone and estradiol following FSH stimulation and ovarian ultrasonography as predictors of IVF outcome. Hum Reprod 20:3178-3183
71. **Franks S** 1995 Polycystic ovary syndrome. N Engl J Med 333:853-861
72. **Polson DW, Adams J, Wadsworth J, Franks S** 1988 Polycystic ovaries--a common finding in normal women. Lancet 1:870-872
73. **Farquhar CM, Birdsall M, Manning P, Mitchell JM** 1994 Transabdominal versus transvaginal ultrasound in the diagnosis of polycystic ovaries in a population of randomly selected women. Ultrasound Obstet Gynecol 4:54-59
74. **Franks S, Roberts R, Hardy K** 2003 Gonadotrophin regimens and oocyte quality in women with polycystic ovaries. Reprod Biomed Online 6:181-184
75. **Laven JS, Mulders AG, Visser JA, Themmen AP, De Jong FH, Fauser BC** 2004 Anti-Mullerian hormone serum concentrations in normoovulatory and anovulatory women of reproductive age. J Clin Endocrinol Metab 89:318-323
76. **Das M, Gillott DJ, Saridogan E, Djahanbakhch O** 2008 Anti-Mullerian hormone is increased in follicular fluid from unstimulated ovaries in women with polycystic ovary syndrome. Hum Reprod 23:2122-2126
77. **Tal R, Seifer DB, Khanimov M, Malter HE, Grazi RV, Leader B** 2014 Characterization of women with elevated antimullerian hormone levels (AMH): correlation of AMH with polycystic ovarian syndrome phenotypes and assisted reproductive technology outcomes. Am J Obstet Gynecol 211:59 e51-58
78. **Lowery JW, de Caestecker MP** 2010 BMP signaling in vascular development and disease. Cytokine Growth Factor Rev 21:287-298

79. **Shi Y, Massague J** 2003 Mechanisms of TGF-beta signaling from cell membrane to the nucleus. Cell 113:685-700
80. **Massague J** 2012 TGFbeta signalling in context. Nat Rev Mol Cell Biol 13:616-630
81. **Mullen AC, Orlando DA, Newman JJ, Loven J, Kumar RM, Bilodeau S, Reddy J, Guenther MG, DeKoter RP, Young RA** 2011 Master transcription factors determine cell-type-specific responses to TGF-beta signaling. Cell 147:565-576
82. **Massague J, Blain SW, Lo RS** 2000 TGFbeta signaling in growth control, cancer, and heritable disorders. Cell 103:295-309
83. **Schmierer B, Hill CS** 2007 TGF[beta]-SMAD signal transduction: molecular specificity and functional flexibility. Nat Rev Mol Cell Biol 8:970-982
84. **Affolter M, Basler K** 2007 The Decapentaplegic morphogen gradient: from pattern formation to growth regulation. Nat Rev Genet 8:663-674
85. **Kicheva A, Gonzalez-Gaitan M** 2008 The Decapentaplegic morphogen gradient: a precise definition. Curr Opin Cell Biol 20:137-143
86. **Gold LI, Jussila T, Fusenig NE, Stenback F** 2000 TGF-beta isoforms are differentially expressed in increasing malignant grades of HaCaT keratinocytes, suggesting separate roles in skin carcinogenesis. J Pathol 190:579-588
87. **Mu Z, Yang Z, Yu D, Zhao Z, Munger JS** 2008 TGFbeta1 and TGFbeta3 are partially redundant effectors in brain vascular morphogenesis. Mech Dev 125:508-516
88. **Massague J** 1998 TGF-beta signal transduction. Annual Review of Biochemistry 67:753-791
89. **Walton KL, Makanji Y, Chen J, Wilce MC, Chan KL, Robertson DM, Harrison CA** 2010 Two distinct regions of latency-associated peptide coordinate stability of the latent transforming growth factor-beta1 complex. Journal of Biological Chemistry 285:17029-17037
90. **Umulis D, O'Connor MB, Blair SS** 2009 The extracellular regulation of bone morphogenetic protein signaling. Development 136:3715-3728
91. **Watabe T, Miyazono K** 2009 Roles of TGF-beta family signaling in stem cell renewal and differentiation. Cell Res 19:103-115
92. **Faure E, Gouedard L, Imbeaud S, Cate R, Picard JY, Josso N, di Clemente N** 1996 Mutant isoforms of the anti-Mullerian hormone type II receptor are not expressed at the cell membrane. Journal of Biological Chemistry 271:30571-30575
93. **Lane AH, Donahoe PK** 1998 New insights into mullerian inhibiting substance and its mechanism of action. J Endocrinol 158:1-6
94. **Pardali E, Goumans MJ, ten Dijke P** 2010 Signaling by members of the TGF-beta family in vascular morphogenesis and disease. Trends Cell Biol 20:556-567
95. **Lopez-Casillas F, Wrana JL, Massague J** 1993 Betaglycan presents ligand to the TGF beta signaling receptor. Cell 73:1435-1444
96. **Lewis KA, Gray PC, Blount AL, MacConell LA, Wiater E, Bilezikjian LM, Vale W** 2000 Betaglycan binds inhibin and can mediate functional antagonism of activin signalling. Nature 404:411-414
97. **Wiater E, Harrison CA, Lewis KA, Gray PC, Vale WW** 2006 Identification of distinct inhibin and transforming growth factor beta-binding sites on betaglycan: functional separation of betaglycan co-receptor actions. Journal of Biological Chemistry 281:17011-17022

98. **Mueller TD, Nickel J** 2012 Promiscuity and specificity in BMP receptor activation. FEBS Lett 586:1846-1859
99. **Muller P, Rogers KW, Jordan BM, Lee JS, Robson D, Ramanathan S, Schier AF** 2012 Differential diffusivity of Nodal and Lefty underlies a reaction-diffusion patterning system. Science 336:721-724
100. **Schier AF** 2009 Nodal morphogens. Cold Spring Harb Perspect Biol 1:a003459
101. **Glister C, Kemp CF, Knight PG** 2004 Bone morphogenetic protein (BMP) ligands and receptors in bovine ovarian follicle cells: actions of BMP-4, -6 and -7 on granulosa cells and differential modulation of Smad-1 phosphorylation by follistatin. Reproduction 127:239-254
102. **Iemura S, Yamamoto TS, Takagi C, Kobayashi H, Ueno N** 1999 Isolation and characterization of bone morphogenetic protein-binding proteins from the early Xenopus embryo. Journal of Biological Chemistry 274:26843-26849
103. **Mulloy B, Rider CC** 2015 The Bone Morphogenetic Proteins and Their Agonists. In: Litwack G ed. Bone Morphogenic Protein: Elsevier Science and Technology; 63-90
104. **Zhang JL, Qiu LY, Kotzsch A, Weidauer S, Patterson L, Hammerschmidt M, Sebald W, Mueller TD** 2008 Crystal structure analysis reveals how the Chordin family member crossveinless 2 blocks BMP-2 receptor binding. Dev Cell 14:739-750
105. **Cash JN, Angerman EB, Keutmann HT, Thompson TB** 2012 Characterization of follistatin-type domains and their contribution to myostatin and activin A antagonism. Mol Endocrinol 26:1167-1178
106. **Stamler R, Keutmann HT, Sidis Y, Kattamuri C, Schneyer A, Thompson TB** 2008 The structure of FSTL3.activin A complex. Differential binding of N-terminal domains influences follistatin-type antagonist specificity. Journal of Biological Chemistry 283:32831-32838
107. **Wiater E, Vale W** 2003 Inhibin is an antagonist of bone morphogenetic protein signaling. Journal of Biological Chemistry 278:7934-7941
108. **Koike N, Kassai Y, Kouta Y, Miwa H, Konishi M, Itoh N** 2007 Brorin, a novel secreted bone morphogenetic protein antagonist, promotes neurogenesis in mouse neural precursor cells. Journal of Biological Chemistry 282:15843-15850
109. **Nakayama N, Han CY, Cam L, Lee JI, Pretorius J, Fisher S, Rosenfeld R, Scully S, Nishinakamura R, Duryea D, Van G, Bolon B, Yokota T, Zhang K** 2004 A novel chordin-like BMP inhibitor, CHL2, expressed preferentially in chondrocytes of developing cartilage and osteoarthritic joint cartilage. Development 131:229-240
110. **Piccolo S, Sasai Y, Lu B, De Robertis EM** 1996 Dorsoventral patterning in Xenopus: inhibition of ventral signals by direct binding of chordin to BMP-4. Cell 86:589-598
111. **Hung W-T, Wu F-J, Wang C-J, Luo C-W** 2012 DAN (NBL1) Specifically Antagonizes BMP2 and BMP4 and Modulates the Actions of GDF9, BMP2, and BMP4 in the Rat Ovary. Biol Reprod 86:158, 151-159
112. **Yamaguchi Y, Mann DM, Ruoslahti E** 1990 Negative regulation of transforming growth factor-[beta] by the proteoglycan decorin. Nature 346:281-284
113. **Barbara NP, Wrana JL, Letarte M** 1999 Endoglin is an accessory protein that interacts with the signaling receptor complex of multiple members of the transforming growth factor-beta superfamily. Journal of Biological Chemistry 274:584-594

114. **Hill JJ, Qiu Y, Hewick RM, Wolfman NM** 2003 Regulation of myostatin in vivo by growth and differentiation factor-associated serum protein-1: a novel protein with protease inhibitor and follistatin domains. Mol Endocrinol 17:1144-1154
115. **de Kretser DM, Hedger MP, Loveland KL, Phillips DJ** 2002 Inhibins, activins and follistatin in reproduction. Hum Reprod Update 8:529-541
116. **Amthor H, Christ B, Rashid-Doubell F, Kemp CF, Lang E, Patel K** 2002 Follistatin regulates bone morphogenetic protein-7 (BMP-7) activity to stimulate embryonic muscle growth. Dev Biol 243:115-127
117. **Sylva M, Moorman AF, van den Hoff MJ** 2013 Follistatin-like 1 in vertebrate development. Birth Defects Res C Embryo Today 99:61-69
118. **Tsuchida K, Arai KY, Kuramoto Y, Yamakawa N, Hasegawa Y, Sugino H** 2000 Identification and characterization of a novel follistatin-like protein as a binding protein for the TGF-beta family. Journal of Biological Chemistry 275:40788-40796
119. **Zimmerman LB, De Jesus-Escobar JM, Harland RM** 1996 The Spemann organizer signal noggin binds and inactivates bone morphogenetic protein 4. Cell 86:599-606
120. **O'Connor-McCourt MD, Wakefield LM** 1987 Latent transforming growth factor-beta in serum. A specific complex with alpha 2-macroglobulin. Journal of Biological Chemistry 262:14090-14099
121. **Hawinkels LJ, Paauwe M, Verspaget HW, Wiercinska E, van der Zon JM, van der Ploeg K, Koelink PJ, Lindeman JH, Mesker W, ten Dijke P, Sier CF** 2014 Interaction with colon cancer cells hyperactivates TGF-beta signaling in cancer-associated fibroblasts. Oncogene 33:97-107
122. **Lopez-Casillas F, Cheifetz S, Doody J, Andres JL, Lane WS, Massague J** 1991 Structure and expression of the membrane proteoglycan betaglycan, a component of the TGF-beta receptor system. Cell 67:785-795
123. **Brown CB, Boyer AS, Runyan RB, Barnett JV** 1999 Requirement of type III TGF-beta receptor for endocardial cell transformation in the heart. Science 283:2080-2082
124. **Lopez-Casillas F, Payne HM, Andres JL, Massague J** 1994 Betaglycan can act as a dual modulator of TGF-beta access to signaling receptors: mapping of ligand binding and GAG attachment sites. J Cell Biol 124:557-568
125. **Kirkbride KC, Townsend TA, Bruinsma MW, Barnett JV, Blobe GC** 2008 Bone morphogenetic proteins signal through the transforming growth factor-beta type III receptor. Journal of Biological Chemistry 283:7628-7637
126. **Lee NY, Kirkbride KC, Sheu RD, Blobe GC** 2009 The transforming growth factor-beta type III receptor mediates distinct subcellular trafficking and downstream signaling of activin-like kinase (ALK)3 and ALK6 receptors. Mol Biol Cell 20:4362-4370
127. **Andres JL, Stanley K, Cheifetz S, Massague J** 1989 Membrane-anchored and soluble forms of betaglycan, a polymorphic proteoglycan that binds transforming growth factor-beta. J Cell Biol 109:3137-3145
128. **Bilandzic M, Stenvers KL** 2012 Reprint of: Betaglycan: A multifunctional accessory. Mol Cell Endocrinol 15:13-22
129. **Moustakas A, Heldin CH** 2009 The regulation of TGFbeta signal transduction. Development 136:3699-3714
130. **Massague J, Seoane J, Wotton D** 2005 Smad transcription factors. Genes Dev 19:2783-2810
131. **Itoh S, ten Dijke P** 2007 Negative regulation of TGF-beta receptor/Smad signal transduction. Curr Opin Cell Biol 19:176-184

132. **Mueller TD, Nickel J** 2012 Promiscuity and specificity in BMP receptor activation. FEBS Lett 586:1846-1859
133. **ten Dijke P, Fu J, Schaap P, Roelen BA** 2003 Signal transduction of bone morphogenetic proteins in osteoblast differentiation. J Bone Joint Surg Am 85-A Suppl 3:34-38
134. **Schmierer B, Hill CS** 2007 TGFbeta-SMAD signal transduction: molecular specificity and functional flexibility. Nat Rev Mol Cell Biol 8:970-982
135. **Rey R, Lukas-Croisier C, Lasala C, Bedecarras P** 2003 AMH/MIS: what we know already about the gene, the protein and its regulation. Mol Cell Endocrinol 211:21-31
136. **Picard JY, Josso N** 1984 Purification of testicular anti-Mullerian hormone allowing direct visualization of the pure glycoprotein and determination of yield and purification factor. Mol Cell Endocrinol 34:23-29
137. **Budzik GP, Swann DA, Hayashi A, Donahoe PK** 1980 Enhanced purification of Mullerian inhibiting substance by lectin affinity chromatography. Cell 21:909-915
138. **Shima H, Donahoe PK, Budzik GP, Kamagata S, Hudson P, Mudgett-Hunter M** 1984 Production of monoclonal antibodies for affinity purification of bovine mullerian inhibiting substance activity. Hybridoma 3:201-214
139. **Cate RL, Mattaliano RJ, Hession C, Tizard R, Farber NM, Cheung A, Ninfa EG, Frey AZ, Gash DJ, Chow EP, et al.** 1986 Isolation of the bovine and human genes for Mullerian inhibiting substance and expression of the human gene in animal cells. Cell 45:685-698
140. **di Clemente N, Jamin SP, Lugovskoy A, Carmillo P, Ehrenfels C, Picard JY, Whitty A, Josso N, Pepinsky RB, Cate RL** 2010 Processing of Anti-Mullerian Hormone Regulates Receptor Activation by a Mechanism Distinct from TGF-beta. Molecular Endocrinology 24:2193-2206
141. **Pankhurst MW, McLennan IS** 2013 Human blood contains both the uncleaved precursor of anti-Mullerian hormone and a complex of the NH2- and COOH-terminal peptides. Am J Physiol Endocrinol Metab 305:E1241-1247
142. **Wilson CA, Diclemente N, Ehrenfels C, Pepinsky RB, Josso N, Vigier B, Cate RL** 1993 Mullerian Inhibiting Substance Requires Its N-Terminal Domain for Maintenance of Biological-Activity, a Novel Finding within the Transforming Growth-Factor-Beta Superfamily. Molecular Endocrinology 7:247-257
143. **Josso N, Belville C, di Clemente N, Picard JY** 2005 AMH and AMH receptor defects in persistent Mullerian duct syndrome. Hum Reprod Update 11:351-356
144. **Vigier B, Tran D, Dubuisson FD, Heyman Y, Josso N** 1983 Use of Monoclonal-Antibody Techniques to Study the Ontogeny of Bovine Anti-Mullerian Hormone. J Reprod Fertil 69:207-214
145. **Belville C, Van Vlijmen H, Ehrenfels C, Pepinsky B, Rezaie AR, Picard JY, Josso N, di Clemente N, Cate RL** 2004 Mutations of the anti-mullerian hormone gene in patients with persistent mullerian duct syndrome: biosynthesis, secretion, and processing of the abnormal proteins and analysis using a three-dimensional model. Mol Endocrinol 18:708-721
146. **Pepinsky RB, Sinclair LK, Chow EP, Mattaliano RJ, Manganaro TF, Donahoe PK, Cate RL** 1988 Proteolytic Processing of Mullerian Inhibiting Substance Produces a Transforming Growth Factor-Beta-Like Fragment. Journal of Biological Chemistry 263:18961-18964

147. **Ragin RC, Donahoe PK, Kenneally MK, Ahmad MF, MacLaughlin DT** 1992 Human Mullerian inhibiting substance: enhanced purification imparts biochemical stability and restores antiproliferative effects. Protein Expr Purif 3:236-245
148. **Almeida J, Ball BA, Conley AJ, Place NJ, Liu IK, Scholtz EL, Mathewson L, Stanley SD, Moeller BC** 2011 Biological and clinical significance of anti-Mullerian hormone determination in blood serum of the mare. Theriogenology 76:1393-1403
149. **Imbeaud S, Carre-Eusebe D, Rey R, Belville C, Josso N, Picard JY** 1994 Molecular genetics of the persistent mullerian duct syndrome: a study of 19 families. Human Molecular Genetics 3:125-131
150. **Akiyama T, Marques G, Wharton KA** 2012 A large bioactive BMP ligand with distinct signaling properties is produced by alternative proconvertase processing Sci Signal 5:ra28
151. **Pankhurst MW, Chong YH, McLennan IS** 2014 Enzyme-linked immunosorbent assay measurements of antimullerian hormone (AMH) in human blood are a composite of the uncleaved and bioactive cleaved forms of AMH. Fertil Steril 101:846-850
152. **Nachtigal MW, Ingraham HA** 1996 Bioactivation of Müllerian inhibiting substance during gonadal development by a kex2/subtilisin-like endoprotease. Proceedings of the National Academy of Sciences 93:7711-7716
153. **Ragin RC, Donahoe PK, Kenneally MK, Ahmad MF, MacLaughlin DT** 1992 Human mullerian inhibiting substance: enhanced purification imparts biochemical stability and restores antiproliferative effects. Protein Expr Purif 3:236-245
154. **Guo J, Shi YQ, Yang W, Li YC, Hu ZY, Liu YX** 2007 Testosterone upregulation of tissue type plasminogen activator expression in Sertoli cells : tPA expression in Sertoli cells. Endocrine 32:83-89
155. **Bae JA, Park HJ, Seo YM, Roh J, Hsueh AJ, Chun SY** 2008 Hormonal regulation of proprotein convertase subtilisin/kexin type 5 expression during ovarian follicle development in the rat. Mol Cell Endocrinol 289:29-37
156. **Kwok SC, Chakraborty D, Soares MJ, Dai G** 2013 Relative expression of proprotein convertases in rat ovaries during pregnancy. J Ovarian Res 6:91
157. **Seidah NG, Khatib AM, Prat A** 2006 The proprotein convertases and their implication in sterol and/or lipid metabolism. Biol Chem 387:871-877
158. **Imbeaud S, Faure E, Lamarre I, Mattei MG, di Clemente N, Tizard R, Carre-Eusebe D, Belville C, Tragethon L, Tonkin C, Nelson J, McAuliffe M, Bidart JM, Lababidi A, Josso N, Cate RL, Picard JY** 1995 Insensitivity to anti-mullerian hormone due to a mutation in the human anti-mullerian hormone receptor. Nature Genetics 11:382-388
159. **Mishina Y, Rey R, Finegold MJ, Matzuk MM, Josso N, Cate RL, Behringer RR** 1996 Genetic analysis of the Mullerian-inhibiting substance signal transduction pathway in mammalian sexual differentiation. Genes Dev 10:2577-2587
160. **Behringer RR, Finegold MJ, Cate RL** 1994 Mullerian-inhibiting substance function during mammalian sexual development. Cell 79:415-425
161. **Knebelmann B, Boussin L, Guerrier D, Legeai L, Kahn A, Josso N, Picard JY** 1991 Anti-Müllerian hormone Bruxelles: a nonsense mutation associated with the persistent Müllerian duct syndrome. Proceedings of the National Academy of Sciences 88:3767-3771
162. **UniProt C** 2007 The Universal Protein Resource (UniProt). Nucleic Acids Res 35:D193-197

163. **Imhoff FM, Yang D, Mathew SF, Clarkson AN, Kawagishi Y, Tate WP, Koishi K, McLennan IS** 2013 The type 2 anti-Mullerian hormone receptor has splice variants that are dominant-negative inhibitors. FEBS Lett 587:1749-1753
164. **Baarends WM, van Helmond MJ, Post M, van der Schoot PJ, Hoogerbrugge JW, de Winter JP, Uilenbroek JT, Karels B, Wilming LG, Meijers JH, et al.** 1994 A novel member of the transmembrane serine/threonine kinase receptor family is specifically expressed in the gonads and in mesenchymal cells adjacent to the mullerian duct. Development 120:189-197
165. **di Clemente N, Wilson C, Faure E, Boussin L, Carmillo P, Tizard R, Picard JY, Vigier B, Josso N, Cate R** 1994 Cloning, expression, and alternative splicing of the receptor for anti-Mullerian hormone. Mol Endocrinol 8:1006-1020
166. **Racine C, Rey R, Forest MG, Louis F, Ferre A, Huhtaniemi I, Josso N, di Clemente N** 1998 Receptors for anti-mullerian hormone on Leydig cells are responsible for its effects on steroidogenesis and cell differentiation. Proc Natl Acad Sci U S A 95:594-599
167. **Baarends WM, van Helmond MJ, Post M, van der Schoot PJ, Hoogerbrugge JW, de Winter JP, Uilenbroek JT, Karels B, Wilming LG, Meijers JH** 1994 A novel member of the transmembrane serine/threonine kinase receptor family is specifically expressed in the gonads and in mesenchymal cells adjacent to the mullerian duct. Development 120:189-197
168. **Tsuji M, Shima H, Yonemura CY, Brody J, Donahoe PK, Cunha GR** 1992 Effect of human recombinant mullerian inhibiting substance on isolated epithelial and mesenchymal cells during mullerian duct regression in the rat. Endocrinology 131:1481-1488
169. **Segev DL, Hoshiya Y, Hoshiya M, Tran TT, Carey JL, Stephen AE, MacLaughlin DT, Donahoe PK, Maheswaran S** 2002 Mullerian-inhibiting substance regulates NF-kappa B signaling in the prostate in vitro and in vivo. Proc Natl Acad Sci U S A 99:239-244
170. **Renaud EJ, MacLaughlin DT, Oliva E, Rueda BR, Donahoe PK** 2005 Endometrial cancer is a receptor-mediated target for Mullerian Inhibiting Substance. Proc Natl Acad Sci U S A 102:111-116
171. **Hoshiya Y, Gupta V, Kawakubo H, Brachtel E, Carey JL, Sasur L, Scott A, Donahoe PK, Maheswaran S** 2003 Mullerian inhibiting substance promotes interferon gamma-induced gene expression and apoptosis in breast cancer cells. Journal of Biological Chemistry 278:51703-51712
172. **Segev DL, Hoshiya Y, Stephen AE, Hoshiya M, Tran TT, MacLaughlin DT, Donahoe PK, Maheswaran S** 2001 Mullerian inhibiting substance regulates NFkappaB signaling and growth of mammary epithelial cells in vivo. Journal of Biological Chemistry 276:26799-26806
173. **Barbie TU, Barbie DA, MacLaughlin DT, Maheswaran S, Donahoe PK** 2003 Mullerian Inhibiting Substance inhibits cervical cancer cell growth via a pathway involving p130 and p107. Proc Natl Acad Sci U S A 100:15601-15606
174. **Catlin EA, Powell SM, Manganaro TF, Hudson PL, Ragin RC, Epstein J, Donahoe PK** 1990 Sex-specific fetal lung development and mullerian inhibiting substance. Am Rev Respir Dis 141:466-470
175. **Catlin EA, Tonnu VC, Ebb RG, Pacheco BA, Manganaro TF, Ezzell RM, Donahoe PK, Teixeira J** 1997 Mullerian inhibiting substance inhibits

branching morphogenesis and induces apoptosis in fetal rat lung. Endocrinology 138:790-796

176. **Segev DL, Ha TU, Tran TT, Kenneally M, Harkin P, Jung M, MacLaughlin DT, Donahoe PK, Maheswaran S** 2000 Mullerian inhibiting substance inhibits breast cancer cell growth through an NFkappa B-mediated pathway. Journal of Biological Chemistry 275:28371-28379
177. **di Clemente N, Josso N, Gouedard L, Belville C** 2003 Components of the anti-Mullerian hormone signaling pathway in gonads. Mol Cell Endocrinol 211:9-14
178. **Gu ZY, Nomura M, Simpson BB, Lei H, Feijen A, van den Eijnden-van Raaij J, Donahoe PK, Li E** 1998 The type I activin receptor ActRIB is required for egg cylinder organization and gastrulation in the mouse. Genes & Development 12:844-857
179. **Mishina Y, Suzuki A, Ueno N, Behringer RR** 1995 Bmpr encodes a type I bone morphogenetic protein receptor that is essential for gastrulation during mouse embryogenesis. Genes Dev 9:3027-3037
180. **Visser JA, Olaso R, Verhoef-Post M, Kramer P, Themmen AP, Ingraham HA** 2001 The serine/threonine transmembrane receptor ALK2 mediates Mullerian inhibiting substance signaling. Mol Endocrinol 15:936-945
181. **Clarke TR, Hoshiya Y, Yi SE, Liu X, Lyons KM, Donahoe PK** 2001 Mullerian inhibiting substance signaling uses a bone morphogenetic protein (BMP)-like pathway mediated by ALK2 and induces SMAD6 expression. Mol Endocrinol 15:946-959
182. **Koenig BB, Cook JS, Wolsing DH, Ting J, Tiesman JP, Correa PE, Olson CA, Pecquet AL, Ventura F, Grant RA, et al.** 1994 Characterization and cloning of a receptor for BMP-2 and BMP-4 from NIH 3T3 cells. Molecular and Cellular Biology 14:5961-5974
183. **Maglott D, Ostell J, Pruitt KD, Tatusova T** 2005 Entrez Gene: gene-centered information at NCBI. Nucleic Acids Res 33:D54-D58
184. **Settle SH, Jr., Rountree RB, Sinha A, Thacker A, Higgins K, Kingsley DM** 2003 Multiple joint and skeletal patterning defects caused by single and double mutations in the mouse Gdf6 and Gdf5 genes. Dev Biol 254:116-130
185. **Pellegrini M, Grimaldi P, Rossi P, Geremia R, Dolci S** 2003 Developmental expression of BMP4/ALK3/SMAD5 signaling pathway in the mouse testis: a potential role of BMP4 in spermatogonia differentiation. J Cell Sci 116:3363-3372
186. **Edson MA, Nalam RL, Clementi C, Franco HL, Demayo FJ, Lyons KM, Pangas SA, Matzuk MM** 2010 Granulosa cell-expressed BMPR1A and BMPR1B have unique functions in regulating fertility but act redundantly to suppress ovarian tumor development. Mol Endocrinol 24:1251-1266
187. **Yi SE, LaPolt PS, Yoon BS, Chen JY, Lu JK, Lyons KM** 2001 The type I BMP receptor BmprIB is essential for female reproductive function. Proc Natl Acad Sci U S A 98:7994-7999
188. **Erickson GF, Shimasaki S** 2003 The spatiotemporal expression pattern of the bone morphogenetic protein family in rat ovary cell types during the estrous cycle. Reprod Biol Endocrinol 1:1-20
189. **Logeart-Avramoglou D, Bourguignon M, Oudina K, Ten Dijke P, Petite H** 2006 An assay for the determination of biologically active bone morphogenetic proteins using cells transfected with an inhibitor of differentiation promoter-luciferase construct. Anal Biochem 349:78-86

190. **Pankhurst MW, McLennan IS** 2015 A specific immunoassay for proAMH, the uncleaved proprotein precursor of anti-Mullerian hormone. Mol Cell Endocrinol S0303-7207(15):Epub ahead of print
191. **Chong YH, Pankhurst MW, McLennan IS** 2015 The Daily Profiles of Circulating AMH and INSL3 in Men are Distinct from the Other Testicular Hormones, Inhibin B and Testosterone. PLoS One 10:e0133637
192. **Gouedard L, Chen YG, Thevenet L, Racine C, Borie S, Lamarre I, Josso N, Massague J, di Clemente N** 2000 Engagement of bone morphogenetic protein type IB receptor and Smad1 signaling by anti-Mullerian hormone and its type II receptor. Journal of Biological Chemistry 275:27973-27978
193. **Tran TT, Segev DL, Gupta V, Kawakubo H, Yeo G, Donahoe PK, Maheswaran S** 2006 Mullerian inhibiting substance regulates androgen-induced gene expression and growth in prostate cancer cells through a nuclear factor-kappaB-dependent Smad-independent mechanism. Mol Endocrinol 20:2382-2391
194. **Macias-Silva M, Hoodless PA, Tang SJ, Buchwald M, Wrana JL** 1998 Specific activation of Smad1 signaling pathways by the BMP7 type I receptor, ALK2. Journal of Biological Chemistry 273:25628-25636
195. **Belville C, Marechal JD, Pennetier S, Carmillo P, Masgrau L, Messika-Zeitoun L, Galey J, Machado G, Treton D, Gonzales J, Picard JY, Josso N, Cate RL, di Clemente N** 2009 Natural mutations of the anti-Mullerian hormone type II receptor found in persistent Mullerian duct syndrome affect ligand binding, signal transduction and cellular transport. Hum Mol Genet 18:3002-3013
196. **Renlund N, O'Neill FH, Zhang L, Sidis Y, Teixeira J** 2007 Activin receptor-like kinase-2 inhibits activin signaling by blocking the binding of activin to its type II receptor. J Endocrinol 195:95-103
197. **Arouche N, Picard JY, Monniaux D, Jamin SP, Vigier B, Josso N, Cate RL, di Clemente N, Taieb J** 2015 The BOC ELISA, a ruminant-specific AMH immunoassay, improves the determination of plasma AMH concentration and its correlation with embryo production in cattle. Theriogenology 84:1397-1404
198. **Herrera B, Inman GJ** 2009 A rapid and sensitive bioassay for the simultaneous measurement of multiple bone morphogenetic proteins. Identification and quantification of BMP4, BMP6 and BMP9 in bovine and human serum. BMC Cell Biol 10:20
199. **Imhoff FM** 2012 New Insights into Müllerian Hormone Signalling. In: Department of Anatomy. Dunedin, New Zealand: University of Otago; 202
200. **Gouedard L, Chen YG, Thevenet L, Racine C, Borie S, Lamarre I, Josso N, Massague J, di Clemente N** 2000 Engagement of bone morphogenetic protein type IB receptor and Smad1 signaling by anti-Mullerian hormone and its type II receptor. Journal of Biological Chemistry 275:27973-27978
201. **Josso N, Clemente N** 2003 Transduction pathway of anti-Mullerian hormone, a sex-specific member of the TGF-beta family. Trends Endocrinol Metab 14:91-97
202. **Mazerbourg S, Sangkuhl K, Luo CW, Sudo S, Klein C, Hsueh AJ** 2005 Identification of receptors and signaling pathways for orphan bone morphogenetic protein/growth differentiation factor ligands based on genomic analyses. Journal of Biological Chemistry 280:32122-32132
203. **Liu F, Ventura F, Doody J, Massague J** 1995 Human type II receptor for bone morphogenic proteins (BMPs): extension of the two-kinase receptor model to the BMPs. Molecular and Cellular Biology 15:3479-3486

204. **Guzman A, Zelman-Femiak M, Boergermann JH, Paschkowsky S, Kreuzaler PA, Fratzl P, Harms GS, Knaus P** 2012 SMAD versus non-SMAD signaling is determined by lateral mobility of bone morphogenetic protein (BMP) receptors. Journal of Biological Chemistry 287:39492-39504
205. **Rosenzweig BL, Imamura T, Okadome T, Cox GN, Yamashita H, ten Dijke P, Heldin CH, Miyazono K** 1995 Cloning and characterization of a human type II receptor for bone morphogenetic proteins. Proc Natl Acad Sci U S A 92:7632-7636
206. **McLennan IS, Chong, Y.H., Kawagishi,Y., Pankhurst, M.W.** 2015 A critical evaluation of whether circulating anti-müllerian hormone is a hormone in adults,with special reference to its putative roles in men. In: Tal IDSaR ed. Anti-Müllerian Hormone: Biology, Role in Ovarian Function, and Clinical Significance: Nova Science
207. **Catlin EA, Ezzell RM, Donahoe PK, Gustafson ML, Son EV, MacLaughlin DT** 1993 Identification of a receptor for human mullerian inhibiting substance. Endocrinology 133:3007-3013
208. **Masiakos PT, MacLaughlin DT, Maheswaran S, Teixeira J, Fuller AF, Jr., Shah PC, Kehas DJ, Kenneally MK, Dombkowski DM, Ha TU, Preffer FI, Donahoe PK** 1999 Human ovarian cancer, cell lines, and primary ascites cells express the human Mullerian inhibiting substance (MIS) type II receptor, bind, and are responsive to MIS. Clin Cancer Res 5:3488-3499
209. **Ha TU, Segev DL, Barbie D, Masiakos PT, Tran TT, Dombkowski D, Glander M, Clarke TR, Lorenzo HK, Donahoe PK, Maheswaran S** 2000 Mullerian inhibiting substance inhibits ovarian cell growth through an Rb-independent mechanism. Journal of Biological Chemistry 275:37101-37109
210. **Pankhurst MW, McLennan IS** 2012 Inhibin B and anti-Mullerian hormone/Mullerian-inhibiting substance may contribute to the male bias in autism. Transl Psychiatry 2:e148
211. **Campbell BK, Clinton M, Webb R** 2012 The role of anti-Mullerian hormone (AMH) during follicle development in a monovulatory species (sheep). Endocrinology 153:4533-4543
212. **Schneyer AL, Wang Q, Sidis Y, Sluss PM** 2004 Differential distribution of follistatin isoforms: application of a new FS315-specific immunoassay. J Clin Endocrinol Metab 89:5067-5075
213. **Phillips DJ, de Kretser DM** 1998 Follistatin: A Multifunctional Regulatory Protein. Frontiers in Neuroendocrinology 19:287-322
214. **Schneyer AL, Hall HA, Lambert-Messerlian G, Wang QF, Sluss P, Crowley WF, Jr.** 1996 Follistatin-activin complexes in human serum and follicular fluid differ immunologically and biochemically. Endocrinology 137:240-247
215. **Sugino K, Kurosawa N, Nakamura T, Takio K, Shimasaki S, Ling N, Titani K, Sugino H** 1993 Molecular heterogeneity of follistatin, an activin-binding protein. Higher affinity of the carboxyl-terminal truncated forms for heparan sulfate proteoglycans on the ovarian granulosa cell. Journal of Biological Chemistry 268:15579-15587
216. **Shimasaki S, Koga M, Esch F, Mercado M, Cooksey K, Koba A, Ling N** 1988 Porcine follistatin gene structure supports two forms of mature follistatin produced by alternative splicing. Biochem Biophys Res Commun 152:717-723
217. **Shimonaka M, Inouye S, Shimasaki S, Ling N** 1991 Follistatin binds to both activin and inhibin through the common subunit. Endocrinology 128:3313-3315

218. **Massague J, Chen YG** 2000 Controlling TGF-beta signaling. Genes Dev 14:627-644
219. **Hashimoto O, Nakamura T, Shoji H, Shimasaki S, Hayashi Y, Sugino H** 1997 A novel role of follistatin, an activin-binding protein, in the inhibition of activin action in rat pituitary cells. Endocytotic degradation of activin and its acceleration by follistatin associated with cell-surface heparan sulfate. Journal of Biological Chemistry 272:13835-13842
220. **Iemura S, Yamamoto TS, Takagi C, Uchiyama H, Natsume T, Shimasaki S, Sugino H, Ueno N** 1998 Direct binding of follistatin to a complex of bone-morphogenetic protein and its receptor inhibits ventral and epidermal cell fates in early Xenopus embryo. Proc Natl Acad Sci U S A 95:9337-9342
221. **Keutmann HT, Schneyer AL, Sidis Y** 2004 The role of follistatin domains in follistatin biological action. Mol Endocrinol 18:228-240
222. **Lin SJ, Lerch TF, Cook RW, Jardetzky TS, Woodruff TK** 2006 The structural basis of TGF-beta, bone morphogenetic protein, and activin ligand binding. Reproduction 132:179-190
223. **Thompson TB, Lerch TF, Cook RW, Woodruff TK, Jardetzky TS** 2005 The structure of the follistatin:activin complex reveals antagonism of both type I and type II receptor binding. Dev Cell 9:535-543
224. **Otsuka F, Moore RK, Iemura S, Ueno N, Shimasaki S** 2001 Follistatin inhibits the function of the oocyte-derived factor BMP-15. Biochem Biophys Res Commun 289:961-966
225. **Jorgez CJ, Klysik M, Jamin SP, Behringer RR, Matzuk MM** 2004 Granulosa cell-specific inactivation of follistatin causes female fertility defects. Mol Endocrinol 18:953-967
226. **Welt C, Sidis Y, Keutmann H, Schneyer A** 2002 Activins, inhibins, and follistatins: from endocrinology to signaling. A paradigm for the new millennium. Exp Biol Med (Maywood) 227:724-752
227. **Matzuk MM, Lu N, Vogel H, Sellheyer K, Roop DR, Bradley A** 1995 Multiple defects and perinatal death in mice deficient in follistatin. Nature 374:360-363
228. **Michel U, Ebert S, Phillips D, Nau R** 2003 Serum concentrations of activin and follistatin are elevated and run in parallel in patients with septicemia. Eur J Endocrinol 148:559-564
229. **Venkatesha S, Toporsian M, Lam C, Hanai J, Mammoto T, Kim YM, Bdolah Y, Lim KH, Yuan HT, Libermann TA, Stillman IE, Roberts D, D'Amore PA, Epstein FH, Sellke FW, Romero R, Sukhatme VP, Letarte M, Karumanchi SA** 2006 Soluble endoglin contributes to the pathogenesis of preeclampsia. Nat Med 12:642-649
230. **Castonguay R, Werner ED, Matthews RG, Presman E, Mulivor AW, Solban N, Sako D, Pearsall RS, Underwood KW, Seehra J, Kumar R, Grinberg AV** 2011 Soluble endoglin specifically binds bone morphogenetic proteins 9 and 10 via its orphan domain, inhibits blood vessel formation, and suppresses tumor growth. Journal of Biological Chemistry 286:30034-30046
231. **Nilsson EE, Larsen G, Skinner MK** 2014 Roles of Gremlin 1 and Gremlin 2 in regulating ovarian primordial to primary follicle transition. Reproduction 147:865-874
232. **Carroll SL, Silos-Santiago I, Frese SE, Ruit KG, Milbrandt J, Snider WD** 1992 Dorsal root ganglion neurons expressing trk are selectively sensitive to NGF deprivation in utero. Neuron 9:779-788

233. **Smeyne RJ, Klein R, Schnapp A, Long LK, Bryant S, Lewin A, Lira SA, Barbacid M** 1994 Severe sensory and sympathetic neuropathies in mice carrying a disrupted Trk/NGF receptor gene. Nature 368:246-249
234. **Nykjaer A, Lee R, Teng KK, Jansen P, Madsen P, Nielsen MS, Jacobsen C, Kliemannel M, Schwarz E, Willnow TE, Hempstead BL, Petersen CM** 2004 Sortilin is essential for proNGF-induced neuronal cell death. Nature 427:843-848
235. **Ge G, Greenspan DS** 2006 BMP1 controls TGFbeta1 activation via cleavage of latent TGFbeta-binding protein. J Cell Biol 175:111-120
236. **Shiga A, Nozaki H, Yokoseki A, Nihonmatsu M, Kawata H, Kato T, Koyama A, Arima K, Ikeda M, Katada S, Toyoshima Y, Takahashi H, Tanaka A, Nakano I, Ikeuchi T, Nishizawa M, Onodera O** 2011 Cerebral small-vessel disease protein HTRA1 controls the amount of TGF-beta1 via cleavage of proTGF-beta1. Hum Mol Genet 20:1800-1810
237. **Wilkinson L, Kolle G, Wen D, Piper M, Scott J, Little M** 2003 CRIM1 regulates the rate of processing and delivery of bone morphogenetic proteins to the cell surface. Journal of Biological Chemistry 278:34181-34188
238. **Ueno N, Ling N, Ying SY, Esch F, Shimasaki S, Guillemin R** 1987 Isolation and partial characterization of follistatin: a single-chain Mr 35,000 monomeric protein that inhibits the release of follicle-stimulating hormone. Proc Natl Acad Sci U S A 84:8282-8286